BERGISCHE
UNIVERSITÄT
WUPPERTAL

INVESTIGATION OF BUILDING ENERGY FLEXIBILITY AT CLUSTER LEVEL FOR A PROMISING ENERGY FLEXIBILITY MARKET

Dissertation
for the award of a doctoral degree
(Dr.-Ing.)

in the
Faculty of Architecture and Civil Engineering of the
University of Wuppertal

Submitted by
Tuğçin Kırant-Mitić
from the place (Kadıköy, Istanbul, Türkiye)

Wuppertal
2025

Chair of the Examination Committee: Prof. Dr. Armin Seyfried
1st Reviewer: Prof. Dr.-Ing. Karsten Voss
2nd Reviewer: Prof. Dr.-Ing. Markus Zdrallek
Member of the Examination Committee: Assoc. Prof. Dr. Rongling Li
Date of Submission: 15 October 2025
Date of Defense: 20 April 2026

Unless otherwise stated, this dissertation is published under a Creative Commons Attribution 4.0 International License (CC BY 4.0). To view a copy of this license, visit https://creativecommons.org/licenses/by/4.0/.

The article "Enhancing Grid Stability and Economic Operation through Heuristic Control: A Simulation Case Study" was originally published in: Proceedings of BauSim Conference 2024: 10th Conference of IBPSA-Germany and Austria. https://doi.org/10.26868/29761662.2024.19 without a Creative Commons license. Under the publishing agreement, the authors retain the copyright and have granted the publisher only a non-exclusive right of use. The CC BY 4.0 license applies only to the version of the article as included in this dissertation.

Not covered by the CC BY license are any third-party materials marked as such, publishers' logos, and publishers' layout and design elements.

URN: urn:nbn:de:hbz:468-2-7009
DOI: 10.25926/BUW/0-1014

FOREWORD

The transition toward a sustainable and resilient energy system requires not only renewable generation but also intelligent and flexible use of energy in buildings. When I began this work, I was motivated by a central question: how can buildings evolve from passive consumers into active, flexible prosumers that support both the market and the distribution grid? This question guided the research assembled in this dissertation.

The work was carried out at the Chair of Building Physics and Technical Building Services (b+tga) at Bergische Universität Wuppertal, under the supervision of Prof. Dr.-Ing. Karsten Voss. His scientific guidance and feedback have been invaluable throughout this journey.

This dissertation was enabled through the InFlex project funding, initiated by Prof. Dr.-Ing. Markus Zdrallek at the Chair of Electric Power Engineering (EVT). The InFlex project provided resources and a collaborative bridge between b+tga and EVT, aligning building and electrical engineering perspectives on flexibility at the interface of buildings and grids. My sincere thanks also go to colleagues at EVT for their open collaboration and ongoing knowledge exchange. This interdisciplinary cooperation was crucial for conducting the research at the building-grid interface.

Subsequently, the work was financed by the Living Lab NRW project, which allowed me to extend and deepen the study, particularly toward cluster-level operation, beyond the scope of the initial project. I would also like to thank my colleagues at the b+tga team, especially Dr.-Ing. Işıl Kalpkırmaz, Dr.-Ing. Karl Walther and Dr.-Ing. Ghadeer Derbas, for their collaboration and friendship. I would also like to thank Dr.-Ing. Tjado Voss for enabling the computing and simulation setup that made the computationally intensive co-simulations feasible.

The research also benefited from participation in the International Energy Agency - Energy in Buildings and Communities Programme, Annex 82 “Energy Flexible Buildings Towards Resilient Low Carbon Energy Systems.” I would like to thank the

operating agent, Assoc. Prof. Dr. Rongling Li, for her leadership throughout the Annex, and all Annex 82 participants for the rich knowledge exchange and constructive discussions that informed both methodology and interpretation.

I am also grateful to the IDA-ICE development team for their timely support in resolving modeling and co-simulation challenges, assistance that significantly accelerated progress and improved model quality.

I gratefully acknowledge the Equal Opportunities & Diversity Staff Unit - Bergische Universität Wuppertal for funding my participation in the Eleventh National Conference of IBPSA-USA (Denver, Colorado). In addition to presenting the conference paper, this support enabled me to take part in the Hackathon, where I won an award for the project “Developing an Interface for Energy Suppliers to Improve Their Operations in Building-Grid Interactions.”

I hope the findings presented here help move building energy flexibility from theoretical potential to verifiable, system-relevant practice.

Tuğçin Kırant-Mitić

TABLE OF CONTENTS

Page

ABBREVIATIONS

BEMS : Building Energy Management System
BEPS : Building Performance Simulation
BGI : Building-Grid Interaction
DER : Distributed Energy Resources
DHW : Domestic Hot Water
DSO : Distribution System Operator
EES : Electrical Energy Storage
EV : Electrical vehicles
GHG : Greenhouse gas
HVAC : Heating, Cooling, Ventilation and Air Conditioning
MPC : Model Predictive Control
PV : Photovoltaic
RBC : Rule-Based Control
RBPC : Rule-Based Predictive Control
RES : Renewable Energy System
RQ : Research Question
TSO : Transmission System Operator

SYMBOLS

Δ**T** **:** Temperature Difference (°C)

LIST OF FIGURES

Page

INVESTIGATION OF BUILDING ENERGY FLEXIBILITY AT CLUSTER LEVEL FOR A PROMISING ENERGY FLEXIBILITY MARKET

SUMMARY

Buildings are becoming prosumers with the electrification of heat and mobility and the spread of rooftop photovoltaic and battery storage. Their operation should follow price and CO_2 signals while prioritizing distribution-level feasibility, including transformer capacity, voltage limits, and node-specific import/export caps. This cumulative dissertation investigates how building-side demand flexibility can be modeled and controlled so that buildings deliver bidirectional value, more specifically, lower cost and emissions for end-users and reliable flexibility for the power grid without compromising comfort.

This dissertation focuses on flexibility at the distribution system level. Specifically, it examines how building´s heating, cooling, air-conditioning and ventilation systems (i.e., heat pumps, thermal storages) and distributed energy resources (i.e., electrical energy storage and photovoltaic) can provide location and time-specific flexibility to manage both market-oriented operation and grid-oriented operation within low-voltage network. The work (i) characterizes distribution system operator needs in the frame of flexibility, (ii) develops and simulates control strategies for buildings such as ranging from price-driven responses to explicit congestion signals, (iii) evaluates performance on realistic German building clusters, and (iv) quantifies benefits in terms of reduced constraint violations and operational cost/indoor thermal comfort impacts for end users. Interactions with transmission system operators are treated as boundary conditions; the primary objective is operational feasibility and value for distribution system operator, ensuring flexibility is applicable, verifiable, and aligned with local network constraints.

In this context, the dissertation has four main contributions. First (building-grid interaction signal evaluation), it develops a joint penalty signal that combines economic (day-ahead price) and environmental (average CO_2-equivalent intensity)

drivers into a single control objective. The analysis compares the composite objective with single-signal control and presents demand-flexibility results for cases where price and CO_2 signals align or conflict. Second, in the single-residential-building context, a simulation case study with heuristic control demonstrates that a small dwelling can deliver grid-oriented and market-oriented operation simultaneously, achieving grid support and cost reduction. Third (single non-residential building operation), it introduces a rule-based predictive control architecture implemented on a building with thermally activated building systems**.** In a co-simulation workflow that couples a white-box building energy performance model with a numerical computing engine, a horizon controller uses day-ahead prices and distribution system operator constraints to schedule preheating/precooling and charge thermal storage in the building mass, while applying comfort via slab and zone temperature limits. Fourth (cluster operation), two transformer-aware case studies in Germany and Switzerland quantify how building-grid interaction signals shape flexibility at the multi-building scale, showing that local constraints, both load-driven and generation-driven, govern performance. Within a calibrated co-simulation framework, the study analyzes cluster operation under price and CO_2eq. intensity signals while enforcing transformer limits, thereby delivering transformer-aware demand-side flexibility.

Overall, the research analyzes both grid-oriented and market-oriented operation, including a sequential “grid-first, market-second” strategy: grid constraints are treated as primary, and economic/environmental objectives are optimized subject to those constraints. The evaluation presents both single-building and multi-building scales: (i) residential and non-residential single buildings and (ii) clusters in different countries (Germany and Switzerland), where transformer-aware scheduling is shown. Methodologically, the work introduces a new control algorithm „Rule-based predictive control“ as an alternative to simple rule-based control and computationally heavy control models. Rule-based predictive control runs in a co-simulation workflow with a calibrated white-box building model, a horizon scheduler, and distribution-level limits.

The results show that the grid-first, market-second approach reliably prevents local violations while still achieving cost and CO_2 benefits. Moreover, rule-based predictive control captures most of the expected performance with only a fraction of the computational effort, and at the cluster scale, transformer-aware control reduces

coincident peaks and curtailment, outperforming single-signal baselines. Parts of this work were undertaken within the InFleX project (EFRE 2014–2020) and the International Energy Agency's EBC Annex 82 - Energy Flexible Buildings Towards Resilient Low Carbon Energy Systems programme, which provided knowledge exchange, shared scenarios, and cross-case comparability. In turn, the dissertation's tools and findings contribute to guidance on assessing and delivering verifiable flexibility.

UNTERSUCHUNG DER GEBÄUDEENERGIEFLEXIBILITÄT AUF CLUSTER-EBENE FÜR EINEN VIELVERSPRECHENDEN ENERGIEFLEXIBILITÄTSMARKT

ZUSAMMENFASSUNG

In dieser kumulativen Dissertation wird untersucht, wie gebäudeseitige Nachfrageflexibilität modelliert und gesteuert werden kann. Dadurch können Gebäude auf der Verteilungsebene bidirektionalen Mehrwert schaffen: niedrigere Kosten und Emissionen für die Endnutzer sowie verlässliche Flexibilität für das Stromnetz, ohne den Nutzerkomfort zu beeinträchtigen. Die Elektrifizierung von Wärme und Mobilität, zusammen mit weitverbreiteten Dach-Photovoltaikanlagen und elektrischen Energiespeichern, macht Gebäude zu Prosumern, deren Betrieb Preis und CO_2 Signalen folgen sollte. Hierbei hat die Machbarkeit auf allen Ebenen der Verteilnetze Vorrang, etwa hinsichtlich Transformatorenkapazitäten, Spannungsgrenzen und knotenspezifischen Import/Exportbegrenzungen.

Der Schwerpunkt der Dissertation liegt auf der Flexibilität im Verteilnetz. Analysiert wird, wie gebäudetechnische Anlagen für Heizung, Kühlung, Klimatisierung und Lüftung (z. B. Wärmepumpen, thermische Speicher) sowie dezentrale Energieressourcen (z. B. elektrische Speichersysteme und Photovoltaikanlagen) orts- und zeitabhängige Flexibilität bereitstellen können, um sowohl marktorientierten als auch netzorientierten Betrieb im Niederspannungsnetz zu ermöglichen. Im Einzelnen werden (i) die Anforderungen des Verteilnetzbetreibers im Rahmen der Flexibilität charakterisiert, (ii) Regelungsstrategien für Gebäude entwickelt und simuliert, wobei diese von preisorientierten Reaktionen bis zu expliziten Engpasssignalen reichen, (iii) die Leistungsfähigkeit an realitätsnahen deutschen Gebäudeclustern evaluiert und (iv) die Vorteile bezüglich verminderter Grenzüberschreitungen und Auswirkungen auf Betriebskosten und Innenraumkomfort für Endnutzer quantifiziert. Interaktionen mit Übertragungsnetzbetreibern werden als Randbedingungen behandelt; das Hauptziel ist die operative Umsetzbarkeit und Wertschöpfung für den Verteilnetzbetreiber, sodass Flexibilität anwendbar, überprüfbar und mit lokalen Netzrestriktionen vereinbar ist.

Die Dissertation leistet vier zentrale Beiträge: Erstens wird eine Bewertung von Gebäude–Netz-Interaktionssignalen vorgenommen, bei der ein gemeinsamer Indikator („joint penalty signal“) entwickelt wird, ökonomische (Day-Ahead-Preise) und ökologische (durchschnittliche CO_2-Äquivalenzintensität) Einflussgrößen zu einem Regelungsziel vereint. Die Analyse vergleicht das zusammengesetzte Regelungsziel mit Einzelziel-Regelungen und stellt Ergebnisse hinsichtlich Nachfrageflexibilität für Situationen dar, in denen Preis- und CO_2-Signale entweder übereinstimmen oder in Konflikt stehen. Zweitens zeigt eine Simulationsfallstudie im Kontext eines einzelnen Wohngebäudes mit heuristischer Regelung, dass auch ein kleines Wohnobjekt gleichzeitig netzorientierten und marktorientierten Betrieb ermöglichen und dabei Netzdienlichkeit und Kostensenkung erreichen kann. Drittens wird für ein Beispiel eines einzelnen gewerblichen Gebäudes eine regelbasierte, prädiktive Regelungsarchitektur eingeführt, die auf Gebäude mit thermisch aktivierten Gebäudesystemen angewendet wird. In einem Co-Simulations-Workflow, der ein White-Box-Gebäudeenergieleistungsmodell mit einem numerischen Optimierungsmodul koppelt, plant eine Optimierungsinstanz (Horizont-Regler) unter Berücksichtigung von Day-Ahead-Preisen und Restriktionen des Verteilnetzbetreibers das Vorheizen/Vorkühlen und das Laden des thermischen Speichers in der Gebäudemasse, wobei Komfortziele durch Begrenzungen der Platten- und Zonentemperaturen gewahrt werden. Viertens quantifizieren zwei Fallstudien in Deutschland und der Schweiz, welche die Transformatorgrenzen explizit berücksichtigen, wie Gebäude–netzbezogene Interaktionssignale die Flexibilität auf Gebäudecluster-Ebene beeinflussen und zeigen, dass sowohl last- als auch erzeugungsgetriebene lokale Netzrestriktionen die Performance determinieren. Im Rahmen eines kalibrierten Co-Simulationsansatzes wird die Clustersteuerung unter Preis- und CO_2-Äquivalenzintensitäts-Signalen analysiert, wobei die Einhaltung von Transformatorgrenzen gewährleistet wird; damit wird nachfrageseitige Flexibilität unter Berücksichtigung der Transformatoren erreicht.

Insgesamt betrachtet die Arbeit sowohl netz- als auch marktorientierten Betrieb, einschließlich einer sequenziellen Strategie „Netz zuerst, Markt danach“: Netzrestriktionen werden als primär behandelt, und ökonomische sowie ökologische Zielgrößen werden unter Beachtung dieser Restriktionen optimiert. Die Evaluierung umfasst sowohl Einzelgebäude (Wohn- und Nichtwohngebäude) als auch Cluster in

unterschiedlichen Ländern (Deutschland und Schweiz), wodurch die Praxis der transformatorbewussten Planung demonstriert wird. Methodisch führt die Dissertation einen neuen Regelungsalgorithmus ein, das „Rule-based predictive control“, welches eine Alternative zu herkömmlicher, regelbasierter Steuerung und rechenintensiven Kontrollmodellen bietet. „Rule-based predictive control“ wird im Co-Simulations-Workflow mit einem kalibrierten physikalischen Gebäudemodell, einer Planungseinheit für den Horizont und Grenzen der Verteilungsebene angewendet.

Die Ergebnisse zeigen, dass der Ansatz „Netz zuerst, Markt danach“ lokale Netzverletzungen zuverlässig verhindert und dennoch Kosten- und CO_2-Einsparungen ermöglicht; dass das „Rule-based predictive control“ den Großteil der erwarteten Leistung bei einem Bruchteil des Rechenaufwands erzielt; und dass auf Clusterebene die Berücksichtigung von Transformatorgrenzen sowohl gleichzeitige Lastspitzen als auch Abregelungen reduziert und gegenüber Einzelziel-Baselines überlegen ist. Teile dieser Arbeit wurden im Rahmen des InFleX-Projekts (EFRE 2014–2020) und des EBC-Annex 82 der Internationalen Energieagentur (Energy Flexible Buildings Towards Resilient Low Carbon Energy Systems Programm) durchgeführt, welche Wissensaustausch, geteilte Szenarien und Fallstudienvergleich ermöglichten. Die in dieser Dissertation entwickelten Werkzeuge und Erkenntnisse bieten eine Grundlage für die Bewertung und Umsetzung verifizierbarer Flexibilität.

1. INTRODUCTION

1.1 Context and Motivation

The global response to climate change has led to a transformation of energy systems, particularly in how electricity is generated, distributed, and consumed. Central to this transformation is the large-scale deployment of renewable energy technologies and the gradual decarbonization of end-use sectors such as buildings. Within the European Union, policy frameworks have reinforced commitments to achieve climate neutrality by 2050 (European Commission 2019, 2021). Germany, as one of the leading actors in the energy transition, aims for greenhouse gas (GHG) neutrality by 2045 (Press and Information Office of the Federal Government | Bundesregierung 2021).

However, the increasing share of renewable energy sources (RES), especially wind and solar photovoltaics (PV), presents new operational challenges to the electric power grid (Hamdi et al. 2024). These resources are inherently variable and weather-dependent, which makes their output difficult to forecast and control. As a result, maintaining grid stability is becoming more complex and requires the development of new flexibility strategies on the demand side (Astapov et al. 2025). At the same time, the growing electrification of heating systems, electric vehicles (EVs), and other household technologies contributes to rising and more volatile peak demands, placing additional stress on local distribution infrastructure, including low-voltage transformers (International Energy Agency 2024).

In this evolving energy landscape, buildings are no longer passive consumers but active participants in energy systems (Liang et al. 2025). Through integrated technologies such as thermal and electrical energy storage, on-site PV generation, and advanced control systems, buildings have the capacity to adjust their energy use in response to external signals and contribute to system-level balancing. This capability is commonly named as building energy flexibility or building-grid interaction (BGI) that it can support objectives such as peak shaving, load shifting, moreover cost and emissions reduction (Marszal-Pomianowska et al. 2019). BGI strategies are

increasingly recognized as essential tools for managing both grid stability and energy system efficiency in a highly electrified (Jensen et al. 2017).

Despite their potential, operationalizing energy flexibility in buildings remains a complex task. Flexibility is not a fixed attribute, but a context-dependent capability influenced by the interaction of system design (Foteinaki et al. 2018; Reynders et al. 2018), control strategies (Péan et al. 2019), user behavior (Li et al. 2017), economic incentives (Shahryari et al. 2018), and grid conditions (Askeland et al. 2025). Aligning building operations with grid needs requires not only the appropriate technical infrastructure but also control approaches that are responsive to dynamic signals and localized constraints (Clauß et al. 2019).

This dissertation explores how building energy systems can be coordinated with power grid requirements through structured control strategies. In particular, it investigates how flexibility can be harnessed using rule-based and predictive control approaches, guided by market (dynamic electricity price) and grid-oriented signals (congestion event). The research builds on simulations of real-world buildings and distribution grid components to better understand the systemic impacts of BGI under various control scenarios.

1.2 Background and State-of-Art

1.2.1 Building-grid interaction

Electric power systems were historically engineered around centralized, dispatchable generation supplying largely passive demand, meaning that, the power grid was run mostly by large power plants that could change output and naturally kept the system stable (Godoy et al. 2024). Power flowed one way from plants to customers (Figure 1) and intraday prices were relatively stable, with less volatility than is common today. (Knaut and Paschmann 2019). As a result, end users had neither incentives nor tools to shift when they used electricity (Eid et al. 2016). On the other hand, buildings used simple local controls aimed at comfort, without mechanisms to coordinate with grid needs or constraints. Under those conditions, a “set it and forget it” approach was sufficient.

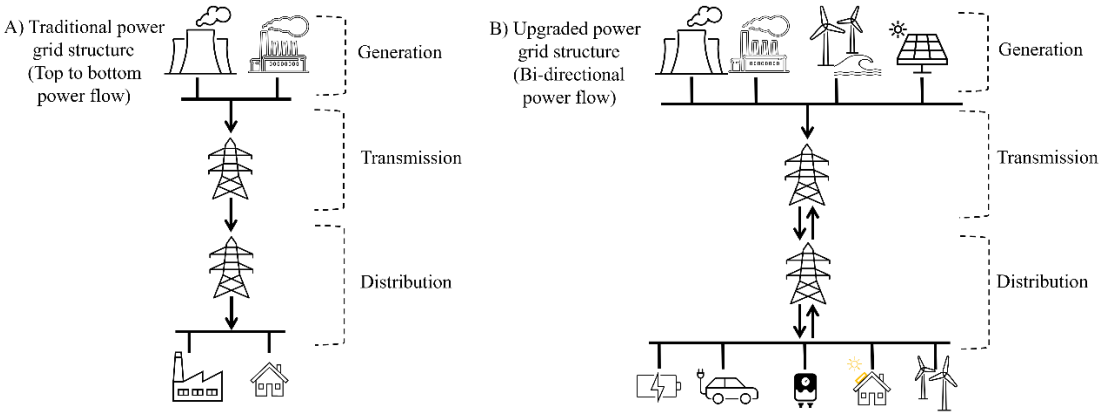

Figure 1: One way and bi-directional power flow.

In recent years, the rapid integration of wind and solar has shifted the generation mix from predominantly dispatchable plants to weather-dependent, more variable output (Toloo et al. 2022). In parallel with changes on the supply side, the role of buildings has shifted from passive consumers to active prosumers that can produce, store, and time-shift energy (Brown et al. 2020). This transformation is driven by building-side electrification, replacing fossil fuel space and water heating with heat pumps and integrating controllable EV charging coordinated by modern building energy management systems (BEMS). In parallel, the spread of embedded distributed energy resources (DER), especially rooftop PV and electrical energy storage (EES) using smart inverters that enable buildings to prioritize self-consumption of on-site generation (Kelepouris et al. 2025).

These developments raise critical concerns. Electrified end uses, e.g., heat pumps, electric domestic hot water (DHW), and EV charging, introduce large, often coincident loads that cluster in a specific time of the day such as late afternoon and evening on cold days. Absent coordination, they increase peak demand, reduce load diversity, cause voltage deviations, accelerate transformer loss-of-life, and bring forward costly feeder and substation upgrades (Xie et al. 2024). In parallel, the spread of rooftop PV and EES has turned formerly one-way distribution networks into two-way systems, for instance many buildings export surplus at the same time (Ruf 2018). If feed-in is unmanaged, e.g., no export limits, limited local storage or load shifting, this creates congestion windows at low and medium voltage levels where distribution system operator (DSO) visibility and control have historically been limited (Konrad et al. 2025).

In light of these challenges, buildings must take part in active coordination with the grid. Practically, this is achieved through grid-interactive operation, in which BEMS uses forecasts (weather, grid signals as prices, DSO constraints) to schedule flexible assets such as heat pumps, DHW production, EV charging, EES, thermal storage, and PV inverters, so that net import/export is shaped without violating thermal comfort, indoor air quality, or equipment limits. In contrast to traditional and static, "set it and forget it" operation, grid-interactive assets continuously sense**,** decide, and act in a closed loop with the power system. To maintain system balance and reliability under these conditions, utility providers must increasingly rely on flexible consumers, e.g. including buildings, to support grid services (Le Dréau et al. 2023).

Such bidirectional coordination requires a well-defined control mechanism that translates grid needs into signals and actions (Li et al. 2022). In practice, this mechanism consists of (i) standardized interfaces for prices, CO_2eq. intensity, and DSO constraints; (ii) forecasting modules for weather, loads, PV, and occupancy; (iii) decision logic from control algorithms that co-optimizes building energy system under thermal comfort, indoor air quality, and equipment constraints; (iv) real-time actuation and monitoring and (v) measurement and verification of the taken action. The mechanism must operate across timescales (seconds to minutes for frequency support; minutes to hours for congestion windows and price signals), and resolve conflicts between economic, CO_2eq. intensity, and DSO objectives via clear priorities.

Without a BGI program, the extra stress from electrification has to be absorbed almost entirely by the network itself. To keep up, the system operators would need to expand the grid to larger service connections (Koralewicz et al. 2023), thicker cables, bigger or additional transformers and substations, and more voltage-control equipment (Federal Ministry for Economic Affairs and Climate-BMWK 28-Sep-25). They may also limit or curtail PV feed-in when many roofs export at the same time (Bucher et al. 2024). During cold-weather evenings, unmanaged heat-pump and EVs loads would raise peaks, transformers aging faster, and increase the risk of overloads and outages (Moghadami et al. 2022). At the system level, higher peaks mean paying for more capacity and reserves, often with higher marginal emissions in those hours. These upgrades are expensive, slow, and planning-intensive (studies, permits, civil works) (Saša Butorac May/2025), so costs rise for everyone (Ma 2025) and there is a real risk of over or underbuilding if conditions change later.

Given this, a well-designed mechanism delivers bidirectional value. For buildings, it enables bill savings through peak reduction and load shifting (Yang et al. 2024), potential revenues from demand response or flexibility services and lower operational CO_2 emission (Yang and Jradi 2025) while maintaining thermal comfort and indoor air quality. For the grid, it secures energy delivery by reducing coincident peaks (Chen et al. 2021), voltage rise, and transformer loading (Haque et al. 2017), increases DER hosting capacity, limits curtailment (Aalami et al. 2010), and provides dependable flexibility for congestion management (Fotouhi Ghazvini et al. 2019) and voltage/frequency support (Ranjan et al. 2021), thereby deferring costly reinforcements.

However, the power grid system has different problems at different layers. Power networks are organized into two complementary layers: the transmission system and the distribution system (Meng et al. 2023). The transmission system moves large quantities of electricity across regions and sets system-wide operating conditions such as wholesale prices, reserve activation, and frequency control. The distribution system delivers electricity to end users and integrates DER. Buildings connect to the distribution layer at low voltage or medium voltage level, yet their operation is increasingly shaped by signals originating at the transmission layer.

1.2.2 National power grid

In Germany, the transmission system (generally between 220kV and 60 kV, however including 380 kV extra high voltage level as treated part of the transmission grid) transports power over long distances and maintains system frequency and short-term balance, while ensuring long-term adequacy (SMARD 2025) (Figure 2). TSOs operate real-time balancing and reserve products and enable wholesale markets (such as day-ahead, intraday). Because variable wind and PV output can change quickly and grid bottlenecks often arise on north/south corridors (Ritter et al. 2025). Therefore, TSOs increasingly rely on flexibility to avoid curtailment and contain costs (Heilmann et al. 2020). Signals that reach buildings indirectly from this layer include wholesale prices and ancillary-service activations.

The distribution system (low voltage ≥230 V; medium voltage ~6–60 kV) delivers electricity to end users (Federal Ministry for Economic Affairs and Climate-BMWK 30-Sep-25) and connects most DER (such as PV, EES, EVs, heat pumps). DSOs face

local, time-specific constraints, i.e., transformer thermal limits, feeder congestion, and voltage quality, which are caused by electrification and clustered PV feed-in. Here, flexibility services from buildings (i.e., load shifting, peak shaving) enable DSOs to keep operations within limits, defer grid reinforcement, and integrate more renewables.

Therefore, flexibility is needed at both layers but for different reasons:
– TSO level: system frequency and balancing, reducing redispatch and curtailment, integrating variable renewables at least cost.

– DSO level: managing location-specific constraints in real time, coordinating many small assets, and maintaining voltage limits.

This dissertation focuses on flexibility at the DSO level. Specifically, it examines how buildings and DER (PV, batteries, EV charging, heat pumps) can provide location and time-specific flexibility to manage transformer thermal limits and congestion within low voltage networks.

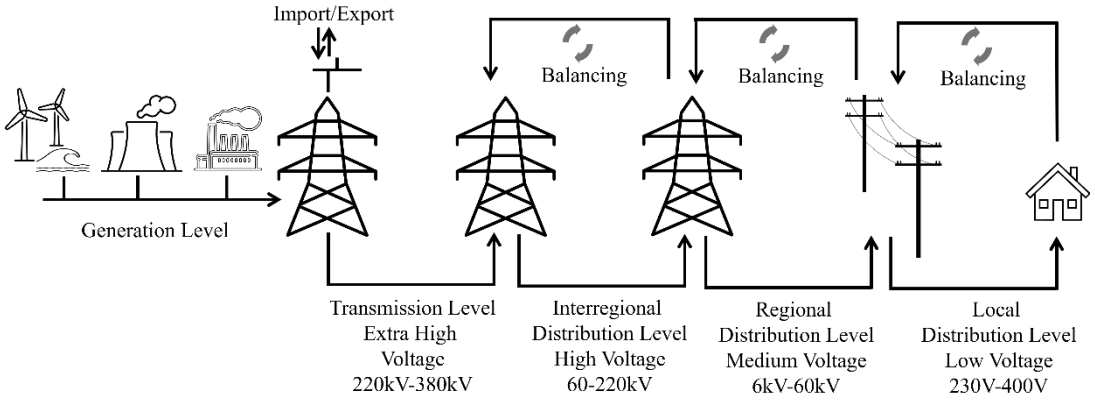

Figure 2: Power network layers in Germany.

1.2.3 Power grid signal

Buildings located at low voltage (mostly residential) or medium voltage (some campuses/industries) and these buildings are increasingly equipped with DER which can affect local grid constraints such as transformer capacity and voltage limits. In order for buildings to participate meaningfully in grid operations, their energy systems must be capable of adjusting operations in response to external control signals. Over the past decade, a wide variety of signal types have been proposed in research and pilot implementations, including:

- **Economic signals**, such as time-of-use tariffs, day-ahead spot market prices, and real-time pricing (Paulat et al. 2019), which encourage cost-efficient load shifting (Schreiber et al. 2015).
- **Environmental signals**, such as grid CO_2 intensity or renewable generation forecasts, which guide energy use toward periods of lower emissions (Huang et al. 2025).
- **Grid condition signals**, including voltage and frequency deviation, transformer thermal load, or local congestion indicators, which reflect operational stress within the distribution network (Maheepala et al. 2025).
- **User-centric or contextual signals**, including occupancy schedules and comfort preferences, typically used within the building's local control layer (Norouziasas et al. 2025).

These control signals are the operational enablers of flexibility, guiding when and how buildings shift or curtail demand. From a system perspective, they offer a scalable and decentralized means of demand-side coordination. From the building perspective, they provide input for optimized operation while maintaining technical and comfort constraints. However, as described in the section National power grid, the signal alignment is not guaranteed. Midday prices can be inexpensive at the wholesale level even while low/medium voltage networks experience reverse power flows and voltage rise from coincident rooftop-PV export; conversely, evening hours may be expensive just as specific transformers impose congestion windows. A second mismatch arises between price and CO_2 intensity (Gabrek and Seifermann 2025): prices can be low on windy nights (often low CO_2), but they may also be low for market dynamics despite a carbon-intensive marginal unit; conversely, when supply is tight, prices can jump to elevated levels even with moderate marginal CO_2. However, the application of these signals poses several challenges:

First, single-signal strategies, which dominate current practice, are often insufficient. For example, price signals may not align with periods of low carbon intensity, especially in markets where fossil-based generators continue to influence marginal prices (Fleschutz et al. 2021). Likewise, responding to CO_2 signals alone may result in higher energy costs or grid stress if demand is concentrated at similar times. As such,

relying on one-dimensional signals may result in suboptimal or even counterproductive behavior from the perspective of broader energy system goals.

Second, when multiple buildings respond to identical signals simultaneously, the resulting synchronized demand shifts can lead to rebound peaks and increased loading of distribution infrastructure (Dewangan et al. 2022). In particular, low-voltage transformers, which serve as bottlenecks in residential and mixed-use grids, are vulnerable to overload and thermal aging under such conditions (Hussain et al. 2023).

Third, current BGI control schemes tend to operate based on fixed or static signal hierarchies. A building may respond exclusively to cost signals, regardless of whether environmental objectives would require different action. Such an action prevents adaptive responses to dynamic grid conditions, especially during congestion, transformer stress events, or unexpected price-emissions decoupling.

Fourth, most BGI simulation studies are conducted on idealized building models or homogeneous clusters, which do not reflect the real-world diversity of building types, climate zones, HVAC systems, and user behaviors. As a result, many findings are difficult to generalize or apply in mixed building communities or urban districts.

In response to these challenges, this dissertation places a strong emphasis on the use of control signals in BGI. It specifically investigates:

- **Economic signals** based on day-ahead price data to guide cost-optimized operation;
- **Environmental signals** using average CO_2eq. intensity from national grid mix data to align energy use with cleaner periods;
- **Grid condition signals**, represented by transformer critical status, modeled according to IEC 60076-7 standards (IEC 60076-7:2005 2005).

The transformer critical status signal is derived from a pre-existing, validated transformer thermal model, developed by an external researcher and applied in this study with permission (Lopes et al. 2018). While this model was not developed as part of this thesis, it has been integrated into analysis to assess how building operation strategies can avoid localized grid constraints such as overheating or accelerated transformer aging.

Moreover, the thesis introduces and compares multi-signal approaches:

- **Joint signals**, which merge economic and environmental inputs to seek trade-offs between cost and emissions.
- **Sequential signals**, which prioritize grid-interactive objectives dynamically, for instance, prioritizing grid operation functionality when a transformer stress condition is triggered and returning to cost or emission-based control otherwise.

Through these explorations, the dissertation aims to advance a more context-aware and system-integrated framework for building-grid interaction, one that reflects the real complexities of signal design, infrastructure constraints, and multi-objective optimization.

1.3 Modelling Effort

This dissertation follows a simulation-based research methodology designed to evaluate the interaction between building energy systems and power grid signals under a range of operational scenarios. The approach combines detailed dynamic building modeling, control algorithm design, BGI signal analysis, and performance evaluation using grid-oriented indicators. Analyzing BGI is inherently a two-level problem: (I) Modeling, which involves accurately representing HVAC systems, PV generation, and thermal comfort in zones; and (ii) Control, which concerns determining the load demand schedule of HVAC systems and the charge/discharge cycles of electrical energy storage (EES) based on the BGI signal. While traditional BEPS tools provide detailed thermal and system modeling capabilities, they are often limited in their capacity to handle complex or adaptive control logic. In contrast, BGI scenarios require real-time interaction with dynamic signals and flexible control structures that may evolve based on external conditions.

To execute such a BGI simulation, the results from the mentioned two main layers must be calculated simultaneously, such that the output of the previous time step becomes the input for the calculation of the next time step. However, under current market conditions, no single software tool is available that can both model building energy systems and design their control based on a given BGI signal (such as a congestion event). Therefore, addressing both levels simultaneously requires a co-simulation environment, as neither the modeling aspects nor the control strategies can

be adequately captured. In this dissertation, a co-simulation environment linking a Building Energy Performance Simulation (BEPS) engine with a numerical tool namely IDA-ICE (IDA-ICE 2023) and MATLAB (MATLAB 2015) is used (Figure 3).

This configuration supports:

- The bidirectional exchange of variables (e.g., indoor temperatures, energy system loads) at high resolution,
- The generation and application of external signals such as electricity prices, CO_2 intensity, and transformer stress indicators,
- The implementation of both building control strategies;

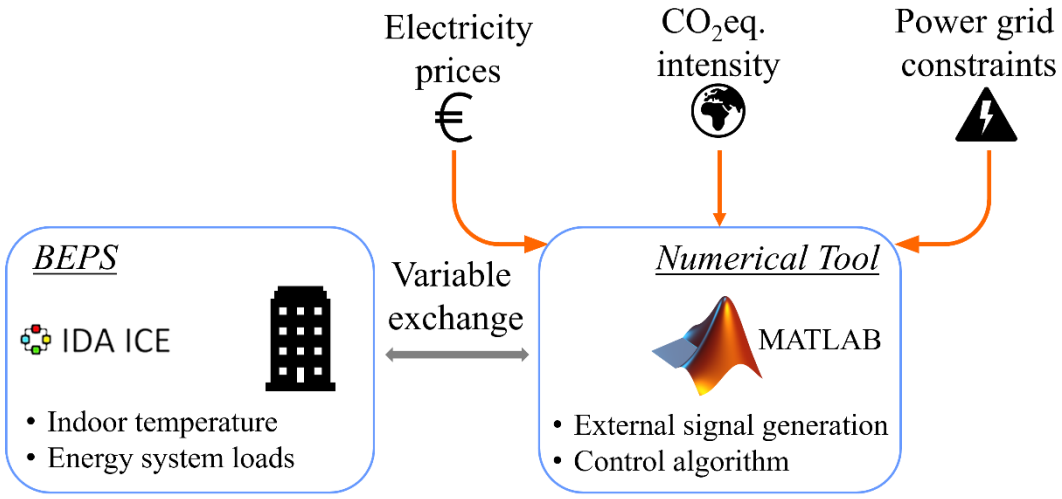

Figure 3: Co-simulation environment linking IDA-ICE and MATLAB for bidirectional data exchange, signal generation, and control implementation.

The co-simulation platform enables the integration of multiple objectives into control decision-making, allowing for real-time responsiveness to joint or sequential signals. A control layer is therefore a prerequisite for any analysis and deployment of BGI. Without such control, the simple operational applications either miss opportunities (e.g., failing to preheat/precool during low energy prices period or before expensive energy prices) or violate constraints (e.g., exceeding a transformer limit or causing rebound discomfort). Control algorithms turn signals into profitable actions with trade-offs among cost, CO_2 emission, indoor thermal comfort, and equipment function. In simple deployments, Rule-Based Control (RBC) encodes if–then pattern such as if price < X charge thermal storage/EES or raise indoor temperature setpoint by ΔT. However, this control type remains straightforward to have a holistic approach. For instance, the setpoint increment of indoor temperature is fixed regardless of how low

electricity price is, however, rather than increasing the indoor temperature by ΔT, maybe ΔT+0.5 could achieve better economical result for that specific day. Addition to its limited capacity for market-oriented operation planning, RBC offers no capability for grid-oriented operation, i.e., transformer stress or congestion windows, since it lacks optimization capability aligned with the required exact BGI signal value. On the other side, there are control algorithms that have optimization features formulating optimization of heat pumps, EV charging, electrical and thermal storage, and more, treating DSO limits as hard constraints and prioritizing comfort and equipment limits. In this context, Model Predictive Control (MPC) is a commonly used method, however it has limitations. Using MPC directly with white-box building models, turns the controller into a nonconvex, mixed-integer dynamic optimization with thousands of states, discontinuities and computationally heavy. Each model evaluation can take seconds to minutes, while MPC requires hundreds of evaluations per solve and must repeat every step. Co-simulation compounds the problem: MPC and the BEPS must exchange setpoints and measurements at every timestep with potential strict time synchronization or mismatched step sizes. Consequently, exploiting MPC in white-box BGI studies is a very complex task .

To address the limitations of simplified methods such as RBC and the computational burden of MPC, this dissertation proposes a Rule-Based Predictive Control (RBPC) approach that jointly optimizes market- and grid-oriented operation while reducing computational effort.

1.4 Research Questions and Objectives

As outlined in the previous section, the growing need for demand-side flexibility in renewable-rich power systems has positioned buildings as active participants in grid operations. However, several critical challenges persist, particularly related to the design and coordination of control signals for BGI. These challenges include the over-reliance on single-objective control inputs, the lack of consideration for localized grid constraints, and the limited adaptability of control strategies to evolving system conditions.

This dissertation addresses these challenges by investigating how different types of control signals, namely, economic, environmental, and congestion based, can be applied individually or in combination to guide flexible building operation. It also

explores the influence of control architecture (e.g., joint vs. sequential signaling) on the effectiveness of BGI in both individual buildings and building clusters.

The overall aim of this research is to contribute to a more integrated and context-aware understanding of how control signals can be utilized to enable effective and grid-supportive building operation.

The dissertation is guided by the following research questions (RQ), and the specific objectives of this research are as follows (Figure 4):

RQ1. What are the trade-offs when combining economic and environmental signals into a joint penalty signal for building control?

Objective: To develop and analyze multi-objective control signal frameworks, including joint signals that combine electricity price and CO_2 intensity, in order to balance environmental and economic goals in demand response.

RQ2. How can BGI co-optimize grid-oriented operation (compliance with distribution-level constraints) and market-oriented operation (minimizing energy cost) at the single-building level, subject to comfort and equipment constraints?

Objective: To integrate and assess power grid signals in building single and cluster operation, with the aim of identifying potential conflicts between building flexibility actions and local grid infrastructure constraints.

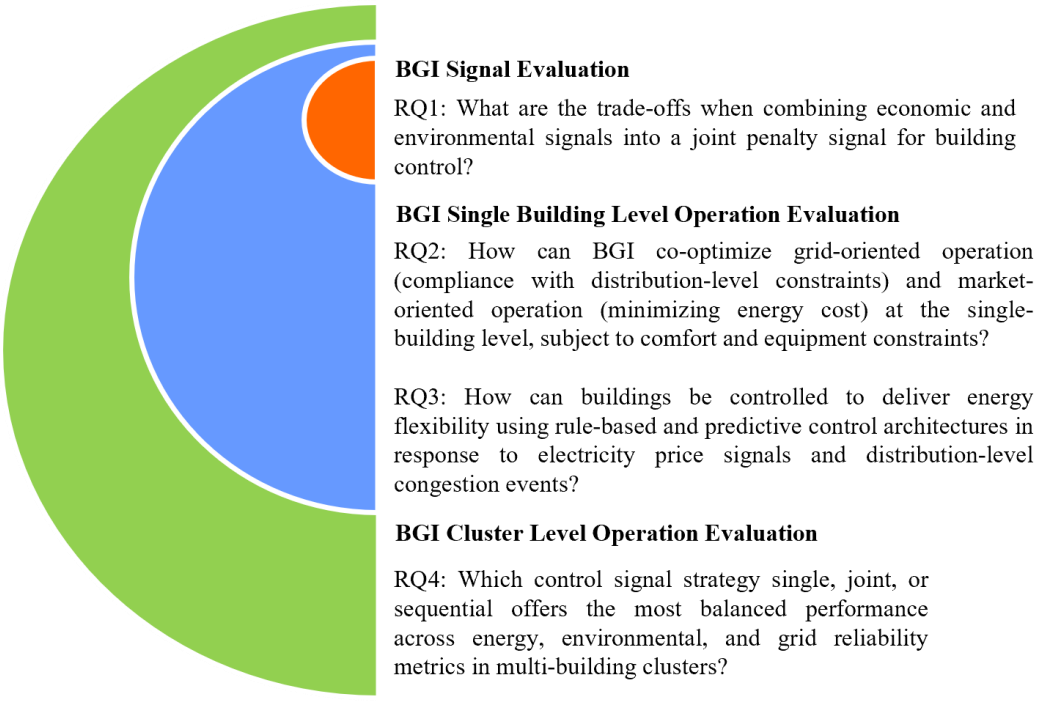

Figure 4: Explored RQ in this dissertation.

RQ3. How can buildings be controlled to deliver energy flexibility using rule-based and predictive control architectures in response to electricity price signals and distribution-level congestion events?

Objective: To compare the performance of single, joint, and sequential signal strategies in different building scenarios and cluster configurations, considering their impact on cost, emissions, and transformer loading.

RQ4. Which control signal strategy single, joint, or sequential offers the most balanced performance across energy, environmental, and grid reliability metrics in multi-building clusters?

Objective: To evaluate the potential of rule-based and predictive control strategies for enabling flexible operation in energy-efficient buildings under dynamic market conditions, using economic signals such as day-ahead electricity prices.

1.5 Organization of the Dissertation

To address these questions, this dissertation follows a cumulative format. The doctoral research is presented through three high-impact, peer-reviewed journal articles that form the core of the thesis (Paper 1, 3 and 4), complemented by supplementary conference papers. Moreover, participation in the International Energy Agency Energy in Buildings and Community - Annex 82 - Energy Flexible Buildings Towards Resilient Low Carbon Energy Systems programme (IEA EBC 30-Sep-25) whose focus aligns directly with BGI significantly strengthened this research. This international platform provided knowledge exchange and led to additional co-authored publications and technical reports.

1.5.1 List of publications

BGI Signal Evaluation

Paper 1: Kırant-Mitić T, Voss K. Development of a Joint Penalty Signal for Building Energy Flexibility in Operation with Power Grids: Analysis and Case Study, Buildings, 2023, https://doi.org/10.3390/buildings13051338.

This paper contributes the signal layer of the BGI by developing a joint penalty signal that combines economic (day-ahead price) and environmental (CO_2eq. intensity) drivers into a single, controllable objective for building operation.

BGI Single Building Level Operation Evaluation

Paper 2: Kırant-Mitić T, Voss K. Enhancing Grid Stability and Economic Operation through Heuristic Control: A Simulation Case Study. Proceedings of BauSim Conference 2024: 10th Conference of IBPSA-Germany and Austria. https://doi.org/10.26868/29761662.2024.19.

This paper provides the baseline for the dissertation by demonstrating, in a simulation case study, how rule-based predictive control can deliver simultaneous grid support and economic benefit using a calibrated building model.

Paper 3: Kırant-Mitić T, Voss K. A Rule-Based Predictive Control Framework for Market and Grid-Oriented Operation in Thermally Activated Buildings, Journal of Building Performance Simulation, 2025, https://doi.org/10.1080/19401493.2025.2565652

This paper introduces a rule-based predictive control (RBPC) method developed in this dissertation. The control architecture is implemented on a building equipped with thermally activated building systems and is designed to optimize market-oriented objectives (energy cost) and grid-oriented objectives (e.g., congestion windows) in a co-simulation environment, subject to comfort and equipment constraints. It operationalizes grid-interactive operation with a horizon scheduler that uses day-ahead prices and distribution-system constraints to plan preheating/precooling and charge thermal storage in the building mass. The controller follows thermal comfort bounds via slab and zone temperature limits.

BGI Cluster Level Operation Evaluation

Paper 4: Kırant-Mitić T, Hall M, Dawes G, Lopes R A. Impact of Building-Grid interaction signals on energy flexibility at cluster Level: Insights from two case studies, Energy and Buildings, 2025, https://doi.org/10.1016/j.enbuild.2025.116235.

This paper advances the dissertation by moving the analysis from single buildings to aggregated, transformer stress aware clusters, and by isolating how different BGI signals shape energy flexibility. Using two energy efficient building clusters (Germany and Switzerland), it compares market-oriented signals (day-ahead price) with environmental signals (marginal CO_2) and grid-oriented constraints (congestion windows), within a co-simulation workflow that links calibrated BEPS models.

Supplementary Papers

Paper 5: Dawes G, Kırant-Mitić T, Jiang Z et al. Energy flexibility at multi-building scales: A review of the dominant factors and their uncertainties, Energy and Buildings, 2025, https://doi.org/10.1016/j.enbuild.2025.116157.

This paper provides a review by synthesizing the dominant drivers of energy flexibility, end uses and electrification (Heat pump/domestic hot water/electrical vehicle), embedded DER (PV/EES/thermal storage), controls, tariffs/signals, occupant behavior, and distribution-level constraints. It develops a categorization of factors and uncertainties (aleatory vs. epistemic) and maps their expected interactions, and aggregation effects.

Paper 6: Le Dréau, J. et al. Developing energy flexibility in clusters of buildings: A critical analysis of barriers from planning to operation, Energy and Buildings, 2023, https://doi.org/10.1016/j.enbuild.2023.113608.

This paper examines BGI at the cluster scale and classifies its full lifecycle from (i) planning, (ii) design to (iii) operation across economic, policy, social, and technical dimensions. My role was contributing to early planning and design stages section.

Paper 7: Forchheim M.H., Kirant-Mitić T., Cano-Tirado D., Zdrallek M., Electrical energy flexibilities' prediction and validation of a real non-residential building through methods of machine learning, IET Conference Proceedings, 2023, https://doi.org/10.1049/icp.2023.0346.

This paper presents data-driven BGI analysis by developing and validating machine-learning models that predict a building's short-term electrical flexibility under realistic disturbances and operational constraints. My role was applying white-box model development and applying rule-based control for BGI analysis that the results were compared to data-driven BGI analysis results.

Paper 8: Cano-Tirado D., Kırant-Mitić T., Forchheim M., Modemann M., Zdrallek M., Kühler D., "Potential Flexible Operation's Assessment of a Non-Residential Building Through a Novel Tool," 2022 IEEE PES Innovative Smart Grid Technologies Conference Europe (ISGT-Europe), Novi Sad, Serbia, 2022, pp. 1-6, https://doi.org/10.1109/ISGT-Europe54678.2022.9960367.

This paper introduces an assessment tool that quantifies the potential for flexible operation in a real non-residential building before a full controller is deployed. The tool treats building load demand data and scenario inputs (i.e., day-ahead prices) to produce flexibility service. My contribution was developing the building load demand formulization to calculate energy consumption.

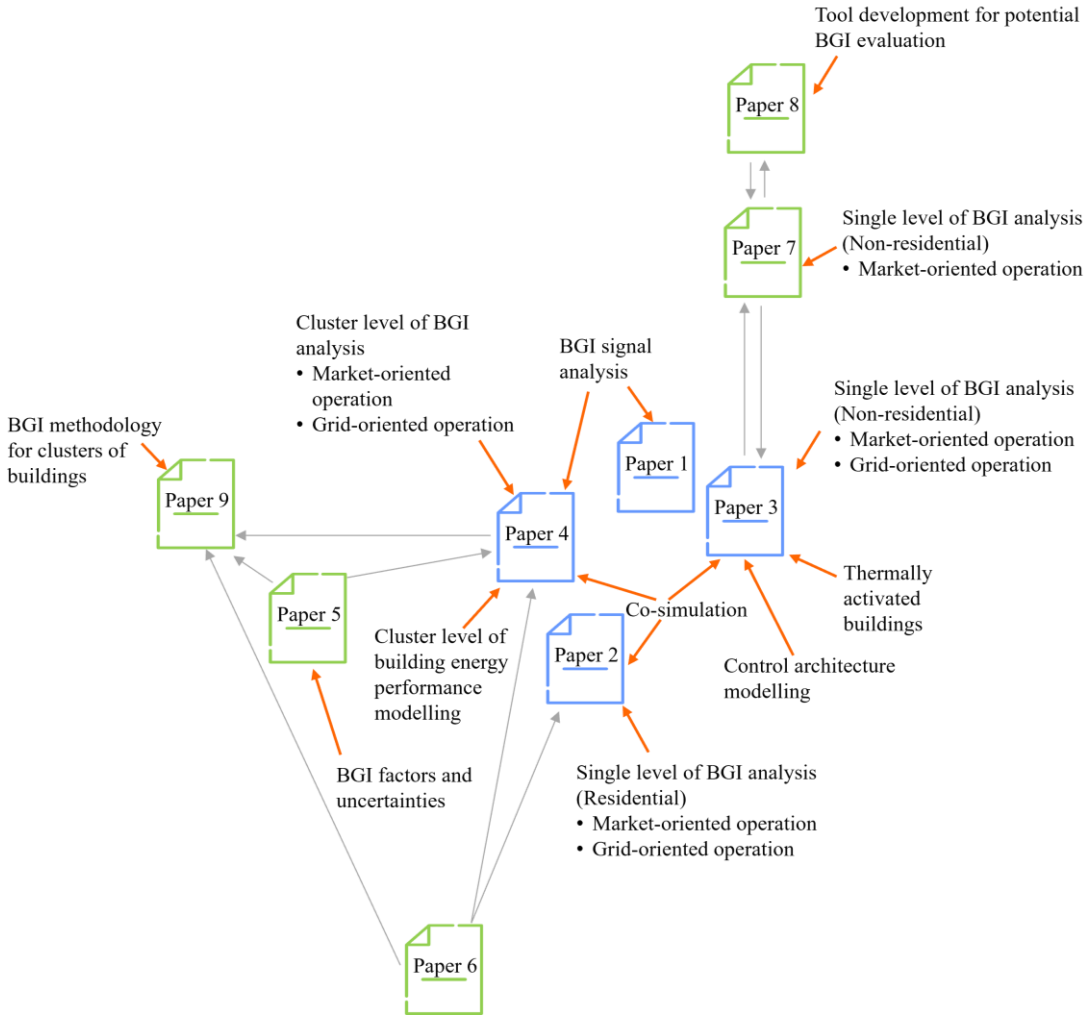

Figure 5: Connection of the papers presented under this dissertation. Blue color icons show the main paper and green color icons reflect the supplementary papers.

Technical Report

Paper 9: Lopes, R. A., Le Dréau, J., Henze, G., Kummert, M., Arteconi, A., Cai, H., Dawes, G., Hall, M., Kazmi, H., Kırant-Mitić, T., Li, R., Madsen, H., Mokhtari, R., O'Neill, Z., Sethuvenkatraman, S., Tohidi, S., Zavřel, V., Willems, S., & White, S. (2025). Methodologies and evaluations of energy flexibility for clusters of buildings: Energy in Buildings and Communities - Technology Collaboration Programme. Technical University of Denmark.

This report consolidates and systematizes evaluation methods for energy flexibility within the IEA EBC framework. While it includes a broader set of studies, I contributed to four: (i) development of BGI at the cluster scale, (ii) a common BGI exercise, (iii) cluster modelling, and (iv) an uncertainty and dominant-factor analysis.

This chapter set out the motivation for the dissertation, stated the research questions and their objectives, and outlined the overall structure. It also listed the associated publications (Figure 5) and clarified each paper's contribution to the research. The next four chapters present the four main papers, one paper per chapter.

REFERENCES

Aalami, H. A.; Moghaddam, M. Parsa; Yousefi, G. R. (2010): Demand response modeling considering Interruptible/Curtailable loads and capacity market programs. In *Applied Energy* 87 (1), pp. 243–250. DOI: 10.1016/j.apenergy.2009.05.041.

Askeland, Magnus; Bjarghov, Sigurd; Rana, Rubi; Morch, Andrei; Taxt, Henning (2025): Smart flexibility in energy communities: Scenario-based analysis of distribution grid implications and economic impacts. In *Smart Energy* 18, p. 100184. DOI: 10.1016/j.segy.2025.100184.

Astapov, Victor; Shabbir, Noman; Rosin, Argo; Kütt, Lauri; Maask, Vahur; Tiismus, Hans (2025): Review of technical solutions addressing voltage and operational challenges in a distribution grid with high penetration of intermittent RES. In *Energy Reports* 14, pp. 1738–1760. DOI: 10.1016/j.egyr.2025.08.019.

Brown, Donal; Hall, Stephen; Davis, Mark E. (2020): What is prosumerism for? Exploring the normative dimensions of decentralised energy transitions. In *Energy Research & Social Science* 66, p. 101475. DOI: 10.1016/j.erss.2020.101475.

Bucher, Ch.; Chen, S.; Adinolfi, G.; Guerrero-Lemus, R.; Ogasawara, Y.; Heilscher, G. et al. (2024): Active Power Management of Photovoltaic Systems – State of the Art and Technical Solutions.

Chen, Lu; Xu, Qingshan; Yang, Yongbiao; Song, Jing (2021): Optimal energy management of smart building for peak shaving considering multi-energy flexibility measures. In *Energy and Buildings* 241, p. 110932. DOI: 10.1016/j.enbuild.2021.110932.

Clauß, John; Stinner, Sebastian; Solli, Christian; Lindberg, Karen Byskov; Madsen, Henrik; Georges, Laurent (2019): Evaluation Method for the Hourly Average CO2eq. Intensity of the Electricity Mix and Its Application to the Demand Response of Residential Heating. In *Energies* 12 (7), p. 1345. DOI: 10.3390/en12071345.

Dewangan, Chaman Lal; Singh, S. N.; Chakrabarti, S.; Singh, Kamini (2022): Peak-to-average ratio incentive scheme to tackle the peak-rebound challenge in TOU pricing. In *Electric Power Systems Research* 210, p. 108048. DOI: 10.1016/j.epsr.2022.108048.

Eid, Cherrelle; Codani, Paul; Perez, Yannick; Reneses, Javier; Hakvoort, Rudi (2016): Managing electric flexibility from Distributed Energy Resources: A review of incentives for market design. In *Renewable and Sustainable Energy Reviews* 64, pp. 237–247. DOI: 10.1016/j.rser.2016.06.008.

European Commission (2019): Communication from the Commission - The European Green Deal. Available online at https://eur-lex.europa.eu/legal-content/EN/TXT/?uri=CELEX:52019DC0640, checked on 24-Aug-25.

European Commission (2021): Fit for 55': delivering the EU's 2030 Climate Target on the way to climate neutrality. Available online at https://eur-lex.europa.eu/legal-content/EN/TXT/?uri=CELEX:52021DC0550, checked on 24-Aug-25.

Federal Ministry for Economic Affairs and Climate-BMWK (28-Sep-25): Grids and infrastructure. BMWI. Available online at https://www.bundeswirtschaftsministerium.de/Redaktion/EN/Artikel/Energy/electricity-grids-of-the-future-01.html, updated on 28-Sep-25, checked on 28-Sep-25.

Federal Ministry for Economic Affairs and Climate-BMWK (30-Sep-25): Grids and infrastructure. BMWI. Available online at https://www.bundeswirtschaftsministerium.de/Redaktion/EN/Artikel/Energy/electricity-grids-of-the-future-01.html, updated on 30-Sep-25, checked on 30-Sep-25.

Fleschutz, Markus; Bohlayer, Markus; Braun, Marco; Henze, Gregor; Murphy, Michael D. (2021): The effect of price-based demand response on carbon emissions in European electricity markets: The importance of adequate carbon prices. In *Applied Energy* 295, p. 117040. DOI: 10.1016/j.apenergy.2021.117040.

Foteinaki, Kyriaki; Li, Rongling; Heller, Alfred; Rode, Carsten (2018): Heating system energy flexibility of low-energy residential buildings. In *Energy and Buildings* 180, pp. 95–108. DOI: 10.1016/j.enbuild.2018.09.030.

Fotouhi Ghazvini, Mohammad Ali; Lipari, Gianluca; Pau, Marco; Ponci, Ferdinanda; Monti, Antonello; Soares, João et al. (2019): Congestion management in active distribution networks through demand response implementation. In *Sustainable Energy, Grids and Networks* 17, p. 100185. DOI: 10.1016/j.segan.2018.100185.

Gabrek, Nadine; Seifermann, Stefan (2025): How the correlation between electricity prices and emission intensity affects the economic and ecological potential of industrial demand-side flexibility measures. In *Journal of Cleaner Production* 518, p. 145863. DOI: 10.1016/j.jclepro.2025.145863.

Godoy, Paulo T. de; Almeida, Adriano B. de; Souza, A. ZambroniC. de; Marujo, Diogo; Souza, Jonas V. (2024): Unified centralized/decentralized voltage and frequency control structure for microgrids. In *Sustainable Energy, Grids and Networks* 38, p. 101366. DOI: 10.1016/j.segan.2024.101366.

Hamdi, Mohamed; El Salmawy, Hafez A.; Ragab, Reda (2024): Incorporating operational constraints into long-term energy planning: The case of the Egyptian power system under high share of renewables. In *Energy* 300, p. 131619. DOI: 10.1016/j.energy.2024.131619.

Haque, A.N.M.M.; Nguyen, P. H.; Bliek, F. W.; Slootweg, J. G. (2017): Demand response for real-time congestion management incorporating dynamic thermal overloading cost. In *Sustainable Energy, Grids and Networks* 10, pp. 65–74. DOI: 10.1016/j.segan.2017.03.002.

Heilmann, Erik; Klempp, Nikolai; Wetzel, Heike (2020): Design of regional flexibility markets for electricity: A product classification framework for and application to German pilot projects. In *Utilities Policy* 67, p. 101133. DOI: 10.1016/j.jup.2020.101133.

Huang, Jiahui; Yuan, Meng; Zou, Zhuo; Sun, Yaojie (2025): Low-carbon economic optimization scheduling in distributed energy systems considering carbon emission responsibility and demand response. In *International Journal of Electrical Power & Energy Systems* 169, p. 110768. DOI: 10.1016/j.ijepes.2025.110768.

Hussain, Sadam; Azim, M. Imran; Lai, Chunyan; Eicker, Ursula (2023): New coordination framework for smart home peer-to-peer trading to reduce impact on

distribution transformer. In *Energy* 284, p. 129297. DOI: 10.1016/j.energy.2023.129297.

IDA-ICE (2023): Equa Simulation AB - IDA indoor climate and energy 4.8 - Simulation Software | EQUA. Available online at https://www.equa.se/en, checked on 15-Aug-23.

IEA EBC (30-Sep-25): Annex 82. Energy Flexible Buildings Towards Resilient Low Carbon Energy Systems. Available online at https://annex82.iea-ebc.org/, updated on 30-Sep-25, checked on 30-Sep-25.

IEC 60076-7:2005 (2005): Power transformers - Part 7: Loading guide for oil-immersed power transformers: International Electrotechnical Commission (29.180), 2005. Available online at https://webstore.iec.ch/en/publication/605, checked on 2024.

International Energy Agency (2024): Empowering Urban Energy Transitions. Paris. Available online at https://www.iea.org/reports/empowering-urban-energy-transitions, checked on 24-Aug-25.

Jensen, Søren Østergaard; Marszal-Pomianowska, Anna; Lollini, Roberto; Pasut, Wilmer; Knotzer, Armin; Engelmann, Peter et al. (2017): IEA EBC Annex 67 Energy Flexible Buildings. In *Energy and Buildings* 155, pp. 25–34. DOI: 10.1016/j.enbuild.2017.08.044.

Kelepouris, Nikolaos S.; Nousdilis, Angelos I.; Bouhouras, Aggelos S.; Christoforidis, Georgios C. (2025): An energy management-based methodology for mutually beneficial interaction between prosumers and distribution system operator. In *Energy Conversion and Management* 346, p. 120433. DOI: 10.1016/j.enconman.2025.120433.

Knaut, Andreas; Paschmann, Martin (2019): Price volatility in commodity markets with restricted participation. In *Energy Economics* 81, pp. 37–51. DOI: 10.1016/j.eneco.2019.03.004.

Konrad, Alexander; Gaugl, Robert; Maier, Christoph; Wogrin, Sonja (2025): Implementing dynamic power feed-in limitations of photovoltaic systems in distribution grids for generation expansion planning. In *Energy Strategy Reviews* 59, p. 101760. DOI: 10.1016/j.esr.2025.101760.

Koralewicz, Marlon; Jakob, Joshua; Bauhaus, Bastian; Zdrallek, Markus (2023): Case study of an integrated expansion planning of coupled large urban electricity, gas and heat grids. In : 2023 International Conference on Future Energy Solutions (FES). 2023 International Conference on Future Energy Solutions (FES). Vaasa, Finland, 12-Jun-23 - 14-Jun-23: IEEE, pp. 1–6.

Le Dréau, Jérôme; Lopes, Rui Amaral; O'Connell, Sarah; Finn, Donal; Hu, Maomao; Queiroz, Humberto et al. (2023): Developing energy flexibility in clusters of buildings: A critical analysis of barriers from planning to operation. In *Energy and Buildings* 300, p. 113608. DOI: 10.1016/j.enbuild.2023.113608.

Li, Rongling; Dane, Gamze; Finck, Christian; Zeiler, Wim (2017): Are building users prepared for energy flexible buildings?—A large-scale survey in the Netherlands. In *Applied Energy* 203, pp. 623–634. DOI: 10.1016/j.apenergy.2017.06.067.

Li, Rongling; Satchwell, Andrew J.; Finn, Donal; Christensen, Toke Haunstrup; Kummert, Michaël; Le Dréau, Jérôme et al. (2022): Ten questions concerning energy flexibility in buildings. In *Building and Environment* 223, p. 109461. DOI: 10.1016/j.buildenv.2022.109461.

Liang, Bomiao; Yang, Jiajia; Wen, Fushuan; Wang, Licheng; Dong, Zhao Yang (2025): Fairness considered aggregation mechanism for consumers and prosumers in electricity distribution networks. In *Electric Power Systems Research* 240, p. 111285. DOI: 10.1016/j.epsr.2024.111285.

Lopes, Rui Amaral; Magalhães, Pedro; Gouveia, João Pedro; Aelenei, Daniel; Lima, Celson; Martins, João (2018): A case study on the impact of nearly Zero-Energy Buildings on distribution transformer aging. In *Energy* 157, pp. 669–678. DOI: 10.1016/j.energy.2018.05.148.

Ma, Jessie (2025): Growing the power system: Expansions on transmission and distribution systems for deep electrification. In *iScience* 28 (6), p. 112662. DOI: 10.1016/j.isci.2025.112662.

Maheepala, M.M.A.L.N.; Li, Hangxin; Robert, Dilan; Meegahapola, Lasantha; Wang, Shengwei (2025): Towards energy flexible commercial buildings: Machine learning approaches, implementation aspects, and future research directions. In *Energy and Buildings* 346, p. 116170. DOI: 10.1016/j.enbuild.2025.116170.

Marszal-Pomianowska, Anna Joanna; Knotzer, Armin; Roberta, Pernetti; Jensen, Søren Østergaard; INTEC, A. E.E.; EURAC; DTI (2019): Characterization of energy flexibility in buildings. [Taastrup]: Danish Technological Institute.

MATLAB (2015): (R2015b). Natick, Massachusetts: The MathWorks Inc.

Meng, Yan; Fan, Shuai; Shen, Yu; Xiao, Jucheng; He, Guangyu; Li, Zuyi (2023): Transmission and distribution network-constrained large-scale demand response based on locational customer directrix load for accommodating renewable energy. In *Applied Energy* 350, p. 121681. DOI: 10.1016/j.apenergy.2023.121681.

Moghadami, Arash; Azizian, Davood; Karimi, Amin (2022): Incorporating demand response effect on transformer replacement planning. In *Electric Power Systems Research* 213, p. 108714. DOI: 10.1016/j.epsr.2022.108714.

Norouziasas, Alireza; Esmaeilzadeh, Ahmad; Yin, Hang; Nord, Natasa; Hamdy, Mohamed (2025): An innovative work time flexibility-based energy management system for decarbonizing office buildings. In *Energy and Buildings* 345, p. 116134. DOI: 10.1016/j.enbuild.2025.116134.

Paulat, Frederik; Korotkiewicz, Kamil; Zdrallek, Markus; Liebelt, Andreas (Eds.) (2019): Local flexibility markets as complement of the Smart Grid. International ETG-Congress 2019. ETG Symposium. Berlin, Offenbach: VDE (ETG-Fachberichte, 158). Available online at https://ieeexplore.ieee.org/document/8836024.

Péan, Thibault Q.; Salom, Jaume; Costa-Castelló, Ramon (2019): Review of control strategies for improving the energy flexibility provided by heat pump systems in buildings. In *Journal of Process Control* 74, pp. 35–49. DOI: 10.1016/j.jprocont.2018.03.006.

Press and Information Office of the Federal Government | Bundesregierung (2021): Climate Change Act 2021. Intergenerational contract for the climate. Available

online at https://www.bundesregierung.de/breg-en/service/archive/climate-change-act-2021-1936846, updated on 24-Aug-25, checked on 24-Aug-25.

Ranjan, Sudhanshu; Latif, Abdul; Das, Dulal Chandra; Sinha, Nidul; Hussain, S. SuhailM.; Ustun, Taha Selim; Iqbal, Atif (2021): Simultaneous analysis of frequency and voltage control of the interconnected hybrid power system in presence of FACTS devices and demand response scheme. In *Energy Reports* 7, pp. 7445–7459. DOI: 10.1016/j.egyr.2021.10.100.

Reynders, Glenn; Amaral Lopes, Rui; Marszal-Pomianowska, Anna; Aelenei, Daniel; Martins, João; Saelens, Dirk (2018): Energy flexible buildings: An evaluation of definitions and quantification methodologies applied to thermal storage. In *Energy and Buildings* 166, pp. 372–390. DOI: 10.1016/j.enbuild.2018.02.040.

Ritter, David; Grafmüller, Dominik; Bauknecht, Dierk; Wingenbach, Marion; Dünzen, Kaya (2025): Electricity market design for 100 % renewable energy in Germany – Challenges and solutions. In *Energy Reports* 14, pp. 634–647. DOI: 10.1016/j.egyr.2025.06.006.

Ruf, Holger (2018): Limitations for the feed-in power of residential photovoltaic systems in Germany – An overview of the regulatory framework. In *Solar Energy* 159, pp. 588–600. DOI: 10.1016/j.solener.2017.10.072.

Saša Butorac (May/2025): EU electricity grids. European Parliamentary Research Service (PE 772.854).

Schreiber, Michael; Wainstein, Martin E.; Hochloff, Patrick; Dargaville, Roger (2015): Flexible electricity tariffs: Power and energy price signals designed for a smarter grid. In *Energy* 93, pp. 2568–2581. DOI: 10.1016/j.energy.2015.10.067.

Shahryari, E.; Shayeghi, H.; Mohammadi-ivatloo, B.; Moradzadeh, M. (2018): An improved incentive-based demand response program in day-ahead and intra-day electricity markets. In *Energy* 155, pp. 205–214. DOI: 10.1016/j.energy.2018.04.170.

SMARD (2025): Transmission system operators. Bundesnetzagentur. Available online at https://www.smard.de/page/en/wiki-article/5884/205528/transmission-system-operators, updated on 30-Sep-25, checked on 30-Sep-25.

Toloo, Mehdi; Taghizadeh-Yazdi, Mohammadreza; Mohammadi-Balani, Abdolkarim (2022): Multi-objective centralization-decentralization trade-off analysis for multi-source renewable electricity generation expansion planning: A case study of Iran. In *Computers & Industrial Engineering* 164, p. 107870. DOI: 10.1016/j.cie.2021.107870.

Xie, Peng; Wang, Han; Jia, Youwei (2024): Decentralized energy management regime for prosumer community Microgrids using flexible tube model predictive control. In *Electric Power Systems Research* 236, p. 110553. DOI: 10.1016/j.epsr.2024.110553.

Yang, Shiyu; Gao, H. Oliver; You, Fengqi (2024): Demand flexibility and cost-saving potentials via smart building energy management: Opportunities in residential space heating across the US. In *Advances in Applied Energy* 14, p. 100171. DOI: 10.1016/j.adapen.2024.100171.

Yang, Yujie; Jradi, Muhyiddine (2025): Multi-objective optimization for balancing CO2 emissions and thermal comfort in a central heat pump system: A case study of a

Danish office building. In *Energy and Buildings* 342, p. 115870. DOI: 10.1016/j.enbuild.2025.115870.

2. PAPER 1

Development of a Joint Penalty Signal for Building Energy Flexibility in Operation with Power Grids: Analysis and Case Study

buildings

MDPI

Article

Development of a Joint Penalty Signal for Building Energy Flexibility in Operation with Power Grids: Analysis and Case Study

Tuğçin Kırant Mitić and Karsten Voss *

School of Architecture and Civil Engineering, University of Wuppertal, Pauluskirchstrasse 7, D-42285 Wuppertal, Germany; kirantmitic@uni-wuppertal.de
* Correspondence: kvoss@uni-wuppertal.de

Abstract: Electricity generation from renewable energy reduces greenhouse gas emissions and, in the long term, the cost of electricity in power grids. However, there is currently no strong positive correlation between greenhouse gas intensity and electricity spot prices in Germany, despite increasing renewable energy penetration. Therefore, energy flexibility programs that rely on demand response may not be fully effective in reducing carbon emissions unless the energy market aligns consistently with carbon emission factors. To address this issue, we propose a model for joint signals consisting of power grid climate gas intensity and price signals that can achieve both environmental and economic benefits for building energy flexibility applications. Next, to assess the maximum possible flexibility hours from the grid side, we explore penalty signal threshold limits with daily and biweekly aggregation. Using a case study, we analyze energy flexibility with joint signals to explore their effect on greenhouse gas emissions and building operation cost. Our results suggest that joint signals can be more effective than a single type of signal in promoting energy flexibility.

Keywords: building energy flexibility; building–grid interaction; dynamic climate gas intensity; joint penalty signal; demand response

check for updates

Citation: Kırant Mitić, T.; Voss, K. Development of a Joint Penalty Signal for Building Energy Flexibility in Operation with Power Grids: Analysis and Case Study. *Buildings* **2023**, *13*, 1338. https://doi.org/10.3390/buildings13051338

Academic Editor: Antonio Caggiano

Received: 30 March 2023
Revised: 8 May 2023
Accepted: 10 May 2023
Published: 20 May 2023

Copyright: © 2023 by the authors. Licensee MDPI, Basel, Switzerland. This article is an open access article distributed under the terms and conditions of the Creative Commons Attribution (CC BY) license (https://creativecommons.org/licenses/by/4.0/).

1. Introduction

The European Commission addresses the climate crisis and intends to decrease the current greenhouse gas (GHG) emissions by at least 55% by 2030 compared to 1990 levels [1]. Looking further ahead, the Commission aims to achieve a further reduction of 55% in 2050 compared to 2030 [2]. Germany, which has high GHG emissions per capita compared to other EU countries and the global average, aims to reduce GHG emissions by 80–95% by 2050 compared to 1990 levels [3]. The country's target for 2040 is a minimum reduction of 88%, with the goal of achieving GHG neutrality by 2045 [4]. On this path, Germany defines limits for the annual climate gas emissions by sectors and an annual control mechanism. To achieve the climate action goals, dissemination of renewable energy systems and energy efficiency investments are positive measures, hence heating systems based on renewable energy sources will be funded. The integration of renewable energy systems (RES) into the power supply is critical on the path to these targets. RES have intermittent form, coming from the variations in solar radiation and wind strength, which can result in variable electricity generation and fluctuating energy supply [5,6]. These changes over time within the power grid create stability issues [7].

National (Transmission) grids are responsible for transmitting electricity over long distances from large power plants to various regions of a country [8]. On the other hand, local (distribution) power grids distribute electricity from the national grid to homes and businesses in a specific area. The national and local power grids are different in design, function, and operational requirements due to the differences in the scale of their operation and the distances they cover [9]. As a result, electricity prices can vary between these

grids due to factors such as generation costs, transmission costs, distribution costs [10,11], and stability issues. Moreover, electricity prices are influenced by the generation mix of electricity sources, which can vary between national and local power grids. Nevertheless, due to the cost reduction of RES technologies and the increasing cost of electricity generation by nonrenewable sources, RES is expected to contribute more significantly to the power grid globally [12].

Increasing electricity production from RES exposes energy providers to challenges in balancing supply and demand efficiently and economically [5]. To ensure efficient allocation of renewable and conventional energy, markets that allow for the trading of new information are crucial [13]. Increasing the flexibility and responsiveness of short-term wholesale markets to accommodate the growing share of renewable energy is suggested by the European Commission [14]. This proposes empowering consumers to participate in electricity markets by providing them with smart meters and dynamic retail tariffs that reflect changing wholesale prices, enabling them to make informed decisions about energy consumption [15]. To address this issue, energy flexibility in buildings as part of demand response management can be used to optimize the load in the power grid [5] based on various external factors such as power grid demand, energy price signal and $CO_{2eq.}$ intensity.

Exploiting the potential of demand response has become an area of growing interest [16]. Demand response involves actions on the demand side by reacting to conditions in the power grid, providing an opportunity to reduce operating costs and GHG emissions [17]. However, the impact of demand–response programs on CO_2 emissions is often inaccurately assessed using dynamic power grid intensity [18]. The dynamic power grid intensity ($CO_{2eq.}$ intensity) refers to the amount of CO_2 emissions released in the generation of one unit of electricity per hour. The marginal emissions factor based on specific generators' CO_2 intensity provides a more accurate estimate of actual reductions rather than grid-average electricity [19]. The merit order dilemma, which refers to the preference for cheaper, more carbon-intensive technologies in the electricity generation process due to their low marginal costs, is often ignored [20]. Since accurately calculating marginal emissions at a given time is complex, identifying marginal generators and isolating their emissions can be challenging [21]. As a result, load shifting through demand–response programs cannot fully exploit the potential for carbon reduction unless the merit order of the energy market is correlated with carbon emission factors [20]. However, due to the mentioned complications, the $CO_{2eq.}$ intensity signal based on average electricity emission factors are used conventionally in the present applications. In other words, the electricity spot price from the energy market and the commonly used $CO_{2eq.}$ intensity value are not always positively correlated, which raises concerns about the optimizing method for both economic and environmental benefits in energy flexibility applications. Although energy storage can facilitate decarbonisation by boosting renewable energy integration in the long run, its effectiveness in reducing GHG emissions in the short term hinges on factors such as the storage technology used and its operational management [22].

The purpose of this paper is to develop a joint signal of price and $CO_{2eq.}$ intensity and use it as a penalty signal for energy flexibility applications in buildings that achieves both environmental and economic savings. Modelling such a signal is a critical issue in building–grid studies to avoid one type of prominent saving since these signals are not always positively correlated. In the literature, there are various studies discussing the price and $CO_{2eq.}$ intensity as a penalty signal to exploit the energy flexibility but, not much attention has been given to the joint influence of these signals and existing research with this focus is limited. One study [23] investigated the joint impact of both price and CO_2 signals in demand–response programmes using Markov–chain load models. Another study [24] conducted a tradeoff analysis between CO_2 emissions and electricity cost achieving both economic and environmental benefits by utilizing various schedules. [25] examined the combined impact of price and CO_2 emissions in demand response programmes and formulated an optimal control model to reduce energy cost and carbon emissions for five

households in South Africa by mixed integer nonlinear programming. Similarly, [26] used mixed integer linear programming for an optimisation model to jointly minimize electricity costs and CO_2 emissions through an optimisation model for home energy management, achieving lower total cost, CO_2 emissions cost, and peak demand shaving. [27] used a mixed integer linear programming model with the ε-constraint method and Pareto curves to examine coordinated scheduling, which resulted in reduced cost and CO_2 emissions. A pilot study to evaluate the influence of real-time price visualisation on electricity consumption, electricity costs, and CO_2 emissions was performed [28]. Since there was a negative correlation between electricity price and $CO_{2eq.}$ intensity in the Swedish electricity market in the period studied, the load shifting results showed a reduction in electricity costs while CO_2 emissions raised.

In this context, this paper introduces two joint penalty signals—concurrence penalty signal and combined penalty signal—and analyses their effectiveness when applied with threshold levels that determine the start of energy flexibility. To achieve this goal, the paper addresses the following research questions:

1. What are the main drivers of the $CO_{2eq.}$ intensity in the German power grid?

The power grid $CO_{2eq.}$ intensity development is discussed in relation to the electricity spot price and energy flow.

2. How does the observation interval affect the definition of penalty signal thresholds?

The paper analyses the upper and lower thresholds for CO_{2eq} intensity and electricity spot price and evaluates the flexibility operation under different observation intervals, such as daily and biweekly, for the heating season. Daily and biweekly observation times refer to the time intervals at which the penalty signals are monitored and used to determine the energy flexibility thresholds.

3. What is the impact of joint penalty signals?

The penalty-unaware status of a case building is compared to different penalty-aware cases using four penalty signals, $CO_{2eq.}$ intensity, electricity spot price (before tax), and two joint signals (concurrence and combined). Their effect on building performance metrics is discussed.

After this introduction (Section 1), this paper is structured as follows: Section 2 shows the calculation methodology of power grid $CO_{2eq.}$ intensity, the threshold calculation of penalty signals and the methods to form the concurrence and combined penalty signals based on $CO_{2eq.}$ intensity and price signals. Section 3 presents the factors influencing the power grid $CO_{2eq.}$ intensity and its relationship with price signal. Additionally, the impact of the different observation intervals on the definition of the penalty signal thresholds is presented. In Section 4, the calculated thresholds are applied in a case study with the described penalty signals, and the result of the simulation results are illustrated. Section 5 discusses the implications of these findings and the analysis. Section 6 concludes the study.

2. Methodology

2.1. Dynamic $CO_{2eq.}$ Intensity Calculation

The dynamic CO_{2eq}. intensity calculation data was collected from ENTSO-e [29], which provides free access to electricity production data and the energy flow information between countries with a time step of 15 or 60 min. The CO_2 emission factors for electricity production technologies are accessible from various resources. In Germany, the grid electricity is generated by 17 different technologies as shown in Table 1.

The production data and the energy flow between countries were obtained for the years 2017–2021, with the interconnected countries for energy flow varying by year. Table 2 presents the yearly average CO_2 emission coefficients of the connected countries. These data were only used as input for the emission calculation resulting from energy trade.

Table 1. Climate gas emissions of various electricity generation technologies in Germany. Climate gases are expressed in CO_2 equivalents (Data source: [30].)

Electricity Production Technology	CO_2 Coefficient ($gCO_{2eq.}$/kWh)
Biomass	70
Fossil brown coal/lignite	1054
Fossil coal-derived gas	433
Fossil gas	433
Fossil hard coal	873
Fossil oil	841
Geothermal	183
Hydro pumped storage-aggregated	14
Hydro run-of-river and poundage	3
Hydro water reservoir	14
Solar	67
Waste	342
Wind offshore	6
Wind onshore	10
Nuclear	68
Other	45
Other renewable	45

Table 2. The $CO_{2eq.}$ intensity of interconnected countries between 2017 and 2021 [31–35].

Country	$CO_{2eq.}$ Intensity ($gCO_{2eq.}$/kWh)				
	2017	2018	2019	2020	2021
Austria	103	100	92	82	82
Belgium	-	-	174	161	140
Czech Republic	472	465	433	437	403
Denmark	179	193	123	109	155
France	69	58	56	51	58
Germany	413	404	344	311	349
Luxembourg	64	65	73	59	55
Netherlands	460	440	392	328	325
Norway	-	-	-	32	27
Poland	778	784	719	710	736
Sweden	10	11	10	9	10
Switzerland	35	35	35	35	35

The $CO_{2eq.}$ intensity in the power grid was influenced by five main factors, including the CO_2 emission coefficient of production technologies (Table 1), the share of technologies in use (from ENTSO-e platform with 60 min data resolution), the CO_2 emission coefficient of imported electricity based on countries (Table 2), and the amount of exported and imported electricity (ENTSO-e). Total CO_2 emissions coming from the production technologies were calculated using the electricity production amount and CO_2 emission coefficients from Table 1 by Equation (1). The average CO_2 emission coefficient of the import countries was used with the amount of imported electricity to calculate the total CO_2 emissions coming from the imported electricity in Equation (2). Total CO_2 emissions coming from the production technologies were reduced by considering the exported electricity to neighbouring countries. In Equation (3), the share of exported electricity in the total electricity production was found and the reduction amount was calculated in Equation (4). The next step focused on the total load in the power grid, presenting the approximate amount of electricity to be consumed by the users. The existing load in the power grid included the produced electricity and the electricity exchange coming from energy transaction Equation (5). Finally,

the grid $CO_{2eq.}$ intensity (Equation (7)) was found by the ratio of total CO_2 emissions in the power grid (Equation (6)) to total load in the power grid.

$$PT_{CO_2\ emission} = \sum_{i=1}^{I}\sum_{h=1}^{H} PT_{i,h} \times CO_{2,_i} \quad (1)$$

$$Import_{CO_2\ emission} = \sum_{j=1}^{J}\sum_{h=1}^{H} IE_{j,h} \times CO_{2eq,_j} \quad (2)$$

$$EE_{\text{Ratio}} = \frac{\sum_{k=1}^{K}\sum_{h=1}^{H} EE_{k,h}}{\sum_{i=1}^{I}\sum_{h=1}^{H} PT_{i,h}} \quad (3)$$

$$Export_{CO_2\ emission} = PT_{CO_2\ emission} \times EE_{\text{Ratio}} \quad (4)$$

$$Load_{Grid} = \sum_{i=1}^{I}\sum_{h=1}^{H} PT_{i,h} + \sum_{j=1}^{J}\sum_{h=1}^{H} IE_{j,h} - \sum_{j=1}^{J}\sum_{h=1}^{H} EE_{i,h} \quad (5)$$

$$Grid_{CO_2\ emission} = PT_{CO_2\ emission} + Import_{CO_2\ emission} - Export_{CO_2\ emission} \quad (6)$$

$$Grid_{CO_2\ intesity=} \frac{Grid_{CO_2\ emission}}{Load_{Grid}} \quad (7)$$

2.2. Threshold Calculation

Thresholds, which represent the boundary points for applying energy flexibility, were dynamically determined based on the observation time and the penalty signal, which in this study are $CO_{2eq.}$ intensity and electricity spot price. In some studies, the observation time is chosen to be "daily" [36,37] or "biweekly" [38]. These observation periods are time intervals at which the penalty signals are monitored and used to determine the energy flexibility thresholds. This implies that 8760 data points per year are taken and aggregated into daily and biweekly intervals.

In the meantime, to approximate the optimal solution, different studies have discussed penalty signal thresholds, which represent the level at when energy flexibility is requested from a building energy system based on this aggregated data. Ref. [39] introduced two adjustable parameters to define the top and bottom threshold for grid interaction signals. In [40], various upper and lower thresholds were used to calculate the number of hours for the set-point adjustment. The thresholds were determined with 25th and 75th percentiles in [36].

In this study, the thresholds as responding to penalty signals were defined by the upper 25% quartile (downward flexibility) and the lower 25% quartile (upward flexibility) using hourly values. Whisker plots were used to assign the penalty signals into quartile groups by percentile analysis. Subsequently, this research compared the results of both aggregation intervals based on the grid status for heating season.

2.3. Development of Penalty Signals and the Simulation Cases

For every aggregation interval, five cases were simulated by a building energy simulation tool to quantify the total CO_2 emissions of the building energy supply, cost, and load profile according to the specified penalty signals. (Table 3).

In the first case (Case Emission), the $CO_{2eq.}$ intensity was exploited as a penalty signal. In the second case (Case Price), price signal was applied. In the third case (Case Concurrence), if the $CO_{2eq.}$ intensity and price signal reflected the same behaviour at the same moment, such as either upward or downward interaction, this synchronised status was used as a signal (Figure 1).

Table 3. The simulation cases based on the penalty signals.

Cases	Penalty Signal
Emission	$CO_{2eq.}$ intensity
Price	Electricity spot price
Concurrence	Simultaneous
Combined	Combined
Reference	Penalty unaware case—Thermostatic valve control

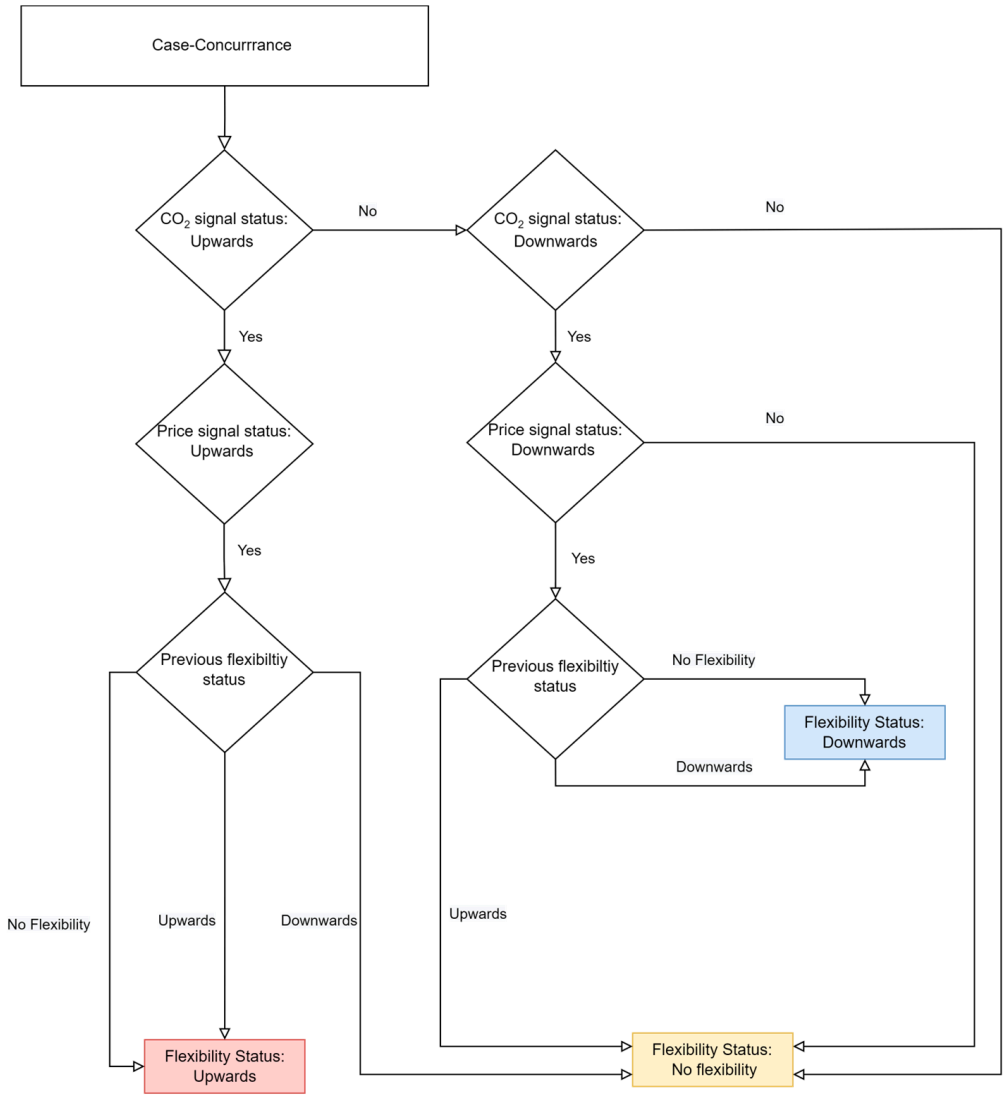

Figure 1. Development of concurrence signal based on the $CO_{2eq.}$ intensity and price signal.

In the fourth case (Case Combined), the combination of $CO_{2eq.}$ intensity and price signals were driven for power grid interaction, such that if one of these signals offered interaction, it was taken into account to develop the combined status. The strategy to form this status was as follows: (1) If both signals offered the same type of power grid interaction state (upwards (+1), downwards (−1), or no interaction (0)), this state was set as the combined signal. (2) If these signals were not harmonised (one is upwards and other is downwards), the previous signal was checked and (2a) the same state as the previous combined signal was chosen; conversely, (2b) if the previous signal was 0 (no interaction), no interaction was continued. (3) If a shift from upwards to downwards or vice versa based on the signals was estimated, it was ignored, and the combined signal was considered as no interaction (Figure 2). Additionally, for (1), the previous signal was checked with the

same purpose. This ensured a smooth transition between the statuses and avoided the sharp changes in the indoor thermal comfort and HVAC operation. Finally, the fifth case (Case Reference) presented the penalty signal-unaware status of the case building.

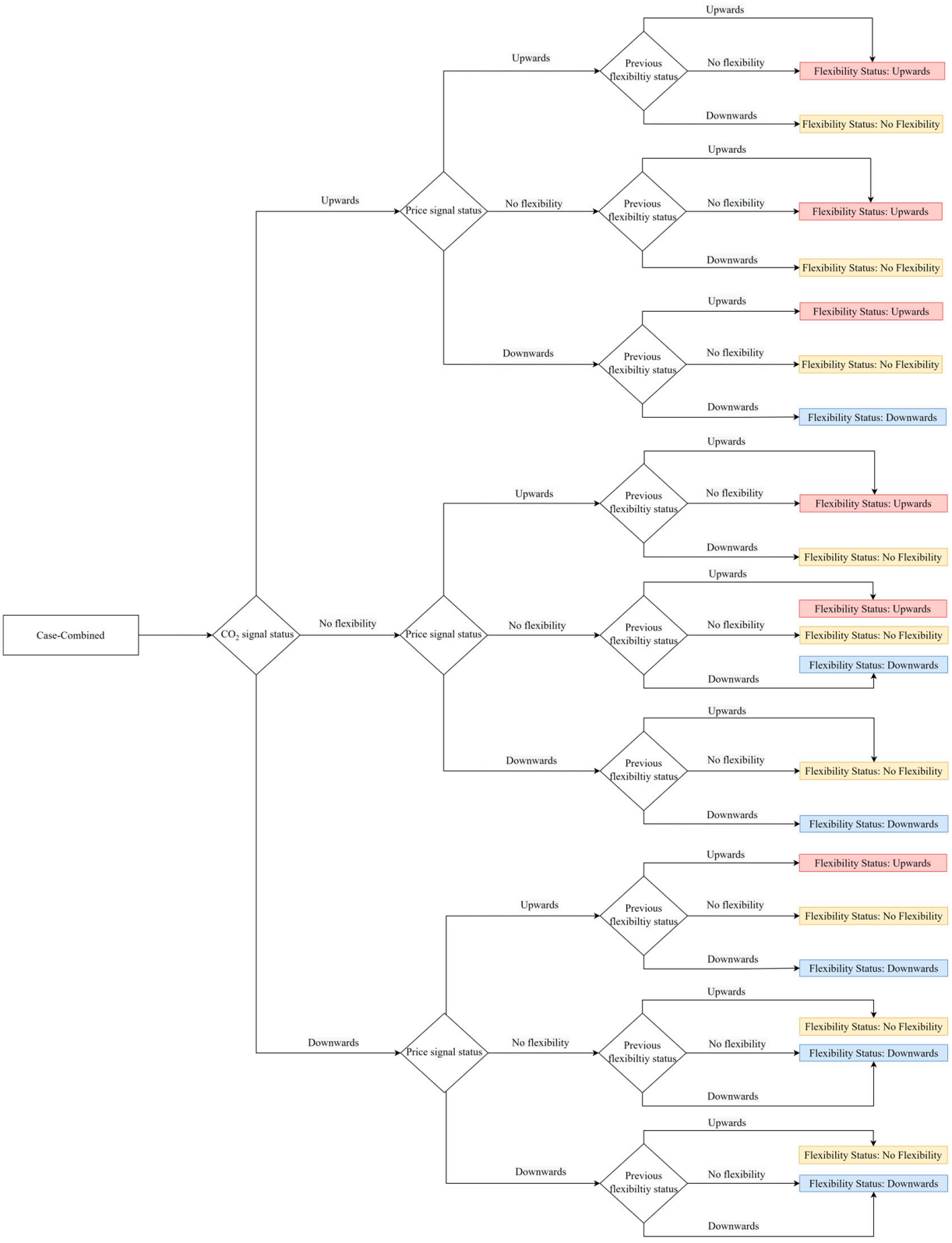

Figure 2. Development of combined signal based on the CO_{2eq}. intensity and price signal.

3. Results

3.1. Dynamic $CO_{2eq.}$ Intensity

Figure 3 presents the share of electricity production technologies between 2017 and 2021. In 2017, the largest contribution was from RES. Although the share of RES decreased in the following years, a growing trend can be observed from 2018 to 2020. Wind energy is the leading technology among RES in Germany, and its overall percentage has been increasing every year. The decreasing trend in production ratio from fossil technologies has reversed, resulting in an increase in 2021. Consequently, electricity generation from RES decreased to nearly 50% in 2021, which was attributed to unfavourable weather conditions [41]. In other words, the current generation in 2021 is approximately 50% dependent on fossil fuel-based power plants.

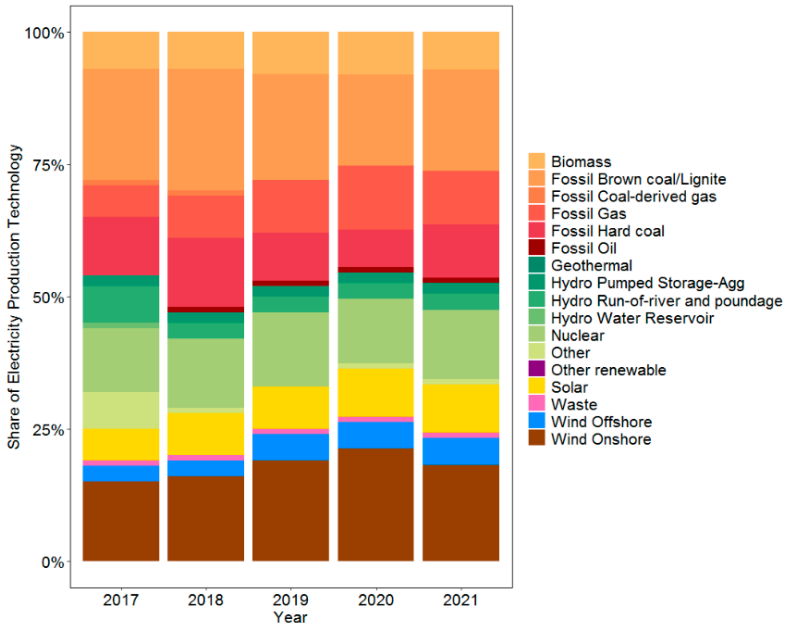

Figure 3. The share of electricity generation technologies in Germany between 2017 and 2021 (Data source: [29]).

Figure 4 presents the grid $CO_{2eq.}$ intensity and electricity spot price for the given years. The yearly average $CO_{2eq.}$ intensity between 2017 and 2021 is calculated as 413, 404, 344, 311, and 439 $gCO_{2eq.}$/kWh, respectively.

The share of electricity production from RES is higher in 2020 compared to other years, leading to lower $CO_{2eq.}$ intensity. Conversely, the highest intensity is observed in 2021 due to a higher share of fossil-based production. The intensity value varies significantly over the year, with the average intensity being approximately 500 $gCO_{2eq.}$/kWh during wintertime and around 300 $gCO_{2eq.}$/kWh in the summer of 2021. The annual average values from Table 2 are reflected in Figure 4 dynamically based on hourly resolution for Germany.

The correlation between the $CO_{2eq.}$ intensity and the electricity spot price is explored for the period between 2017 and 2021, and is illustrated in Figure 5. The results show an upward trend in the correlation factor over this period. As the share of RES in electricity generation increases, a stronger relationship is observed between cheaper generation and CO_2 emission-free generation, particularly between 2017 and 2020. Therefore, the behaviour of $CO_{2eq.}$ intensity as a penalty signal on the energy flexibility reflects the behaviour of the price signal, especially in 2020, when the highest correlation is observed. However, a drastic change occurs in 2021, attributed to the rise of fossil-based production and the increase in electricity spot price by approximately three times compared to 2020 [41]. Further analysis of the relation between $CO_{2eq.}$ intensity and the load in the power grid reveals no significant correlation, thus it is not presented in this study.

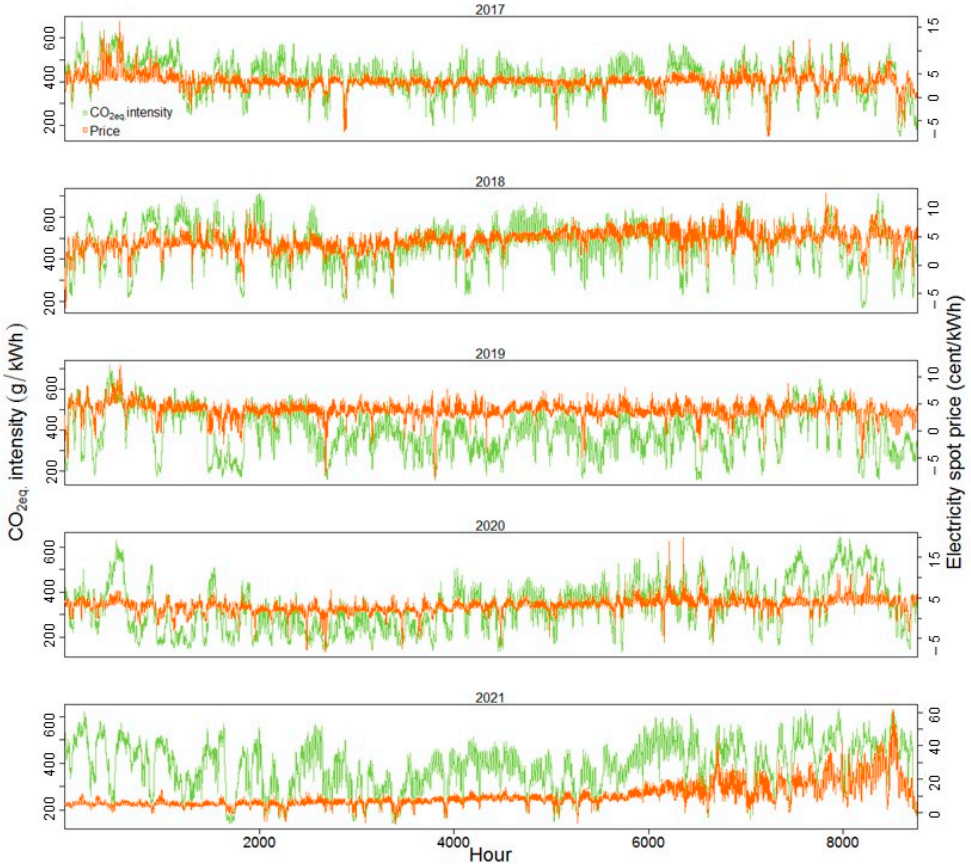

Figure 4. Hourly $CO_{2eq.}$ intensity and electricity spot price between 2017 and 2021 (Data source for electricity spot price: [29]).

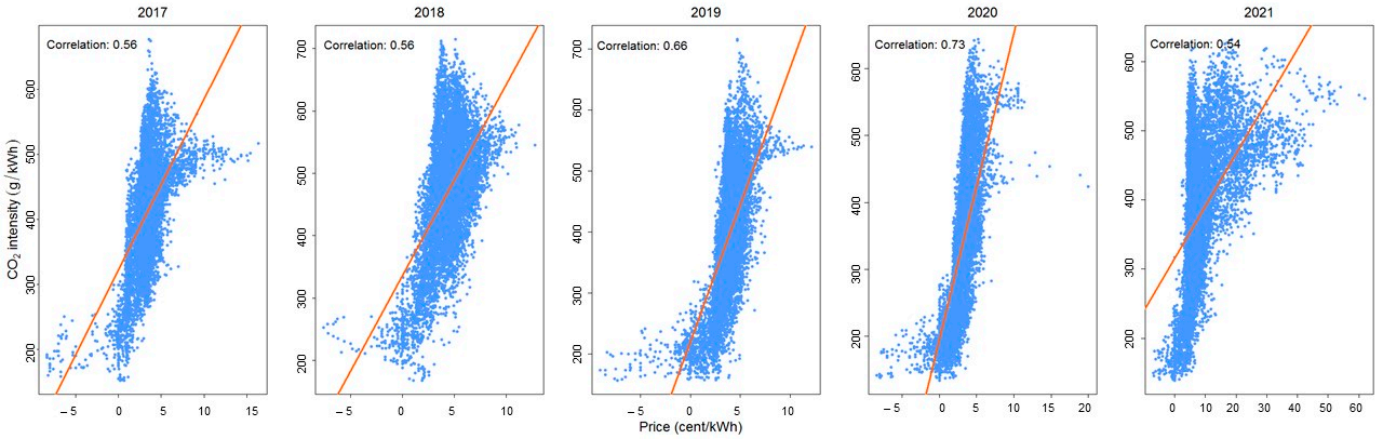

Figure 5. Correlation of hourly $CO_{2eq.}$ intensity and electricity spot price (Data source for electricity spot price: [29]).

As described in Section 2.1, the $CO_{2eq.}$ intensity calculation considers the CO_2 emission from the imported energy, hence, in Figure 6, the $CO_{2eq.}$ intensity profile during import period is examined. One of the highest energy flows to Germany is from the Czech Republic. Along with the import, the $CO_{2eq.}$ intensity in the German power grid rises.

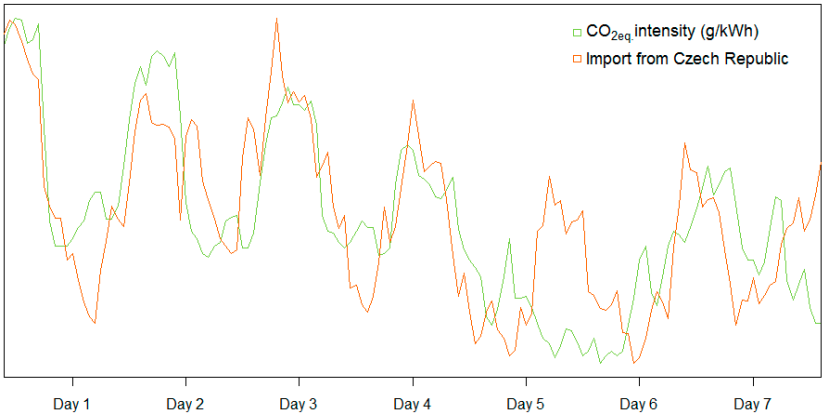

Figure 6. Correlation of hourly $CO_{2eq.}$ intensity and imports with interconnected countries.

3.2. Penalty Signals Threshold

Figure 7 presents the penalty signal thresholds for $CO_{2eq.}$ intensity and electricity spot price for daily aggregation in 2021. The price thresholds vary for each daily aggregation and fluctuate over the course of the year. This raises concerns about the choice of a threshold for a particular day, e.g., selecting the threshold for day_n may result in no positive grid interaction on day_{n+1} or a loss of potential flexibility application hours. Similarly, $CO_{2eq.}$ intensity thresholds vary significantly between days, requiring a threshold to be set for each day. Additionally, the daily $CO_{2eq.}$ intensity thresholds exhibit larger differences throughout the year than the electricity spot price thresholds.

Figure 7. Upper and lower threshold of price and $CO_{2eq.}$ signals with daily observation (red lines represent the upper 25th percentile (downward action) and green lines show the lower 25th percentile (upward action)).

Figure 8 shows the results for biweekly aggregation, with a total of 26 intervals over the course of a year. The electricity spot price threshold values are close to each other among observations than those at daily aggregation, although differences are observed

among the seasons. Conversely, $CO_{2eq.}$ intensity threshold exhibits distinct variations during the year.

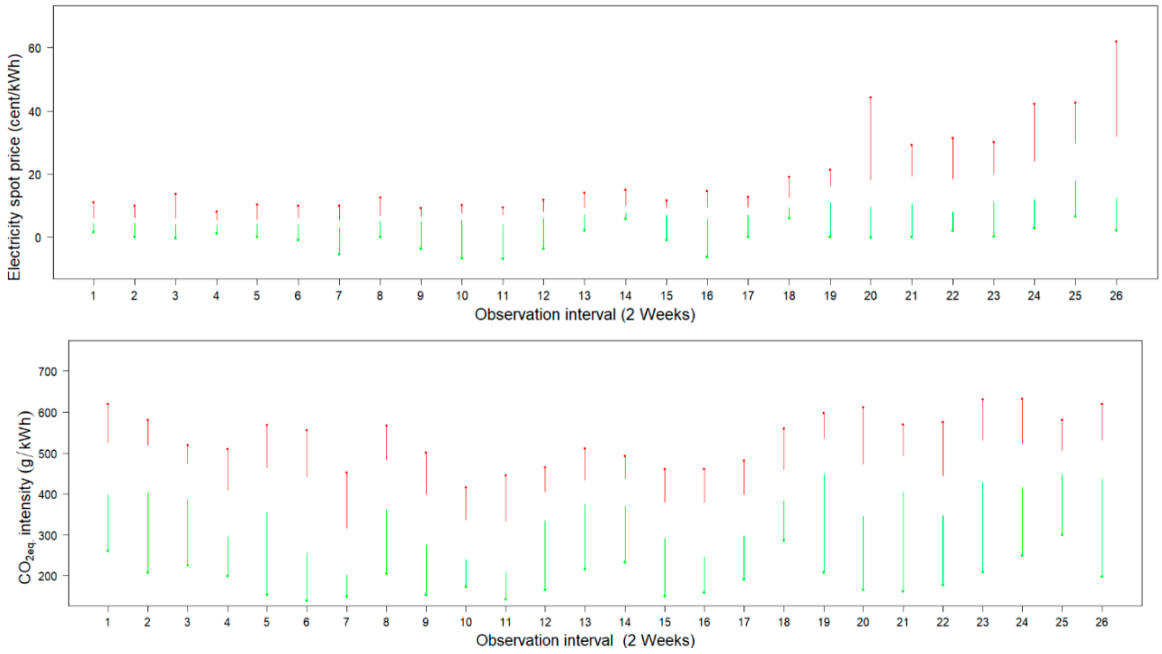

Figure 8. Upper and lower threshold of price and $CO_{2eq.}$ signals with 2 weeks' observation (red lines represent the upper 25th percentile (downward action) and green lines show the lower 25th percentile (upward action)).

The benchmark for threshold limits for $CO_{2eq.}$ intensity signal and price signal between daily and biweekly aggregation was assessed using the upper quartile and lower quartile for the heating season, and the results with the maximum possible flexibility operation hours are presented in Tables 4 and 5. The penalty-aware times are grouped into upward and downward periods. Upward time represents the hours during a day when the penalty signal is less than the lower limit and downward time stands for the periods when the dynamic signal is higher than the upper limit. In Table 4, the differences between aggregations are found as following: In daily aggregation, flexibility application is possible while dynamic $CO_{2eq.}$ intensity signal is higher than 481 $gCO_{2eq.}$/kwh or lower than 447 $gCO_{2eq.}$/kwh for Day 1. The maximum possible flexibility operation hours from the grid side are 6 and 5 h for upward and downward action, respectively. In the case of biweekly aggregation, there can be flexibility when the $CO_{2eq.}$ intensity signal is higher than 531 $gCO_{2eq.}$/kwh and lower than 435 $gCO_{2eq.}$/kwh on the same day, and these are the limits for the next 13 days. On Day 1, the entire day is offered for the upward energy flexibility. By the last day, Day 14, almost no interaction presents based on the calculation results of biweekly aggregation. For this day, 6 h of upward and downward actions are found by the daily aggregation. Comparing the daily and biweekly aggregation cases, a 50% difference is observed for threshold limits, which is the main factor for the variability seen for possible flexibility hours. Besides, rather than having a switch between upward and downward actions, as in the daily aggregation case, the building is intended to have one type of operation in biweekly aggregation.

Table 5 presents the thresholds for the price signal and the maximum possible interaction hours for the heating season. Similar to the $CO_{2eq.}$ intensity signal case, the daily aggregation case shows 5 and 6 h of upward and downward action on Day 1, respectively. However, some days exhibit significant differences by biweekly aggregation by enabling 19 h of upwards flexibility. On Day 14, the flexibility by biweekly aggregation is found as 16 h of downward flexibility. Yet, nearly equal number of flexibility hours (5 and 6 h) for both upwards and downwards are possible with daily aggregation.

Table 4. The thresholds of $CO_{2eq.}$ intensity based on daily and biweekly aggregation—heating season.

	Daily—$CO_{2eq.}$ Intensity Signal				Biweekly—$CO_{2eq.}$ Intensity Signal			
	Upper	Lower	Upward	Downward	Upper	Lower	Upward	Downward
	($gCO_{2eq.}$/kwh)		(Hour)		($gCO_{2eq.}$/kwh)		(Hour)	
Day 1	481	447	6	5			24	0
Day 2	499	465	6	6			7	2
Day 3	527	467	6	5			3	2
Day 4	494	440	6	7			0	9
Day 5	473	333	5	6			7	2
Day 6	553	513	7	5			14	2
Day 7	515	492	6	7	531	435	0	23
Day 8	539	497	6	5			0	10
Day 9	481	408	5	7			0	15
Day 10	508	456	7	5			13	2
Day 11	499	473	6	6			4	6
Day 12	464	426	6	6			0	4
Day 13	488	453	5	5			13	0
Day 14	513	481	6	6			0	2

Table 5. The thresholds of price signal based on daily and biweekly observation intervals in the heating season. (Data source for electricity spot price: [29]).

	Daily—Price Signal				Biweekly—Price Signal			
	Upper	Lower	Upward	Downward	Upper	Lower	Upward	Downward
	(cent/kwh)		(Hour)		(cent/kwh)		(Hour)	
Day 1	23	17	5	6			19	0
Day 2	21	9	6	6			6	0
Day 3	33	19	7	6			12	0
Day 4	29	13	5	6			3	11
Day 5	24	10	6	6			8	1
Day 6	34	20	7	6			9	0
Day 7	28	20	5	6	32	12	2	13
Day 8	28	21	7	6			3	2
Day 9	24	11	5	6			1	0
Day 10	32	19	7	6			12	0
Day 11	37	20	6	6			5	13
Day 12	34	24	6	6			4	14
Day 13	41	26	6	6			0	14
Day 14	39	27	5	6			0	16

4. A Case Study

The threshold limits are applied to the office zones of a university building assumed to be equipped with an air source heat pump with a constant COP of 4. The university building is located in Wuppertal, Germany and has a total net floor area of 860 m^2 (only for the case zone as presented in Figure 9).

The simulation employs measured climate data from the university weather station and power grid $CO_{2eq.}$ intensity and electricity spot price data from 2021 as penalty signals. The U-values of the external walls (0.22 $W/m^2.K$), window (1.3 $W/m^2.K$), roof (0.20 $W/m^2.K$) and floor (0.28 $W/m^2.K$) were defined as well as the occupancy and ventilation profile (Mon.–Fri. 8:00 a.m. to 6:00 p.m.) in the simulation model. The indoor air temperature set points are designated as the flexibility option.

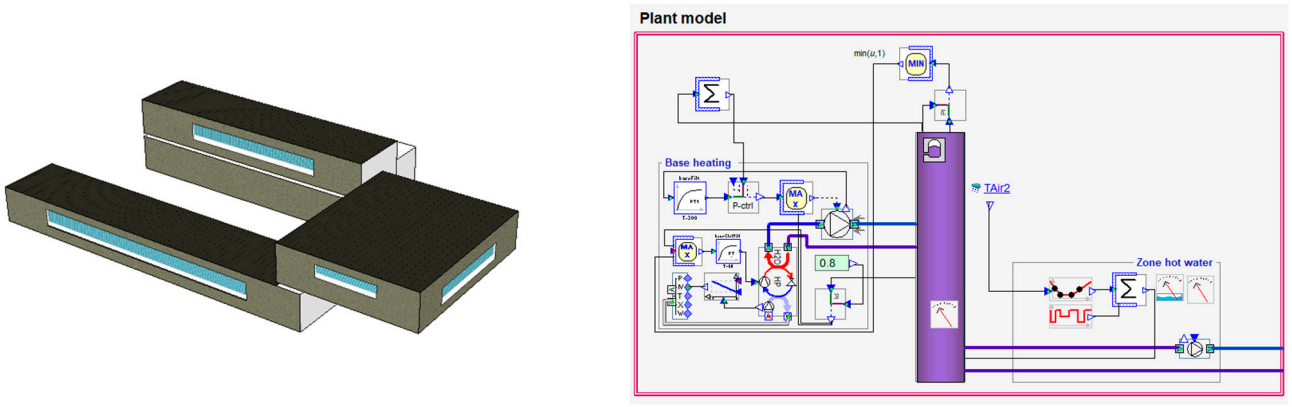

Figure 9. (**A**) The building zone and (**B**) plant model for the simulated case.

The simulation was conducted in hourly time step resolution using the IDA-ICE simulation tool [42], and all five cases are simulated, as outlined in Section 2.3. Daily and biweekly aggregation intervals are used for the simulation for a year, and a rule-based control (RBC) algorithm is employed. The calculated thresholds from Section 3.2 are inserted as input into the control macro, and the indoor temperature levels are adjusted according to the input flexibility status. The indoor temperature set points are 20 °C, 21 °C, and 22 °C for downward flexibility status, no flexibility status and upward flexibility status, respectively, during the heating season. Figure 10 presents the emissions, cost based on the electricity spot market prices (not end user costs), load demand profile, indoor temperature, and the possible flexibility status for Day 1 (from Table 4) as a representative day during the heating season based on daily aggregation, while Figure 11 presents the same metrics for biweekly aggregation intervals (Day 1 from Table 5). The analysis and comparison of the results of the entire 14 days are given in Table 6 with the reference case results. In this research, a simple thermostatic case is simulated for the reference case, and the given costs represent electricity usage coming from the heat pump operation, excluding other zone usage-related costs. It is assumed that end user costs follow the spot market cost profile.

Table 6. The results of the simulated cases for two weeks—heating season.

	Case Emission		**Case Price**		**Case Concurrence**		**Case Combined**		**Case Reference**
	1 Day	**2 W**	**1 Day**	**2 W**	**1 Day**	**2 W**	**1 Day**	**2 W**	**-**
Load demand (kWh)	690	710	715	740	740	730	710	740	875
CO_2 emission ($kgCO_{2eq.}$)	620	615	690	650	685	690	665	640	840
Cost (Euro)	310	280	245	240	300	305	290	250	380

The minimisation objective is achieved for both daily and biweekly aggregation as illustrated in Figures 10 and 11. The results comparison of observation intervals indicates that savings are higher on biweekly aggregation intervals except for Case Concurrence. In Case Emission, CO_2 emissions are reduced by 26% and 27% with daily and biweekly aggregation, respectively. In Case Price, around a 35% decrement of costs is observed. In Case Concurrence, emission is reduced by 18%, while the cost change is reduced by around 27%. In Case Combined, a 21% and 24% downward change on emissions, besides, a 24% and 34% less cost is calculated for daily and biweekly aggregation, respectively.

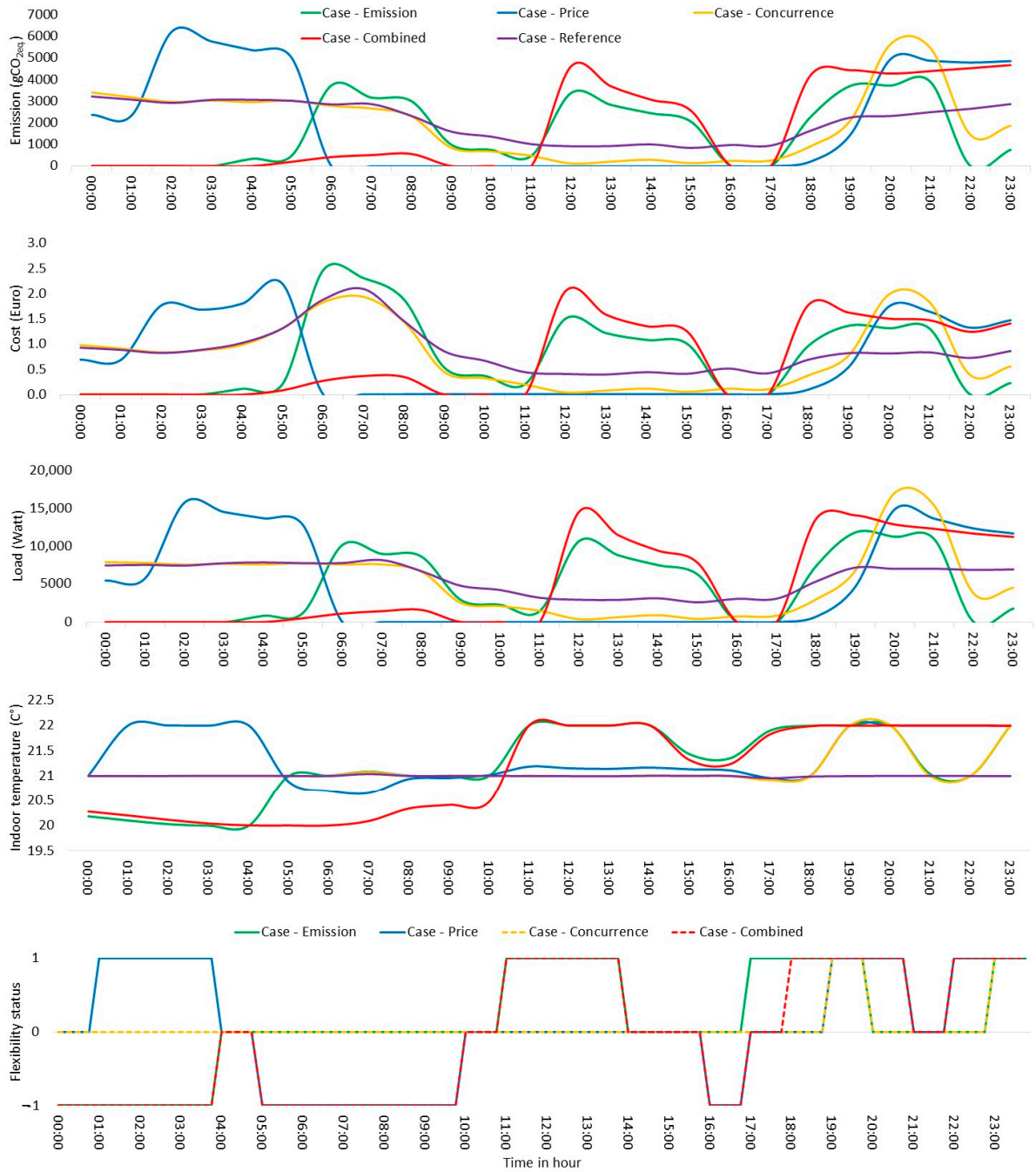

Figure 10. Simulation results of penalty signal with daily aggregation threshold—heating season.

Table 7 provides a comprehensive overview of the yearly savings achieved by the different cases during the heating season. Based on the optimisation parameter (such as emissions for Case Emission and cost for Case Price, etc.), higher savings are calculated in the daily aggregation interval case by a small margin. Case Price results in the highest cost savings, followed by Case Combined. Likewise, the difference in emission savings between Case Emission and Case Combined is negligible. Although the results of Case Concurrence exhibit improvement compared to the reference case, they do not yield any substantial advantage in terms of final metrics. Single penalty signals, such as $CO_{2eq.}$ intensity and price signals, maximise savings for their respective optimisation parameters. However, a holistic optimisation approach can be achieved as demonstrated by Case Combined.

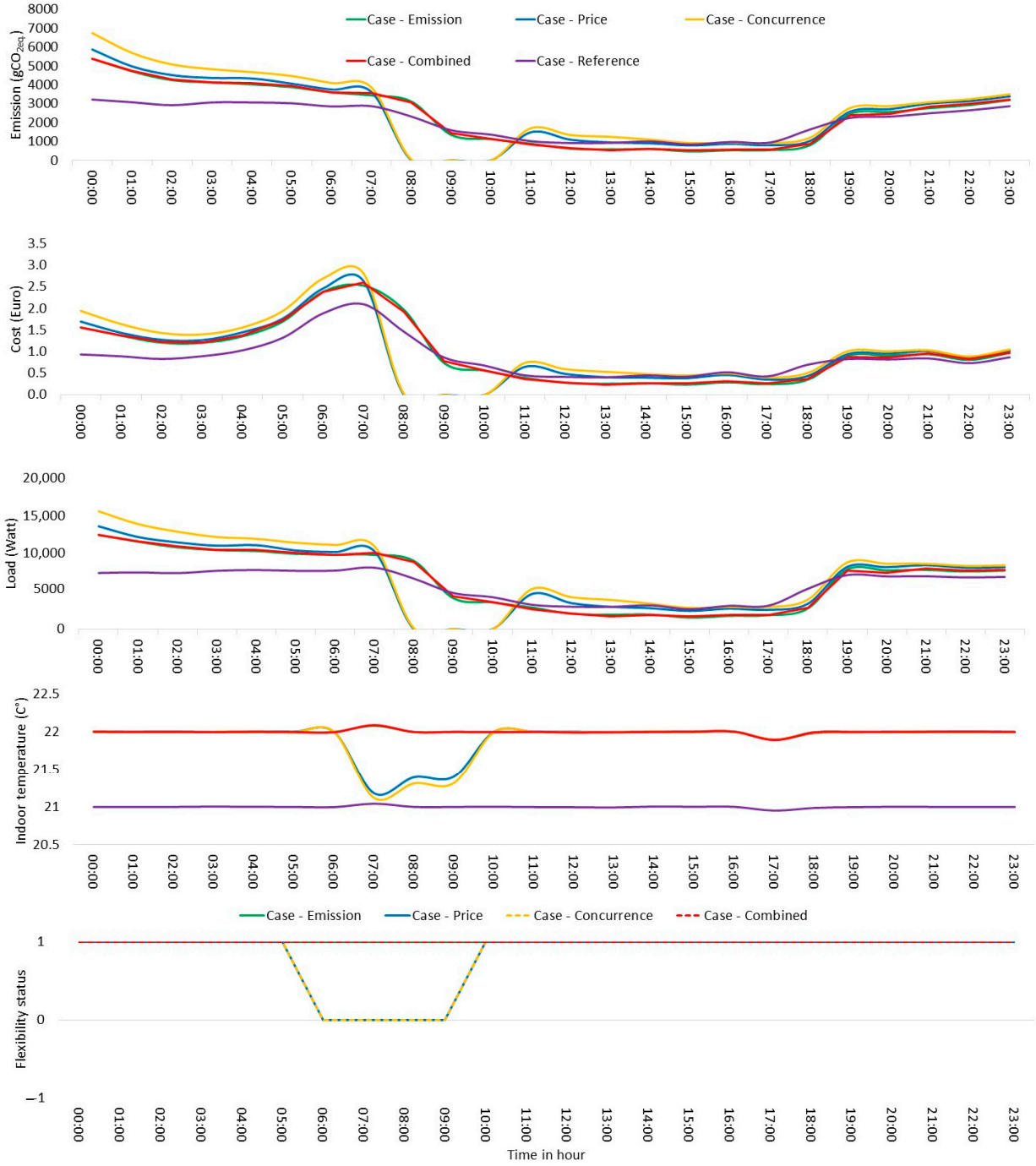

Figure 11. Simulation results of penalty signal with a biweekly observation threshold—heating season.

Table 7. The results of the simulated cases for entire heating season in a year.

	Case Emission		Case Price		Case Concurrence		Case Combined		Case Reference
	1 Day	**2 W**	**1 Day**	**2 W**	**1 Day**	**2 W**	**1 Day**	**2 W**	**-**
Load demand (kWh)	20,800	22,200	20,400	21,350	21,000	22,000	20,800	21,700	23,300
CO_2 emission ($kgCO_{2eq.}$)	5660	5900	6170	6120	6240	6260	5900	5960	8290
Cost (Euro)	1500	1450	1270	1300	1530	1515	1360	1330	2070

5. Discussion

The relation between $CO_{2eq.}$ intensity and share of electricity production type are assessed between 2017 and 2021. Following this, the correlation of $CO_{2eq.}$ intensity and electricity spot price is analysed. The decrement of the positive correlation in the last year is highlighted. Moreover, it is seen that the $CO_{2eq.}$ intensity does not depend on local generation technologies but also on the $CO_{2eq.}$ intensity of the interconnected countries. The expansion of the power grid through neighbouring countries limits the value of environmental returns of the existing local RES. Despite the ongoing action plan and the increasing penetration of RES, the share of fossil-fuel based electricity generation does not demonstrate a steady decrease. For a nonemission power grid, the operated generation technology types of the interconnected countries are critical as the local technologies.

Two joint penalty signals and their modelling approach with the motivation of acquiring both environmental and economic savings are introduced. In addition to a single type of penalty signal implementation, their joint impact was able to address improved performance in terms of environment, cost, and load demand. The results from Case Combined presents an option for building operations which ensure remarkable savings on metrics compared to the other cases. Even though each of these parameters can be enhanced more by individual signals (either $CO_{2eq.}$ or price), the overall average outcome is found to be favourable.

The building energy flexibility analysis by applying different penalty signals considering the upper and lower quartiles was performed with the calculated power grid $CO_{2eq.}$ intensity data and historical electricity spot price (before tax) data from the ENTSO-E platform. Two aggregation intervals, namely daily and biweekly, were used for threshold analysis. These thresholds were incorporated into two joint penalty signals as concurrence and combined signals. The approach to develop these signals was described. An office zone group's energy performance, presenting CO_2 emission, cost, load demand, and indoor temperature, was simulated by a building energy simulation tool using the mentioned penalty signals for five given cases. The main findings are listed below:

- The approach for aggregation intervals of penalty signals plays a critical role for the determination of thresholds and the maximum possible interaction hours from the grid side. In the heating season, marked differences were observed for upper and lower thresholds between aggregation intervals.
- Biweekly aggregation intervals might provide an improved building performance based on the time of the year during heating season. However, no significant difference is found between aggregation intervals in the yearly metrics.
- With Case Combined, the environmental and economic performance closely approximates that of Case Emission and Case Price, respectively, thereby achieving the research's objective of minimizing both metrics to nearly the same level.
- Biweekly aggregation reduces peak demand compared to daily aggregation and results in less indoor temperature fluctuation.

The modelling approach of the combined signal ensures more flexibility hours than a single penalty signal, thereby improving both environmental and economic metrics with the use of a joint signal.

6. Conclusions

A simple-structured methodology is presented to calculate the dynamic climate gas emission intensity in the power grid. The calculation method can be used to generate the CO_2 penalty signal in the energy flexibility studies. The main drivers of the emission signals were investigated, following the impact of production technology types, and their share and electricity import in the local power grid are discussed. The relation of $CO_{2eq.}$ intensity was compared to electricity spot price and energy use as a penalty signal in energy flexibility. The biggest challenge was to collect reliable climate gas emission factors of the production technologies and the average emission intensity of the countries, because available data from various sources are not consistent. However, data of electricity production from

technologies was easily accessible through transparency platform. For precise emission intensity calculation, the dynamic $CO_{2eq.}$ intensity of the interconnected countries should be considered rather than the average value for energy trade. However, this would complicate the calculation process, especially if there is more than one bidding zone in the connected country. As the penetration of RES is increasing in Germany, a bidding zone configuration might be needed to ensure congestion management. In such a situation, the grid emission intensity in Germany should be calculated on a bidding zone basis and the relation with the price signal should be assessed separately. Additionally, the self-consumption of the production plants should be considered for a more accurate outcome.

A joint signal is necessary for the current mixed power grid but may not be required for future grids based solely on renewable energy sources. In such a scenario, the order of merit for electricity generation could change, potentially simplifying the calculation challenges of marginal emission factors. Then, the dynamic power grid intensity and electricity spot prices would be positively correlated and employed in building energy flexibility applications.

Author Contributions: T.K.M.: resources, visualization, methodology, conceptualization, formal analysis, writing—original draft, writing—review & editing. K.V.: supervision, conceptualization, writing—review & editing. All authors have read and agreed to the published version of the manuscript.

Funding: This research was performed in the context of the research project "InFleX" [EFRE programme by the European Union] grant number [EFRE-0801826].

Acknowledgments: Authors would like to acknowledge IEA-EBC Annex 82 members for conducting scientific discussions and providing knowledge exchange.

Conflicts of Interest: The authors declare no conflict of interest.

Nomenclature

Abbreviations

$CO_{2eq.}$	Carbon dioxide equivalent emissions
COP	Coefficient of performance
GHG	Greenhouse gas
HVAC	Heating, ventilation, and air conditioning
RES	Renewable energy system

Indices

$h \in$ H	Index and set of hours (hour)
$i \in$ I	Index and set of electricity production technologies (-)
$j \in$ J	Index and set of import countries (-)
$k \in$ K	Index and set of export countries (-)

Parameter

$CO_{2,i}$	CO_2 equivalent emission coefficient of electricity production technology i
$CO_{2eq,j}$	$CO_{2eq.}$ intensity of country j

Variables

$EE_{k,h}$	Exported electrical energy to interconnected country k at hour h (kWh)
EE_{Ratio}	Ratio of exported electrical energy (-)
$Export_{CO_2\ emission}$	Total CO_2 emission of exported electricity to interconnected country from Germany ($gCO_{2eq.}$)
$Grid_{CO_2\ emission}$	Total CO_2 emission in the power grid ($gCO_{2eq.}$)
$Grid_{CO_2\ intesity}$	Dynamic $CO_{2eq.}$ intensity in the power grid ($gCO_{2eq.}$/kWh)
$Load_{Grid}$	Total load in the power grid (kwh)
$Import_{CO_2\ emission}$	Total CO_2 emission of imported electricity from interconnected country to Germany ($gCO_{2eq.}$)
$IE_{j,h}$	Imported electrical energy from country j at hour (kWh)
$PT_{i,h}$	Generated electricity from production technology i at hour h (kWh)
$PT_{CO_2\ emission}$	Total CO_2 emission from electricity production technology at hour h ($gCO_{2eq.}$)

References

1. Climate Action, 2030 Climate Target Plan. Available online: https://ec.europa.eu/clima/eu-action/european-green-deal/2030-climate-target-plan_en (accessed on 5 August 2022).
2. Communication from The Commission to The European Parliament, The Council, The European Economic and Social Committee and The Committee of the Regions. 2020. Available online: https://eur-lex.europa.eu/legal-content/EN/TXT/?uri=CELEX:52020DC0562 (accessed on 5 August 2022).
3. Federal Ministry for the Environment, Nature Conservation, Building and Nuclear Safety (BMUB). Climate Action Plan 2050: Principles and Goals of the German Government's Climate Policy. 2016. Available online: https://www.bmuv.de/en/publication/climate-action-plan-2050-en (accessed on 3 March 2023).
4. Climate Change Act: Climate Neutrality by 2045. Available online: https://www.bundesregierung.de/breg-de/themen/klimaschutz/climate-change-act-2021-1936846 (accessed on 7 August 2022).
5. Lashmar, N.; Wade, B.; Molyneaux, L.; Ashworth, P. Motivations, barriers, and enablers for demand response programs: A commercial and industrial consumer perspective. *Energy Res. Soc. Sci.* **2022**, *90*, 102667. [CrossRef]
6. Bando, S.; Sasaki, Y.; Asano, H.; Tagami, S. Balancing control method of a microgrid with intermittent renewable energy generators and small battery storage. In Proceedings of the 2008 IEEE Power and Energy Society General Meeting—Conversion and Delivery of Electrical Energy in the 21st Century, Pittsburgh, PA, USA, 20–24 July 2008; pp. 1–6.
7. Makolo, P.; Zamora, R.; Lie, T.-T. The role of inertia for grid flexibility under high penetration of variable renewables—A review of challenges and solutions. *Renew. Sustain. Energy Rev.* **2021**, *147*, 111223. [CrossRef]
8. Eto, J.H.; Alvarado, F.L.; Dagle, J.E.; Hauer, J.F.; Widergren, S.E.; Gross, G.; Overbye, T.; Hirst, E.; Kirby, B.; Meyer, D.; et al. National Transmission Grid Study. 2002. Available online: http://energy.gov/oe/downloads/national-transmission-grid-study-2002 (accessed on 3 March 2023).
9. Executive Office of the President. *Economic Benefits of Increasing Electric Grid Resilience to Weather Outages*; Technical Report; President's Council of Economic Advisers and the U.S. Department of Energy's Office of Electricity Delivery and Energy Reliability: Washington, DC, USA, 2013.
10. Sahari, A. Electricity prices and consumers' long-term technology choices: Evidence from heating investments. *Eur. Econ. Rev.* **2019**, *114*, 19–53. [CrossRef]
11. Li, J.; Ge, S.; Liu, H.; Zhang, S.; Wang, C.; Wang, P. Distribution locational pricing mechanisms for flexible interconnected distribution system with variable renewable energy generation. *Appl. Energy* **2023**, *335*, 120476. [CrossRef]
12. Kroposki, B.; Johnson, B.; Zhang, Y.; Gevorgian, V.; Denholm, P.; Hodge, B.M.; Hannegan, B. Achieving a 100% Renewable Grid: Operating Electric Power Systems with Extremely High Levels of Variable Renewable Energy. *IEEE Power Energy Mag.* **2017**, *15*, 61–73. [CrossRef]
13. Knaut, A. *Essays on the Integration of Renewables in Electricity Markets*; Köln Universität: Köln, Germany, 2017. Available online: https://kups.ub.uni-koeln.de/7729/ (accessed on 25 February 2023).
14. Widuto, A. *Reforming the EU Electricity Market*; European Parliamentary Research Service: Brussels, Belgium, 2023.
15. European Union Agency for the Cooperation of Energy Regulators. Energy Bills Continue to Be Very Different across EU Member States: The new Energy Retail and Consumer Protection Volume. Available online: https://documents.acer.europa.eu/Media/News/Pages/Energy-bills-continue-to-be-very-different-across-EU-Member-States.aspx (accessed on 3 March 2023).
16. Dahl Knudsen, M.; Petersen, S. Demand response potential of model predictive control of space heating based on price and carbon dioxide intensity signals. *Energy Build.* **2016**, *125*, 196–204. [CrossRef]
17. Saberi, K.; Pashaei-Didani, H.; Nourollahi, R.; Zare, K.; Nojavan, S. Optimal performance of CCHP based microgrid considering environmental issue in the presence of real time demand response. *Sustain. Cities Soc.* **2019**, *45*, 596–606. [CrossRef]
18. Hawkes, A.D. Estimating marginal CO2 emissions rates for national electricity systems. *Energy Policy* **2010**, *38*, 5977–5987. [CrossRef]
19. Bigazzi, A. Comparison of marginal and average emission factors for passenger transportation modes. *Appl. Energy* **2019**, *242*, 1460–1466. [CrossRef]
20. Fleschutz, M.; Bohlayer, M.; Braun, M.; Henze, G.; Murphy, M.D. The effect of price-based demand response on carbon emissions in European electricity markets: The importance of adequate carbon prices. *Appl. Energy* **2021**, *295*, 117040. [CrossRef]
21. Zohrabian, A.; Mayes, S.; Sanders, K.T. A data-driven framework for quantifying consumption-based monthly and hourly marginal emissions factors. *J. Clean. Prod.* **2023**, *396*, 136296. [CrossRef]
22. Bardwell, L.; Blackhall, L.; Shaw, M. Emissions and prices are anticorrelated in Australia's electricity grid, undermining the potential of energy storage to support decarbonisation. *Energy Policy* **2023**, *173*, 113409. [CrossRef]
23. Song, M.; Alvehag, K.; Widén, J.; Parisio, A. Estimating the impacts of demand response by simulating household behaviours under price and CO2 signals. *Electr. Power Syst. Res.* **2014**, *111*, 103–114. [CrossRef]
24. Wu, J. *Scheduling Smart Home Appliances in the Stockholm Royal Seaport*; School of Electrical Engineering, Automatic Control, KTH Royal Institute of Technology: Stockholm, Sweden, 2012.
25. Setlhaolo, D.; Xia, X. Combined residential demand side management strategies with coordination and economic analysis. *Int. J. Electr. Power Energy Syst.* **2016**, *79*, 150–160. [CrossRef]
26. Pooranian, Z.; Abawajy, J.H.; Conti, M. Scheduling Distributed Energy Resource Operation and Daily Power Consumption for a Smart Building to Optimize Economic and Environmental Parameters. *Energies* **2018**, *11*, 1348. [CrossRef]

27. Zhang, D.; Evangelisti, S.; Lettieri, P.; Papageorgiou, L.G. Economic and environmental scheduling of smart homes with microgrid: DER operation and electrical tasks. *Energy Convers. Manag.* **2016**, *110*, 113–124. [CrossRef]
28. Nilsson, A.; Stoll, P.; Brandt, N. Assessing the impact of real-time price visualization on residential electricity consumption, costs, and carbon emissions. *Resour. Conserv. Recycl.* **2017**, *124*, 152–161. [CrossRef]
29. ENTSO-E Transparency Platform. Available online: https://transparency.entsoe.eu/dashboard/show (accessed on 8 July 2022).
30. Bavarian State for the Environment. Calculate Your Greenhouse Gas Emissions with the CO2 Calculator. Available online: https://www.umweltpakt.bayern.de/energie_klima/fachwissen/217/berechnen-sie-ihre-treibhausgasemissionen-mit-co2-rechner (accessed on 16 August 2022).
31. European Environment Agency. CO_2 Emission Intensity from Electricity Generation. Available online: https://www.eea.europa.eu/data-and-maps/daviz/sds/co2-emission-intensity-from-electricity-generation-5/@@view (accessed on 16 August 2022).
32. Carbon Footprint. Country Specific Electricity Grid Greenhouse Gas Emissions Factors. Available online: https://www.carbonfootprint.com/docs/2019_06_emissions_factors_sources_for_2019_electricity.pdf (accessed on 16 August 2022).
33. Nowtricity. CO_2 Emissions Per kWh in Norway. Available online: https://www.nowtricity.com/country/norway/ (accessed on 16 August 2022).
34. European Environment Agency. Greenhouse Gas Emission Intensity of Electricity Generation by Country. Available online: https://www.eea.europa.eu/data-and-maps/daviz/co2-emission-intensity-9/#tab-chart_2_filters=%7B%22rowFilters%22%3A%7B%22ugeo%22%3A%5B%22Germany%22%5D%7D%3B%22columnFilters%22%3A%7B%7D%7D (accessed on 16 August 2022).
35. Statista. Emissions. Available online: https://www.statista.com/markets/408/topic/949/emissions/#overview (accessed on 16 August 2022).
36. Hall, M.; Geissler, A. Comparison of Flexibility Factors and Introduction of A Flexibility Classification Using Advanced Heat Pump Control. *Energies* **2021**, *14*, 8391. [CrossRef]
37. Clauß, J.; Stinner, S.; Solli, C.; Lindberg, K.B.; Madsen, H.; Georges, L. Evaluation Method for the Hourly Average CO_{2eq}. Intensity of the Electricity Mix and Its Application to the Demand Response of Residential Heating. *Energies* **2019**, *12*, 1345. [CrossRef]
38. Le Dréau, J.; Heiselberg, P. Energy flexibility of residential buildings using short term heat storage in the thermal mass. *Energy* **2016**, *111*, 991–1002. [CrossRef]
39. Georges, E.; Garsoux, P.; Masy, G.; d'Aertrycke, G.D.; Lemort, V. (Eds.) Analysis of the flexibility of Belgian residential buildings equipped with heat pumps and thermal energy storage. In Proceedings of the CLIMA 2016 Conference and 12th REHVA World Congress, Aalborg, Denmark, 22–25 May 2016.
40. Clauß, J.; Stinner, S.; Sartori, I.; Georges, L. Predictive rule-based control to activate the energy flexibility of Norwegian residential buildings: Case of an air-source heat pump and direct electric heating. *Appl. Energy* **2019**, *237*, 500–518. [CrossRef]
41. Fraunhofer Institute for Solar Energy Systems ISE. Public Net Electricity Generation in Germany in 2021: Renewables Weaker Due to Weather—Fraunhofer ISE. Available online: https://www.ise.fraunhofer.de/en/press-media/news/2022/public-net-electricity-in-germany-in-2021-renewables-weaker-due-to-weather.html (accessed on 10 August 2022).
42. Equa Simulation AB, IDA Indoor Climate and Energy 4.8. 2018. Available online: https://www.equa.se/en/ (accessed on 20 September 2022).

Disclaimer/Publisher's Note: The statements, opinions and data contained in all publications are solely those of the individual author(s) and contributor(s) and not of MDPI and/or the editor(s). MDPI and/or the editor(s) disclaim responsibility for any injury to people or property resulting from any ideas, methods, instructions or products referred to in the content.

3. PAPER 2

Enhancing Grid Stability and Economic Operation through Heuristic Control: A Simulation Case Study

BauSIM 2024 in Wien
23. September – 26. September

Enhancing Grid Stability and Economic Operation through Heuristic Control: A Simulation Case Study

Tuğçin Kırant-Mitić[1], Karsten Voss[1]
University Wuppertal, Germany, E-Mail: kirantmitic@uni-wuppertal.de

Abstract

A positive interaction between buildings and power grids can enhance green power utilization. Notwithstanding these advancements, the unforeseen voltage stability challenges, leading to critical grid states, remains a salient concern. In this research, the power demand optimization of a case building is accomplished through the application of rule-based predictive heuristic control, with a primary focus on achieving economical operation while considering the requests from the smart grid system. As part of the Solar Decathlon Europe 21/22 competition, one of the competition buildings is exploited as case building. Cost optimized operation of the building is driven by historical electricity spot prices from the power grid of Germany. The critical grid state measurements of smart grid system are undertaken by the local utility company. During critical status, the building is expected to respond to the smart grid system by decreasing the power demand. To conduct the analysis, a co-simulation environment is developed between IDA-ICE and MATLAB. The power demand profiles of subcomponents — namely, heat pump, photovoltaic, electrical energy storage, and user-related loads— are simulated by IDA-ICE, while cost and power optimization is run in MATLAB. In conclusion, this research demonstrates an approach to support grid stability challenges through building-grid interaction.

Introduction

A positive interaction between buildings and power grid can increase green energy usage by introducing dynamic electricity prices within energy market (Zhao et al. 2015). However, despite this advancement, challenges such as unexpected voltage stability issues remain significant. In such scenarios, it becomes necessary to respond to signals from the smart grid system (SGS) by adjusting building operations to support the SGS operation. The integration of smart grid technology into building operations is referred to as building-grid interaction.

In case of voltage instability in the SGS operation, the buildings are informed by SGS technologies to adapt their operation to ensure the resilient SG operation. To achieve this, the building operation should be optimized by control algorithms. Building energy management systems are capable to receive the signal from SGS and apply demand optimization using model predictive control (MPC), rule-based control, reinforcement learning control (Zhou et al. 2023), heuristic control (Dengiz et al. 2019) and more.

Heuristics-based controls exploit the simple rules derived from experimental and practical experiences (Sánchez et al. 2019). Executing control algorithms such as MPC can be computationally expensive, but this can be mitigated by using a heuristic approach. For building energy optimization, RPHC enables the definition of selected operation setpoints to be evaluated for the solution. Therefore, control algorithms evaluate the given values rather than all possible values within a setpoint range, thus finding the solution faster. On the other hand, the RPHC approach may not provide the optimal solution since it evaluates only predefined values, not all possible values. As a result, it provides an applicable solution, though a better solution may exist. To adopt a simplified approach, (Gudi et al. 2012) evaluated household appliance scheduling for cost optimization using heuristic control with a set of defined rules, resulting in a 20% cost reduction. (Dengiz et al. 2019) applied rule-based heuristic control to minimize the heating cost of a residential area. (Cano-Tirado et al. 2024) applied a heuristic genetic algorithm to schedule a charging infrastructure operation to support SGS operation.

Novelty

In this research, the power demand optimization of a case building is accomplished through the application of RPHC, with a primary focus on achieving economical operation while

considering the requests from the SGS. In this paper, the authors discuss: 1) development and application of RPHC, 2) building a co-simulation environment, and 3) finally optimizing building operations based on the multiple signals from SGS.

Cost optimized operation of the building is driven by electricity spot prices from the German power grid for the year 2023. The critical grid state measurements of a transformer station for the same year are undertaken by the local utility Wuppertaler Stadtwerke. On critical status, the buildings are expected to decrease the power demand at the exact amount SGS needs.

As part of the Solar Decathlon Europe 21/22 competition (SDE 21/22 2022), one of the competition buildings “MIMO” (MIMO 2023) is exploited as case building in this research. More information about the building is given in Simulation section.

The co-simulation environment has been developed to ensure communication between a building energy simulation tool IDA-ICE (IDA-ICE 2023) and numeric computing program MATLAB (MATLAB 2015). Within this framework, RPHC is applied in MATLAB by employing cost optimization. The power demand profiles of distinct subcomponents - namely, the heat pump, photovoltaic array (PV), electrical storage system (ESS), and user-related loads such as lighting and plug-in devices - are simulated by IDA-ICE. These simulated profiles are then stored in MATLAB, serving as input for the calculation. The manipulated variables are the supply temperature of the thermal buffer tank (TBT) and charging/discharging value from ESS, which drives the heuristic strategy. In Co-simulation environment section, this framework is described in detail. This research is conducted only in the simulation environment and has not been applied to the real-existing building.

Simulation

The case building, MIMO, is an all-electric demonstration building equipped with an air-water heat pump (for heating purposes only) that has a thermal capacity of 5.28 kW. It is modelled with a constant coefficient of performance of 4.41. The building comprises three zones (such as community room, residential unit 1 and residential unit 2) and has a net conditioned area of 85 m^2. Utilizing TBT to fulfill both space heating and domestic hot water requirements, the efficient distribution of heat is achieved through the integration of underfloor and wall heating units. Aiming for self-sufficiency, a PV with a rated capacity of 2.8 kWp, adding to this power generation is a lithium-ion ESS with a capacity of 2.5 kWh are installed in the building. These systems are integrated into the building's energy model (Figure 1) using the building energy simulation tool IDA-ICE.

A

B

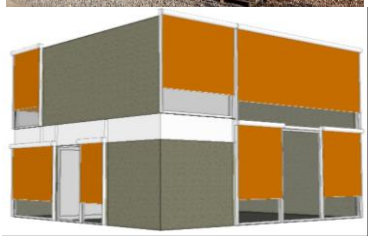

Figure 1: The picture of the case building (Sigurd Steinprinz, University of Wuppertal) (A) and the energy model view (B)

The building energy model is calibrated by monitored data during the competition period when there is a test phase for co-heating (mid-June 2022) to assess the thermal performance of the building. The results from the test period and the IDA-ICE simulation are compared as given in Figure 2, leading to accurate outcomes.

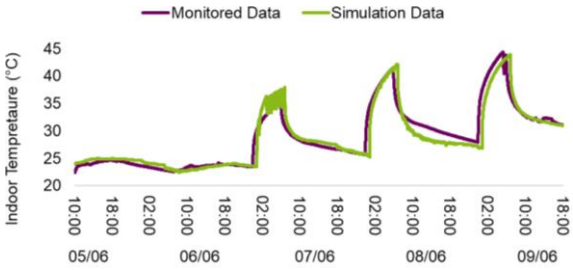

Figure 2: The indoor temperature profile of the case building for the calibration process

This paper presents a comprehensive analysis of a representative one-day heating period (18 January 2023) in response to the SGS signals within the developed co-simulation environment. The assessment is conducted between the building's business-as-usual case (BAU) and building-grid interaction case. These comparisons are performed for both before and after grid critical states, presenting optimized building operation in response to the dynamic grid environment. In this context, following cases are analyzed:

1-BAU case: In this reference case, MIMO operates under a signal-unaware condition, meaning it does not engage in active building-grid interaction. The building operates independently, with indoor temperature setpoints remaining

constant (16°C for community room and 20°C for residential units). The ESS is charged by the installed PV and discharges to cover the building's energy demand, thus operating on a self-sufficiency basis. Consequently, there are no additional measures implemented to minimize costs, unlike in scenarios involving active building-grid engagement, which is discussed in the following section.

2- Building-grid interaction case: In this scenario, the building receives signals from SGS to manage two types of operational statuses: grid-oriented and market-oriented operations (Figure 3). When the building participates in building-grid interaction, it becomes eligible to take part in the flexibility market, allowing it to consume power at more favorable prices. In response, the building assumes the responsibility of supporting the SGS in the event of critical voltage instability in the power grid, thus creating a win-win situation.

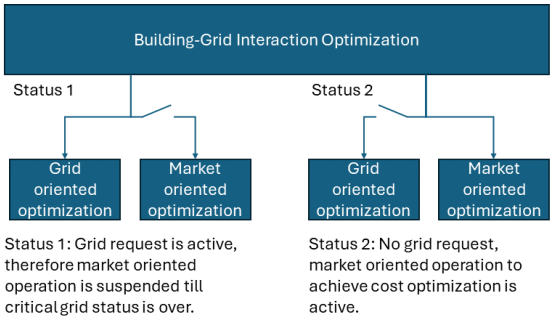

Figure 3: The two types of status occur in building-gird interaction case

In this context, the operational priority is to ensure grid stability. Therefore, the building continually monitors grid request signals. If no such signal is detected, the building then operates under a market-oriented approach to optimize operational costs by taking advantage of the flexibility market prices. To actualize the building-grid interaction case, there are several steps to be followed:

Step 1: The grid-oriented status occurs rarely, as it represents a critical situation that arises unexpectedly. The flexibility market are announced one day in advance, allowing buildings use this time to optimize their operations (e.g., temperature setpoints, EES discharging/charging actions) for the most cost-effective overall operation (referred to as Status 2 in Figure 3). For this purpose, control algorithms, such as RPHC, are applied. This is the first step executed in the co-simulation environment so that the best economical solution is found for the case building. The use of control algorithm in this research is discussed in Rule-Based Predictive Heuristic Controlsection.

Step 2: When RPHC decides the building´s setpoints and actions for market-oriented operation, they are scheduled to be applied the following day. However, if the SGS issues a request for grid support during a day when market-oriented operation is active (referred to as Status 1-Figure 3), it requires the execution of a separate optimization algorithm. This algorithm is tasked with identifying the solution to assist the grid, which involves calculating the precise setpoints and actions needed to achieve the specific reduction in power demand requested by the SGS. The effectiveness of these adjustments is assessed using the load matching index (LMI) mentioned in the Results section. This step is executed by another RPHC script in MATLAB, which is distinct from script applied in Step 1.

Step 3: Upon fulfilling the SGS's power reduction request, the building resumes market-oriented operation. However, due to the adjustments made during the grid-oriented optimization phase, the initial setpoints/actions determined in Step 1 no longer apply. Consequently, new market-oriented setpoints/actions need to be recalculated for the remainder of the day, based on the adjustments implemented in Step 2. To accomplish this, a separate RPHC script is executed in MATLAB, aimed at optimizing operational costs under the new conditions. This ensures that the building operates in the most economically advantageous manner for the rest of the day. If there is no grid request from SGS on a specific day, the building's operation continues according to the market-oriented setpoints, and actions determined in Step 1.

Co-simulation environment

In this research, two separate calculations are carried out, each requiring different programs designed to meet specific needs. These include: (1) determining building energy performance results, including HVAC operation values and thermal comfort values, and (2) implementing advanced control algorithms for demand optimization based on SGS requests and optimal cost results. Importantly, these calculations must be performed concurrently, as the results for the next time step depend on the outcomes of the previous time step in this dynamic calculation environment. To address this challenge, a co-simulation framework is established, enabling an analysis of building-grid interaction. Specifically, this research utilizes a co-simulation environment that integrates IDA-ICE (for building energy simulation) and MATLAB (for RPHC implementation).

The initial connection between IDA-ICE and MATLAB is established using a given MATLAB

script from the IDA-ICE developers. Following this, the script is improved by implementing RPHC. The initial script enables the channel connection to IDA-ICE to send and receive data using import and export modules. To avoid data loss between these programs, high resolution time steps such as one to five minutes are favorable. However, the computational burden during the co-simulation limits this process, causing the simulation to collapse before completing the defined simulation time (such as 24 hours). After testing several time steps, the time step for continuous simulation is set to 15 minutes. The determination of the proper time step involved conducting several runs and evaluating indicators such as simulation stability, data transmission stability, and the completeness of IDA-ICE simulation outputs in local directory. However, as mentioned above, data loss is a critical problem since the exported data from IDA-ICE is an input for the cost optimization calculation in MATLAB and if there is a mismatch between calculated final values and exported values. RPHC receives incorrect values, leading to performance gap between the simulated case and real case practice. To avoid this problem, another approach is applied: IDA-ICE saves the simulation results in ".prn" format in a local directory. In MATLAB, an additional section is written as part of the RPHC script to call and read the .prn files. These read data are accurate and provide reliable inputs for RPHC. Therefore, the data transferred by the export module are neglected. It should be noted that this problem is not observed during the data import process from MATLAB to IDA-ICE, but vice versa.

Another challenge in the co-simulation environment is long calculation times. For an accurate energy performance calculation, as much as different setpoints sent by MATLAB, more building performance cases are simulated in IDA-ICE allowing to the calculation of the most cost-effective result in RPHC among many different scenarios. Each simulation case means additional simulation time. Also, how long the control horizon should be (6 hours, 12 hours etc.) is another factor to consider. Therefore, some simplifications are applied to reduce the computational burden. These simplifications are explained in the Rule-Based Predictive Heuristic Control section.

The co-simulation framework is controlled mainly by MATLAB which provides the commands to set up a channel connection, create storage for transferred data and finally launches IDA-ICE. In other words, after setting up the co-simulation environment, the user doesn't use IDA-ICE anymore directly, since everything is controlled by MATLAB. After launching IDA-ICE, the simulation time "from when to when" is assigned by MATLAB script, following, the setpoints/actions values are sent to IDA-ICE. During the simulation time span, the data transfer between two programs continues. At each time step, the data "sent to" and "received from" are stored in MATLAB for post-processing, in addition to the IDA-ICE storage. Once the simulation period concludes, MATLAB issues a command for IDA-ICE to terminate its operation. MATLAB then pauses momentarily to ensure all IDA-ICE data storages are properly closed, preventing any data overlap that could be caused by the upcoming simulation. This process outlines just one simulation scenario for RPHC. However, this workflow will be repeated from the beginning for each existing RPHC scenario. The development methodology of the simulation scenarios is explained in section Rule-Based Predictive Heuristic Control.

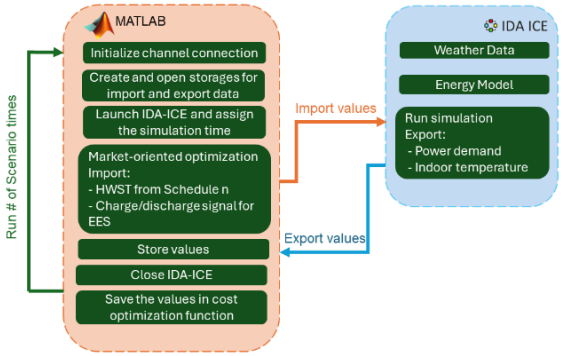

Figure 4: The co-simulation environment workflow for the market- oriented optimization (Step 1)

As mentioned in the Novelty section, the manipulated variables are the supply temperature of TBT and charging/discharging value of ESS. The explained co-simulation workflow is illustrated in Figure 4 for market-oriented optimization. In grid-oriented optimization, the primary objective is to reduce power demand by the amount requested by the SGS. The initial strategy involves exploiting the ESS to initiate discharge. In this context, the request signal (binary 0/1) and the specific amount of demand reduction required are transmitted to IDA-ICE (Figure 5). If the discharged power amount from ESS does not meet the SGS's request (which is captured from return values by IDA-ICE), various TBT setpoints are then simulated until a value close to the requested demand reduction is achieved.

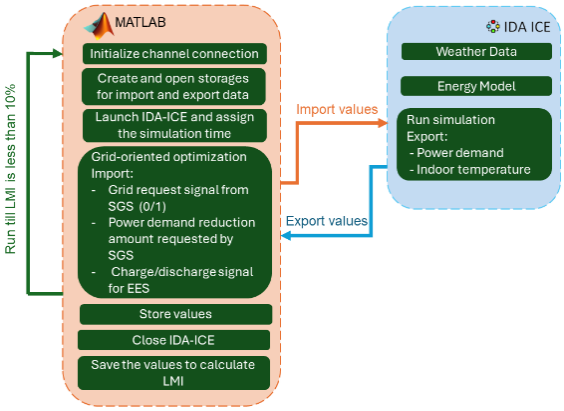

Figure 5: The co-simulation environment workflow for the grid-oriented optimization (Step 2)

SGS Signals

In this research, hourly day-ahead energy unit prices (before tax) are used for the optimization of a representative heating day - the 8th of January 2023 - which is sourced from the ENTSO-E Transparency Platform (ENTSO-E Transparency Platform Jan-2024).

In the BAU case, the TBT setpoints are determined by a heating curve that depends on the outdoor temperature. However, for the building-grid interaction scenario, the setpoints are adjusted in response to electricity price signals. To facilitate this, the hourly price signal is categorized into three levels: cheap, normal, and expensive, using a quartile analysis (25th percentile) for the simulation day. During periods identified as having the lowest electricity costs (falling within the lower quartile of day-ahead prices), the building's control system can adjust the TBT setpoints for zone heating (domestic hot water temperatures are not influenced by this operation) to be either 2.5°C or 5.0°C higher than the reference setpoint established in the BAU scenario. For durations categorized under the normal price level, two options are provided for the TBT setpoint temperatures: either 2.5°C or 5.0°C lower than the BAU reference setpoint. During periods with high electricity prices, the heat pump is turned off. If the indoor temperature is jeopardized during this period, the TBT setpoints are reverted to the standard operating temperatures defined for the BAU scenario. The motivation for limiting setpoint temperatures is to reduce the computational burden by decreasing the number of possible simulation scenarios, generating combinations only with the predefined values in RPHC. This method allows the RPHC to test specific provided setpoints, rather than attempting every possible setpoint within a given range, which could be extensive.

Secondly, as mentioned earlier, an SGS signal is triggered in cases of critical voltage instability. In this case study, we utilize real monitored data provided by the local utility. This data, collected from a transformer in Wuppertal, reflects the power demand of a neighborhood, reaching up to 100 kW. On average, a demand exceeding 50 kW triggers a yellow status, indicating slight stress on the local transformer. If the demand exceeds approximately 65 kW, it signifies a critical situation requiring buildings to support power grid stability. These thresholds are considerably higher than the peak demand observed for the case study building from the SDE 21/22 competition, which is designed for efficient energy consumption and has a peak power demand of approximately 3.0 kW during the heating period. Consequently, the building's contribution to transformer support would be minimal. To address this discrepancy, we normalize the monitored data to a scale ranging from 2 kW to 10 kW, where the yellow and red statuses are triggered after 5 kW and 6.5 kW, respectively.

Rule-Based Predictive Heuristic Control

RPHC runs various scenarios to optimize the overall operating costs of the case building by aligning them with a market-oriented operation. Here the main concern is to decrease the computation time as RPHC running with a white-box model results in long simulation times, e.g., 15 hours for a day optimization. In this context, two simplifications are conducted limiting the possible setpoints to develop the RPHC scenarios and dividing the prediction horizon (24 hours) into four control horizons.

In the SGS Signals section, the approach to limit the possible setpoints are explained. For each time step, there are two possible TBT setpoints based on the price category: During cheap price periods, either 2.5°C or 5°C above than BAU case, and during normal price period either 2.5°C or 5°C below than BAU case. Using these values, a set of simulation scenarios is developed by combining all the possible setpoints throughout a day. For example, if one hour has a cheap price with two temperature options, and the next hour has a normal price with two different temperature options, we combine these options to form four unique scenarios. When we apply this method over six continuous hours, the number of possible scenario combinations increases greatly.

Alongside the prediction horizon (24 hours), the co-simulation process includes a six-hour control horizon (Figure 6). Each control horizon comprises a series of #n simulation scenarios, categorized according to the price signal category over the control horizon. The initial control horizon predicts the optimal demand

profile from 00:00 to 06:00. The inputs for the next control horizon are the setpoint values determined and saved from the previous control horizon. During the second control horizon, simulations run from 00:00 to 12:00. For the interval from 00:00 to 06:00, the setpoint values established in the first control horizon are used, and new setpoint values for the period from 06:00 to 12:00 are projected using the RPHC. Once the final setpoint values are obtained, they are saved and employed in the following control horizon. This approach is maintained throughout the prediction horizon. Following each control horizon, the power demand outcomes for each scenario, as computed by IDA-ICE, are stored in MATLAB. These results are then utilized for the cost calculation. The scenario yielding the most favorable cost outcome is selected as the final decision.

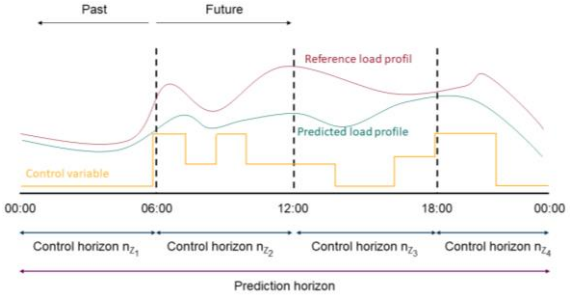

Figure 6: Prediction and control horizons in RPHC application

In the case study, an SGS signal occurs before 19:00 indicating that the predicted power demand from market-oriented optimization between 19:00-20:00 should be reduced by 1300 W due to an impending critical situation. In the Results section, the capability of the building´s energy system to respond this demand is analyzed and the outcomes are presented for each optimization as described in the Simulation section in addition to the LMI. LMI serves as an indicator to show the effectiveness of the response ratio to the power grid's demand. LMI is formulated as following:

$$LMI = \frac{P_{Market-oriented\ opt.} - P_{Grid-oriented\ opt.}}{P_{SGS\ request}} \quad (1)$$

P=Power demand from grid (Watt)

Results

This case study requires an analysis of cost optimization and demand reduction optimization in response to SGS signals, as well as a reevaluation of cost optimization for the remainder of the day after adjusting the operational setpoints to support the SGS. In this analysis, various optimization scenarios are compared on an hourly basis to the BAU case, with a focus on key performance metrics: the power demand of the heat pump, the state of charge of the ESS, the power demand from the grid, the temperature of the TBT, the indoor temperature of residential unit-1, LMI and total operational cost calculation.

In Figure 7, the ESS state of charge shows the storage utilization under different operational strategies. The BAU approach demonstrates a relatively uniform state of charge, suggesting an absence of strategic charging actions from the power grid, attributed to a strategy focused on self-sufficiency. Given that solar irradiance is typically weak during a standard heating period day, the EES cannot be charged, preventing the building from utilizing the EES's potential. On the other hand, market-oriented operation suggests an adaptive charging/discharging strategy to use lower electricity prices to charge, presented by significant charging levels, specifically during overnight.

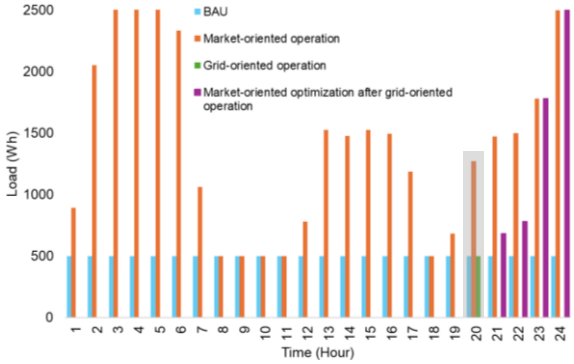

Figure 7: EES state of charge for different operation cases

In market-oriented optimization, the amount of stored energy increases between 19:00-20:00 due to a plan to charge up (using 800 W for charging). However, when it comes to supporting the grid, this charging plan isn't used. Instead, the stored energy decreases, showing that the EES is discharged by 250 W. This discharging phase is necessary to minimize the power demand from grid as requested by SGS. By changing the planned actions for the EES, power demand from grid is decreased by 1050 W in total. This action underlines the ESS's role in providing flexibility and its ability to manage between market-driven objectives and grid-supportive actions. However, since this amount is not sufficient, further action, such as, changing the heat pump power demand, is considered in the next step.

Heat pump power demand is given in Figure 8. In the BAU scenario, demand reflects a non-responsive system to price signals or grid requests. It operates only based on the thermal needs of the building. Reversely, the market-

oriented operation presents a dynamic adjustment to the fluctuating prices throughout the day.

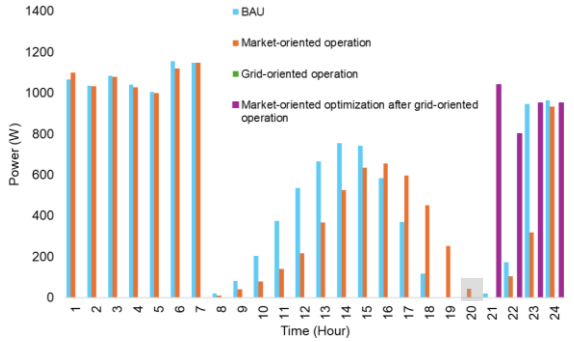

Figure 8: Heat pump power demand for different operation cases

During grid-oriented operation, to closely match the power demand reduction requested by SGS and considering that the EES strategy alone cannot fully achieve this, it becomes necessary to reduce heat pump operation, if possible, without jeopardizing thermal comfort. In this context, the heat pump operation is suspended, and the power demand of 50 W is avoided. Following the grid-oriented response, the market-oriented optimization after grid-optimization case shows an increment in demand.

Fehler! Verweisquelle konnte nicht gefunden werden. illustrates the building's total power demand from the grid under various operational strategies. In the BAU scenario, power demand remains steady at approximately 2000 W throughout the day, indicating a non-adaptive energy strategy since it doesn't take part in the energy flexibility market, however, market-oriented operation is characterized by fluctuating demand, reflecting active participation.

During grid-oriented operation, there's a notable decline in demand at 20:00, when the building has decreased its grid energy use, to match load reduction as requested from SGS. With EES and heat pump power reduction strategy, 1100 W of decrement is achieved. Following this, the market-oriented optimization after grid-responsive action shows a rise in demand, that considers both the previous support provided to the grid and current market pricing. This presents the building's role as a proactive consumer that maintains cost-effective energy habits. As previously stated, SGS requested a reduction in demand of 1300 W. Through the implementation of the applied measure, a reduction of 1100 W in demand is achieved. Based on the given formula (1), LMI is calculated to be 85%.

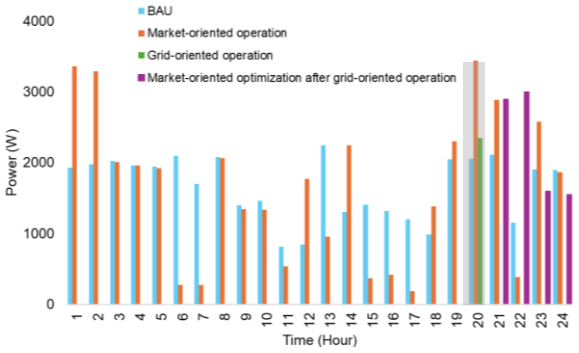

Figure 9: Final power demand for different operation cases

Figure 10 shows the upper layer temperature of TBT over a 24-hour period for different optimization cases. Due to stratification, the water is supplied to the heating units from the upper layer, ensuring the highest temperature water is used for heating purposes. The tank is designed with 8 layers, which helps maintain distinct temperature gradients and enhances the efficiency of the thermal storage system. The BAU line presents the temperature based on the heating curve. For market-oriented optimization, the temperature fluctuates more, adjusting to cost variations and showing a more responsive approach to energy pricing. During the grid optimization, the temperatures go down since the heat pump operation is suspended. However, on the following hour, the temperature rises again.

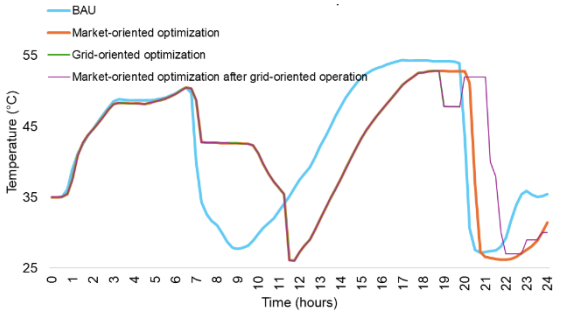

Figure 10: Thermal buffer tank upper layer temperature for different operation cases

Figure 11 tracks the indoor temperature under different scenarios, indicating how the thermal comfort is influenced by each strategy. The temperature under the BAU approach is quite stable, suggesting that the heating system maintains a consistent setting since it doesn't interact with dynamic pricing. The market-oriented result also presents similar behavior to the BAU case, since the manipulated RPHC variable is not indoor temperature profile, but TBT temperature. In this research, the motivation was to keep the indoor temperature stable as possible so that the occupants do not sense the interaction measures between the building and SGS. However, due to changes in the heat pump

operation plan during the grid-oriented operation case, we observed a slight increase in indoor temperature, approximately by 1°C, in the post-operation scenario.

In addition to the power reduction, another crucial aspect to consider is the potential economic benefit. In the BAU scenario, the total operational cost for the analyzed day is 5.64 €. Participation in the flexibility market reduced this cost to 5.45 €. Following market optimization and subsequent grid optimization, the final operational cost is determined to be 5.5 €.

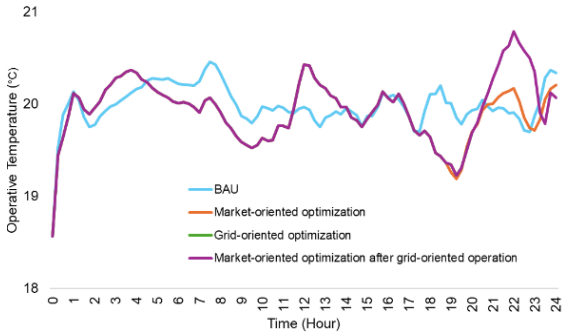

Figure 11: Indoor temperature of the residential unit-1 for different operation cases

Conclusion

The positive interaction between buildings and the power grid is incentivized by participation in the energy flexibility market to support SGS operations. Nevertheless, the practical analysis of this issue highlights the challenges of implementing load optimization simulation modelling using control strategies. The complexity of these problems surpasses the capabilities of a single program, introducing computational complications and necessitating a co-simulation environment.

In this research, a co-simulation environment between a building performance simulation program and numerical program is presented with a case study. It showcases a win-win situation to enhance grid stability and pursue cost reductions. The results are evaluated with several metrics. It is found that, with control algorithms, multiple signal optimization such as load and cost, can be achieved. However, in a highly energy-efficient experimental building like MIMO, achieving high LMI values and significant cost reductions is constrained. This limitation arises because such buildings are designed to operate at a high level of energy efficiency in BAU scenario. Consequently, the potential for realizing higher cost benefits is also limited.

References

Cano-Tirado, D.; Forchheim, M.; Asman, M.; Zdrallek, M.; Palmer, S. (Eds.) (2024): Potential Grid-Oriented and Market-Oriented Optimisation of a Local Charging Infrastructure Through a Genetic Algorithm. 18. Symposium Energieinnovation. Graz/Austria, 14.-16.02.2024.

Dengiz, Thomas; Jochem, Patrick; Fichtner, Wolf (2019): Demand response with heuristic control strategies for modulating heat pumps. In *Applied Energy* 238, pp. 1346–1360. DOI: 10.1016/j.apenergy.2018.12.008.

ENTSO-E Transparency Platform (Jan-2024): Day-ahead Prices. Available online at https://transparency.entsoe.eu/dashboard/show, updated on Jan-2024, checked on Jan-2024.

Gudi, Nikhil; Wang, Lingfeng; Devabhaktuni, Vijay (2012): A demand side management based simulation platform incorporating heuristic optimization for management of household appliances. In *International Journal of Electrical Power & Energy Systems* 43 (1), pp. 185–193. DOI: 10.1016/j.ijepes.2012.05.023.

IDA-ICE (2023): Equa Simulation AB - IDA indoor climate and energy 4.8 - Simulation Software | EQUA. Available online at https://www.equa.se/en, checked on 15-Aug-23.

MATLAB (2015): (R2015b). Natick, Massachusetts: The MathWorks Inc.

MIMO (2023): MIMO - Minimal Impact Maximum Output - Solar Decathlon Europe 21. Available online at https://mimo-hsd.de/de/, checked on 15-Aug-23.

Sánchez, Cristian; Bloch, Lionel; Holweger, Jordan; Ballif, Christophe; Wyrsch, Nicolas (2019): Optimised Heat Pump Management for Increasing Photovoltaic Penetration into the Electricity Grid. In *Energies* 12 (8), p. 1571. DOI: 10.3390/en12081571.

SDE 21/22 (2022): Solar Decathlon Europe. Available online at https://sdeurope.uni-wuppertal.de/de/, checked on 15-Aug-23.

Zhao, Yang; Lu, Yuehong; Yan, Chengchu; Wang, Shengwei (2015): MPC-based optimal scheduling of grid-connected low energy buildings with thermal energy storages. In *Energy and Buildings* 86, pp. 415–426. DOI: 10.1016/j.enbuild.2014.10.019.

Zhou, Xinlei; Xue, Shan; Du, Han; Ma, Zhenjun (2023): Optimization of building demand flexibility using reinforcement learning and rule-based expert systems. In *Applied Energy* 350, p. 121792. DOI: 10.1016/j.apenergy.2023.121792.

4. PAPER 3

A Rule-Based Predictive Control Framework for Market and Grid-Oriented Operation in Thermally Activated Buildings

JOURNAL OF BUILDING PERFORMANCE SIMULATION
https://doi.org/10.1080/19401493.2025.2565652

OPEN ACCESS Check for updates

A rule-based predictive control framework for market and grid-oriented operation in thermally activated buildings

Tuğçin Kırant-Mitić and Karsten Voss

Department of Building Physics and Technical Services, Faculty of Architecture and Civil Engineering, University of Wuppertal, Wuppertal, Germany

ABSTRACT

The integration of renewable energy into power grids introduces instability due to generation intermittency, necessitating demand-side flexibility strategies. Building-grid interaction, particularly for thermally activated building systems, offers a solution by dynamically adjusting power demand. These buildings exploit thermal mass of their structural elements, such as concrete slabs with embedded water pipes, to shift thermal loads. This study investigates an all-electric office building with concrete core activation, employing a rule-based control strategy and introducing a rule-based predictive control framework to optimize market-oriented and grid-oriented operations. A co-simulation environment integrating a building performance simulation tool with numerical optimization is developed. Results show that the rule-based predictive control improves cost savings by 2.2% compared to rule-based control while ensuring grid support, achieving a load matching grid index of 88.6% during congestion events. The proposed approach enables sequential demand flexibility, balancing economic efficiency and grid stability while offering an alternative to advanced control algorithms.

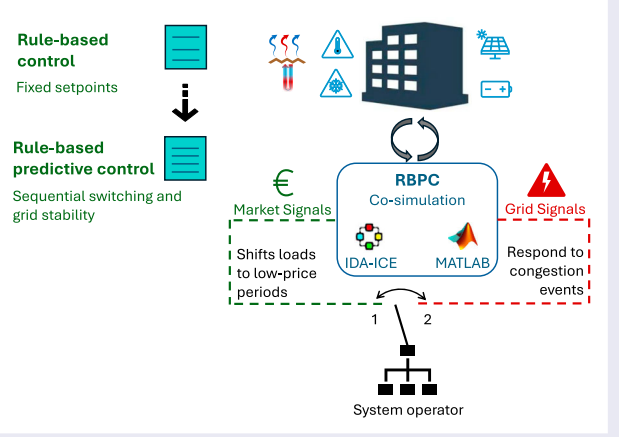

ARTICLE HISTORY
Received 25 February 2025
Accepted 18 September 2025

KEYWORDS
Thermally activated building systems; co-simulation; energy flexibility markets; market-oriented operation; grid-oriented operation; demand response

Introduction

Background

In traditional energy supply systems, electricity demand in buildings is primarily met by a centralized utility grid, where generation is largely stable and can be adjusted to accommodate demand fluctuations (Powell et al. 2024). However, the transition to a decarbonized energy system has introduced new challenges in balancing electricity supply and demand (Valkering et al. 2023). The increasing integration of distributed energy resources (DERs), such as solar photovoltaic (PV) and wind power, has led to greater reliance on intermittent generation (Y. Li et al. 2020). This intermittency often results in a mismatch between energy generation and consumption, which, if not managed effectively, can compromise power grid stability.

Buildings, as major electricity consumers, have the potential to play an important role in mitigating these imbalances by providing demand-side flexibility (Liu et al. 2023). By actively participating in building-grid interaction, buildings can adjust their energy consumption patterns in response to market signals or grid constraints (Balaras 1996). This flexibility enables buildings to align

CONTACT Tuğçin Kırant-Mitić tugcin.kirant_mitic@uni-wuppertal.de

© 2025 The Author(s). Published by Informa UK Limited, trading as Taylor & Francis Group.
This is an Open Access article distributed under the terms of the Creative Commons Attribution License (http://creativecommons.org/licenses/by/4.0/), which permits unrestricted use, distribution, and reproduction in any medium, provided the original work is properly cited. The terms on which this article has been published allow the posting of the Accepted Manuscript in a repository by the author(s) or with their consent.

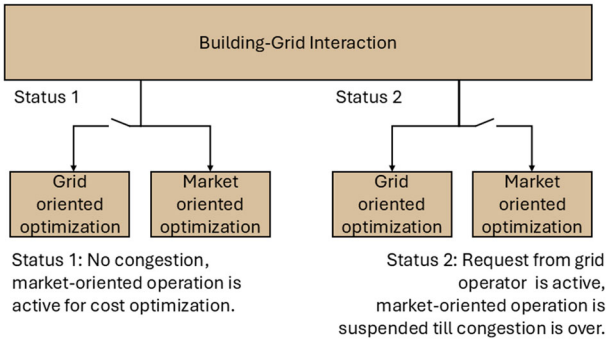

Figure 1. The sequential activation of market-oriented and grid-oriented operations.

their demand with fluctuating renewable generation, reducing grid stress and enhancing the overall efficiency of energy distribution.

Within this framework, energy markets serve as key enablers for the efficient distribution of electricity while ensuring grid stability (L. Yang et al. 2024). In the European power grid system, the day-ahead market, intraday market, and balancing market each contribute to different aspects of system reliability (Federal Ministry for Economic Affairs and Energy 2015). However, with the increasing penetration of decentralized energy systems, demand-side flexibility has become an essential resource, leading to the development of the flexibility market. The flexibility market enables DERs, including buildings and electric vehicle fleets, to offer demand-side flexibility by shifting or reducing their consumption in response to market signals or grid operator requests (Lustenberger et al. 2024).

Buildings can participate in the flexibility market in two main ways. First, they can apply market-oriented operation that they can optimize their demand through dynamic pricing mechanisms such as day-ahead market prices (Alahäivälä et al. 2017). This approach allows buildings to shift their energy demand to periods of lower electricity prices, reducing overall costs. Second, buildings can actively participate in the flexibility market by offering load shifting and demand reduction services to grid operators in case of congestion issues (Esmat, Usaola, and Moreno 2018). This operation, which will be called grid-oriented operation after this point, is driven by congestion events rather e.g. physical grid constraints, rather than market-based incentives such as cost savings, CO_2 reduction, or price-based load shifting. When congestion occurs, the market-oriented operation is suspended as grid stability has higher priority. After ensuring the congestion is resolved, the operation is switched back to the market-oriented operation as illustrated in Figure 1.

In this research, congestion refers to a power overload in a substation as also described in Haque et al. (2017), Du et al. (2023). To solve a congestion event, buildings must adjust their load demand by the amount requested by the distribution system operator. However, developing control algorithms to implement operational changes at the requested demand level is a challenging task. Designing an effective control algorithm requires not only achieving an optimal solution, but also controller modelling performance. This research introduces a novel control algorithm for sequential market and grid-oriented operation in a building equipped with Thermally Activated Building Systems (TABS), implemented within a co-simulation environment. To evaluate its effectiveness, the algorithm's outputs are compared with the results of a rule-based control (RBC) analysis.

Addition to the congestion issues, frequency and voltage stability are essential aspects of broader grid resilience. However, these parameters are typically managed at the transmission or substation level using supply-side resources (e.g. spinning reserves, inverters) and very fast control mechanisms. Buildings equipped with fast-responding assets such as batteries, electric vehicles, or smart inverters could only provide ancillary services like frequency support and voltage control.

Thermally activated building systems and their control

TABS embed heating and cooling elements within the building structure, harnessing building envelope as thermal reservoirs (Arteconi et al. 2014). In recent years, TABS have garnered growing favour due to their capacity to deliver enhanced thermal comfort and heightened energy efficiency (Chen, Li, and Feng 2021) making use of environmental heat sources and sinks. TABS contribute to energy efficiency by allowing slightly lower heating setpoints and higher cooling setpoints while maintaining comfort (Rhee and Kim 2015; Salt 1985).

Since this system is characterized by water pipes embedded in building structure, it exhibits a sluggish response to control signals attributable to their substantial thermal inertia. This constraint hinders the control system's ability to quickly address sudden thermal load changes leading to increased energy consumption from frequent mode switches (Tian and Love 2009). However, by integrating a buffer tank as an energy buffer and implementing a well-structured thermal charging control strategy, fluctuations in TABS operation can be minimized. To assess the effectiveness of this implementation, it should be analyzed as a potential strategy for building-grid interaction, ensuring that TABS can provide both energy efficiency and demand flexibility.

TABS are typically regulated controlling supply water temperature and flow rate (Gwerder et al. 2008; Rhee, Olesen, and Kim 2017). The heating/cooling curve adjusts the supply water temperature based on outdoor air temperature, and water flow rate to individual zones aligns with indoor set point temperatures (Lim et al. 2006; Olesen 2007). Some research suggests that slab or floor surface temperatures can be used for control (Cho and Zaheeruddin 1999; Shin et al. 2015). In addition to the diverse manipulation variables, the operation mode, either continuous or intermittent, can also be implemented (Cho and Zaheer-uddin 1999). In continuous mode, the system is continuously monitored and controlled by thermostat feedback. Conversely, in the latter case, the operation is implemented where the system is active during specific hours throughout the day.

The integration of TABS with renewable energy sources and heat pumps can effectively reduce reliance on primary energy sources, enhances overall energy efficiency and consequently leading to a subsequent decrease in operational costs (Chen, Li, and Feng 2021). In these hydronic systems, thermal energy is mostly extracted from the ground as a resource to be utilized by a heat pump (Self, Reddy, and Rosen 2013) and is then distributed to the building structure via embodied piping to charge the envelope. However, this underscores the necessity for the development of more sophisticated building control strategies to effectively harness the potential synergy between hydronic systems, renewable energy sources, and the building envelope for optimal energy management.

To address this challenge, innovative building control approaches have been developed (R. Li et al. 2022). These approaches consider the building's thermal characteristics, heating, ventilation, and air conditioning (HVAC) system, and dynamic grid pricing or CO_2 emission factors. They exploit the building envelope as a structural thermal storage medium, offering a pathway to harness building-grid interaction potential. This ensures that energy demand aligns with periods of lower cost and availability (Reynders, Nuytten, and Saelens 2013). However, the interaction of the building when congestion occurs in a power grid is not discussed. The existing research is primarily limited to analyzing market-oriented operation or environmentally friendly operation. It remains an open question how a TABS building can contribute to grid stability while remaining unaffected by its own sluggish thermal response during power instability.

The complexity of advanced control algorithms

Market-oriented operations can be analyzed using different control algorithms such as RBC, reinforcement learning, fuzzy logic, model predictive control (MPC) and more (Jensen et al. 2017). Each of these control algorithms has its own advantages and limitations when compared to one another. As the modelling complexity of the control algorithm increases, its capability to find solutions that maximize cost savings also improves. On the other side, in grid-oriented operations, basic control algorithms such as RBC are insufficient for determining accurate set-points, as they lack the capability to compute optimal solutions, necessitating the implementation of sophisticated control strategies.

Advanced control algorithms, such as MPC and reinforcement learning are widely applied in energy management due to their ability to handle constraints, predict future states, and optimize multi-step decision-making (Drgoňa et al. 2020). However, despite their advanced performance, their practical implementation remains challenging due to their demanding modelling requirements.

Even though white-box MPC models capture building physics in depth, they are often too heavy to run at the few-minute resolutions needed for real-time control. Wang et al. (2023) showed that a white-box MPC based on IDA-ICE–Matlab co-simulation is impractical for multi-room heating. The iterative, multi-zone calculations in IDA-ICE impose a heavy computational burden, and the data exchange between IDA-ICE and MATLAB is complex, undermining real-time optimization. This underscores the practical limits of white-box MPC and motivates reduced-order or grey-box replacement for deployable controllers. For instance, Khatibi et al. (2022) replaced the reference white box model with a second-order state-space model and corrected with a Kalman-style prediction for MPC implementation. Similarly in Wei and Calautit (2024), the authors proceeded with an RC surrogate of the white-box model because its low-order state-space form enables efficient optimization within MPC. Another critical point is the deployment of MPC in building automation system as it generally requires specialist expertise during both design and implementation (Killian and Kozek 2016). Because each building energy system is tailored to a specific building, controllers and plant models are non-transferable and costly for engineers. Constructing and maintaining these models also imposes substantial computational demands and depends on detailed mathematical representations of the building. Additionally, this means required engineering modelling effort is an additional cost as it requires heavy work to obtain a reliable MPC model (Sturzenegger et al. 2016).

Compared to MPC, reinforcement learning can perform better on overcoming on challenges such as non-linearity, and dynamic changes (Al Sayed et al. 2024).

However, reinforcement learning requires substantial monitored operational data for training. For new or planned buildings, such data are unavailable, making direct deployment of reinforcement learning on the energy system technically infeasible. At the same time, demand response is increasingly institutionalized, e.g. driven by higher shares of variable renewables, so policies, standards, and incentive programs now encourage designing and operating buildings for grid-interactive operation. However, without monitored operational data (or a calibrated white-box model), deploying reinforcement learning in those buildings is not technically feasible. Also, it should also be noted that training a reliable reinforcement learning model can last several months, resulting in high computational costs (Dey et al. 2023).

As mentioned above, the process of developing the mathematical model necessities an accurate representation of the building's thermal behaviour, energy consumption, and interaction with external market signals. Given the complex thermal inertia of buildings, particularly those equipped with TABS, a highly detailed model must be developed, which increases computational effort (X. Yang et al. 2024). For practical applications, particularly in grid-oriented operation, the computational demands of these advanced algorithms pose significant barriers to scalability. In real-world implementations, their complexity may result in delayed decision-making.

To address the computational and implementation challenges of advanced control algorithms while maintaining predictive capabilities, this research adopts Rule-Based Predictive Control (RBPC) as an alternative control approach. Unlike conventional predictive controls, RBPC follows a predefined rule-based logic by developing several setpoint scenarios (not a fixed setpoint as applied in RBC) that adjust based on conditions such as energy prices and grid constraints. This approach enables finding suboptimal solutions for proactive energy management while implementing simplified predictive control.

RBPC integrates a prediction approach, ensuring flexibility in both market-oriented and grid-oriented operations. In market-oriented operation, RBPC pre-schedules energy consumption based on day-ahead electricity price forecasts, shifting demand to low-cost periods. In grid-oriented operation, it reacts to grid congestion events, dynamically adjusting heating and cooling activation to alleviate grid stress. This balance between predictive control and modelling simplicity makes RBPC a practical alternative for real-world building energy applications. In Table 1, the important terms used in the study are listed.

Table 1. Key terms used in the study.

Term	Description
RBC	Rule-based control
RBPC	Rule-based predictive control
Market-oriented operation	An operational mode optimizes building energy usage based on electricity price signal
Grid-oriented operation	An operational mode focused on supporting grid stability

The need for co-simulation environment

Traditional building performance simulation (BPS) tools are often insufficient for analyzing grid-oriented operation, as they primarily focus on building-level energy performance without considering interactions with the power grid. Moreover, integrating advanced control algorithms is limited in BPS. A comprehensive assessment of grid-oriented operations requires a co-simulation environment where BPS tools are integrated with numerical computing tools (Le Dréau et al. 2023).

In this research, the analysis is conducted using a co-simulation environment that integrates BPS and numerical computing tool for optimization and control implementation. By this coupled setup, the real-time evaluation of RBPC in grid-driven operations is enabled to enhance building-grid interaction while maintaining occupant comfort.

The novelty

Despite extensive research on demand-side flexibility, market-oriented operation, and control strategies for TABS, most existing studies primarily focus on optimizing building energy consumption in response to dynamic electricity prices. However, the potential of TABS-equipped buildings to actively support grid stability during congestion events remains largely unexplored. This research addresses this gap by introducing a novel sequential control framework that integrates both market and grid-oriented operations, ensuring cost-efficient operation as well as grid flexibility and stability. Within this scope, the key contributions of this study include:

- Development of RBPC as an efficient alternative to complex control algorithms.
- Establishment of a detailed co-simulation framework, coupling BPS with a numerical computing tool for real-time control implementation.
- Unlocking the market-oriented operation of TABS using RBC and RBPC.
- Comparing the RBPC results to RBC results to demonstrate the effectiveness of proposed control algorithm.

Figure 2. View of the case building (Staff n.d.).

- Deployment of two distinct control signals: day-ahead electricity prices for market-driven optimization and real substation congestion values for grid-oriented response.
- Comprehensive evaluation of building envelope and energy system performance when a TABS-equipped building participates in the flexibility market, analyzing surface temperature variations, heat flux distribution, and indoor operative temperatures across different office zones (Southeast, Southwest, Northeast, Northwest).

The RBC results for market-oriented operation are first analyzed over a representative week and compared to baseline operation to illustrate the activation of building-grid interaction. Subsequently, a selected day from this period is examined to compare RBPC with RBC in market-oriented operation, highlighting its impact on operational performance. Finally, RBPC is applied for grid-oriented operation. Additionally, the study quantifies shifted electrical energy demand, grid consumption changes, cost variations, and the load matching grid index, offering new insights into the economic and operational advantages of RBPC for market and grid integrated TABS control.

The case study building

The case study building (Figure 2), with an energy reference area of 2,600 m^2, is situated in Niederanven, Luxembourg (Lichtmess 2018). This region is characterized by an annual average temperature of 11°C and a global horizontal radiation of 150 W/m^2 (Stackhouse 2023), representative of typical climate conditions in Central Europe.

It is designed to utilize its concrete ceilings as a dual conduit for thermal energy transfer and air distribution. The building's heating and cooling demands are met by a geothermal borehole setup consisting of a heat pump system, which draws energy from a field of 21 geothermal probes, each extending to a depth of 100 metres, and offering a total heating capacity of 57 kW and a Coefficient of Performance (COP) of 4. Ground temperature fluctuations are more pronounced at depths shallower than 0.8 m, decreasing with greater depth (Hanova and Dowlatabadi 2007). Ground source heat pumps harness the stable ground temperature, warmer than the winter air and cooler than the summer air (Lee 2011). The building fulfills its cooling requirements passively by harnessing a geothermal probe field with a capacity of 74 kW, along with the implementation of automated nighttime window ventilation for enhanced natural temperature regulation. In periods of prolonged cooling demand, the heat pump system is dual-purposed to provide cooling, with a capacity of 45 kW, effectively employing the ground or the probe field as an energy-efficient re-cooler to sustain comfortable indoor temperatures. Figure 3 illustrates the comprehensive HVAC system of the case building, detailing the interplay between various system components and their interactions with electrical and environmental energy sources.

The building design incorporates pipe coils in the lower zones of the concrete ceilings, mirroring the principle of underfloor heating. These coils circulate water, subtly adjusting the ceiling temperature to 24°C for heating purposes or reducing it to 18°C to cool the space during warmer months. In this research, a continuous mode by thermostat feedback is conducted. Indoor air quality is actively managed by introducing fresh air through an air handling unit (AHU) with a substantial capacity of 11,000 m^3/h, regulated by indoor CO_2 levels to ensure a healthy indoor environment. The system boasts a heat recovery efficiency of 80%, with a specific fan power of 0.51 $W/(m^3/h)$, striking a balance between energy efficiency and air quality. In the pursuit of energy independence, the building's electrical demand is predominantly satisfied by a rooftop PV installation which of 35 kW_p. Complementing this, a lithium-ion electrical energy storage (EES) with a capacity of 20 kWh is employed to capitalize on the PV system's energy yield, storing excess power for use. It has 87% round-trip efficiency. The battery could discharge to 20% of its capacity. In BPS, energy losses were accounted for by applying a loading/unloading efficiency of 87%, which ensures that the battery does not store or deliver energy at 100% efficiency during charge and discharge cycles. Degradation effects were not included as this work focuses on short-term operational performance.

Simulation

The analysis presented in this paper was conducted using BPS tool IDA-ICE-version 4.8 (IDA-ICE 2023). To ensure

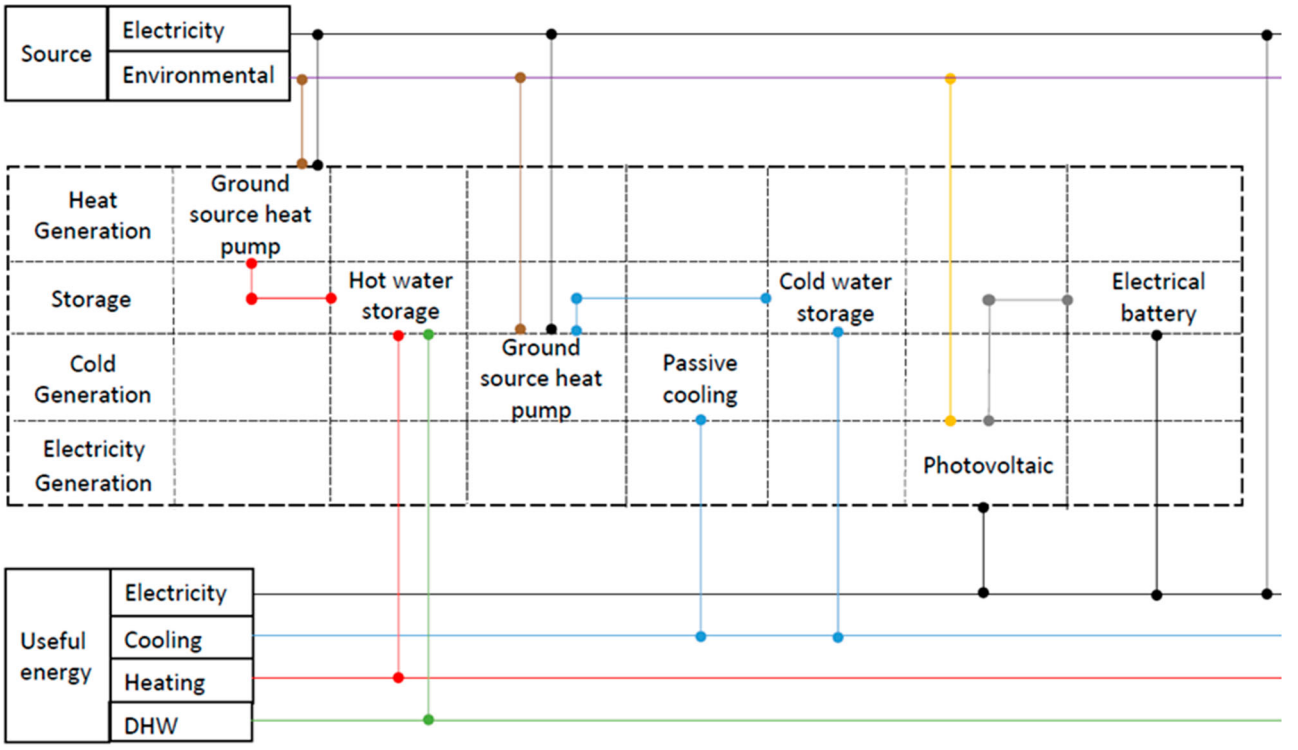

Figure 3. Integration of HVAC system components with energy resources in the case building.

accuracy, the simulation's energy profiles including heat pump, circulation pumps, AHU fans, PV, EES, lighting, and user-related loads were calibrated against historically monitored data. The resulting RMSE for indoor temperature was 0.9 °C, MAE was 0.8 °C, and MBE was −0.06 °C, indicating good agreement between simulated and measured values and meeting commonly accepted thresholds for thermal zone calibration. The annual difference in heating energy use was 8.7%, while the difference in cooling energy use was 6.1%.

Following this calibration, a specialized energy model was developed within IDA-ICE to examine the market and grid-oriented operations (Figure 4). The building operation analysis in this research specifically focuses on optimizing energy use during the heating period. Concurrently, the system's control strategy includes feedback from indoor temperature sensors. Moreover, the surface temperature is continuously monitored to ensure that the operation stays within the specified thermal limits.

The system employs a continuous operation mode in reaction to thermostat readings to minimize temperature oscillations within the space. In baseline operation, electricity generated by the PV system initially meets the building's electrical demand and any surplus generation is then used to charge the EES. Notably, the EES does not charge from the power grid or any other external sources.

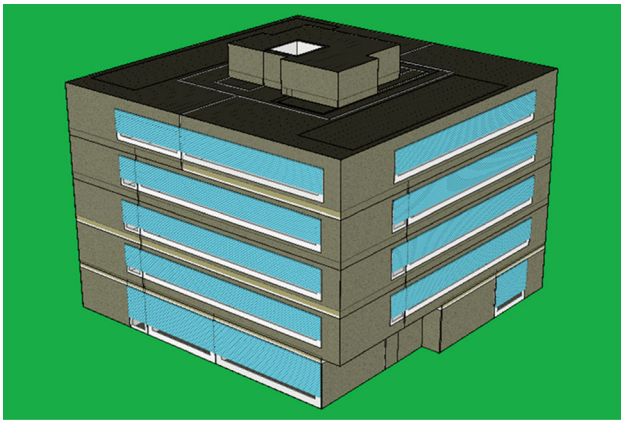

Figure 4. Energy model view of the case building.

Operational cases

In this research, five different operational cases are investigated (Figure 5). The first operation is Business-as-Usual [case(1)] where baseline operation is analyzed. In this operation, no control signal as electricity price or grid power change request is implemented. In case(1), the heat pump operation is adjusted by a predefined heating curve, which responds to changes in ambient temperature. More information about the heating curve is given in the following section.

To conduct market-oriented operation, the utilization of heating curve is adapted by integrating day-ahead

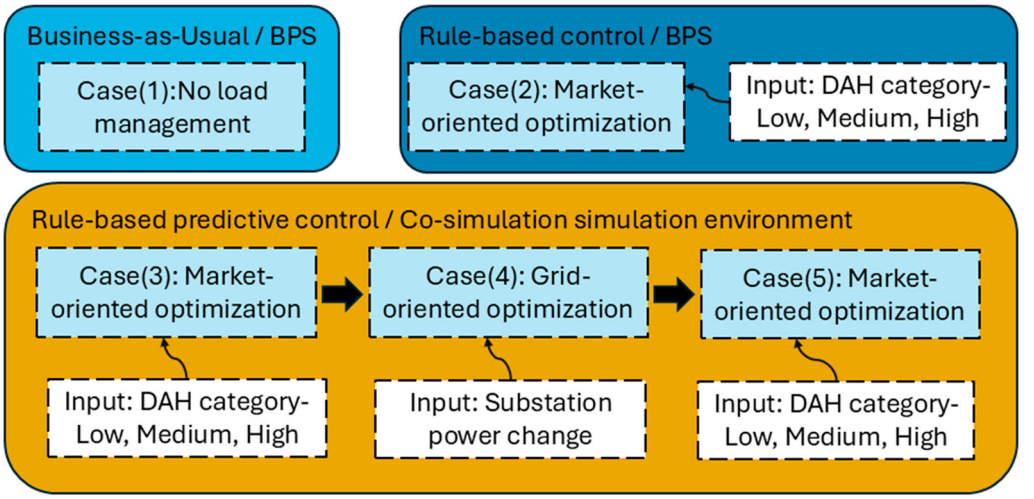

Figure 5. The analyzed operational cases.

prices. On the other hand, to achieve comparative analysis, market-oriented operation is evaluated using two control strategies as RBC [case(2)] and RBPC [case(3)]. RBC operates entirely within the BPS tool and does not require a co-simulation environment. In contrast, RBPC requires a numerical computing tool to determine cost-saving operational scenarios by simulating multiple predefined setpoints. Therefore, RBPC is implemented within a co-simulation framework. Grid-oriented operation [case(4)] is activated when congestion is detected during case(3). Under these conditions, case(3) is suspended to prioritize grid stability. To mitigate this, it is assumed that the distribution system operator informs the building aggregator in advance, enabling buildings to shift their demand proactively. Once the congestion is resolved, the system returns to market-oriented operation. However, as the previously forecasted setpoints from case(3) are overridden during case(4), a new cost-optimized setpoint adjustment is required. This launches the execution of case(5) as a post market-oriented operation, ensuring the building resumes cost-effective operation after grid stabilization.

In principle, the building continuously monitors grid request signal, and if no request is detected, it operates under case(3), optimizing energy costs using day-ahead prices. However, if the aggregator issues a power change request, the building temporarily shifts to case(4), adjusting its demand to stabilize the grid before reverting to market-oriented operation.

Control strategies

Market-oriented operation

During market-oriented operations, the building-grid interaction is examined using historical day-ahead electricity spot prices (before taxes and surcharges) from the 2022 Germany-Luxembourg bidding zone data in hourly resolution, which serve as a control signal to facilitate market-oriented optimization. Figure 6 (A) illustrates the price data for a representative week of December 5th to December 11th used in the simulation, which is sourced from ENTSO-E Transparency Platform (2022).

To conduct the analysis, the hourly price signal is grouped into three levels as cheap, normal, and expensive using 25% quartile analysis for each simulation day (Figure 6 (B)). During periods when day-ahead prices are at their lowest, as determined by the lower quartile of historical spot prices, the building's control system adjusts the setpoint temperature of the buffer tank, which has a capacity of 4500 litres. As mentioned earlier, two different control algorithms, RBC and RBPC, are applied in this research. Consequently, two different approaches are used to optimize the heat pump supply temperature setpoint to the buffer tank. In RBC, the setpoint temperature is increased by 2°C above case(1) when electricity prices fall into the cheap category as given in Figure 7. Conversely, when prices are in the normal flexibility category, the control system lowers the setpoint temperature by 2°C to prevent excessive energy consumption.

In RBPC, however, a predictive approach is used to enhance flexibility. Instead of using a single predefined adjustment, multiple setpoints as 1°C, 2°C, or 3°C above case(1) are considered to evaluate different possible operational scenarios (Figure 7) during cheap price durations.

This allows the control system to anticipate and react dynamically to price fluctuations, optimizing energy use more effectively. Unlike RBC, during the normal price category, the supply temperature setpoint in RBPC is lowered by either 1°C, 2°C, or 3°C below case(1), providing additional adaptability to price variations. During

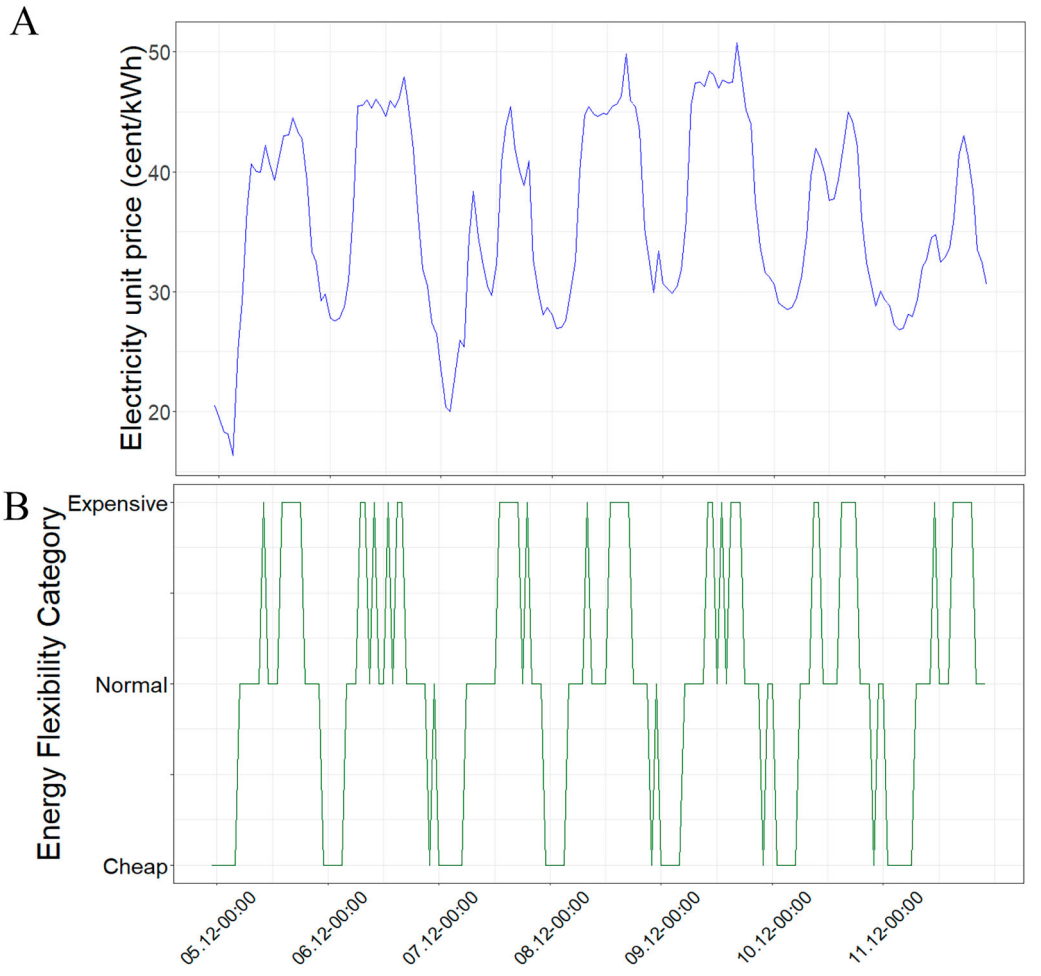

Figure 6. Electricity unit price (before tax and surcharges)-(A) and its categorization as a control signal for case (2) operation-(B).

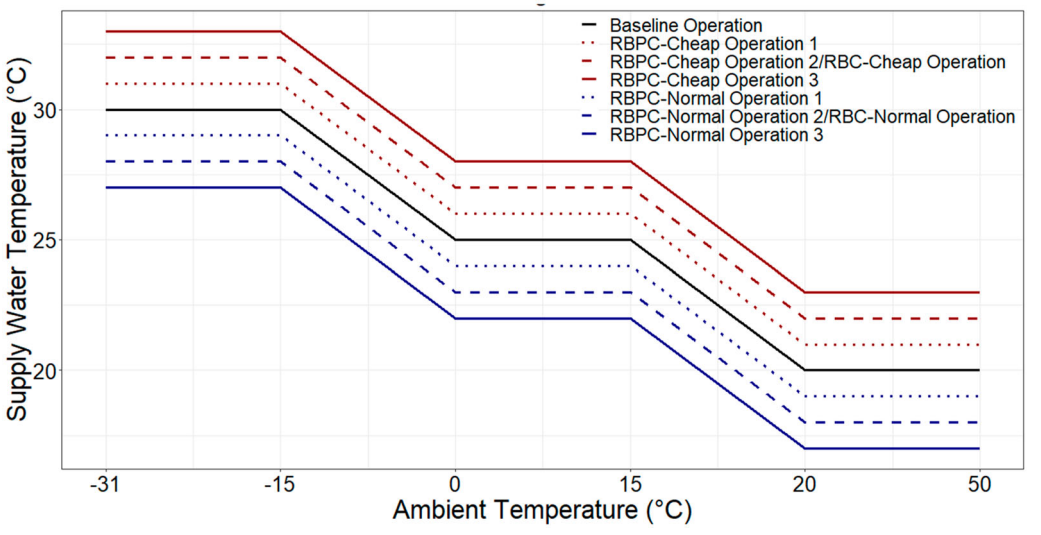

Figure 7. The HC based on the outdoor temperature.

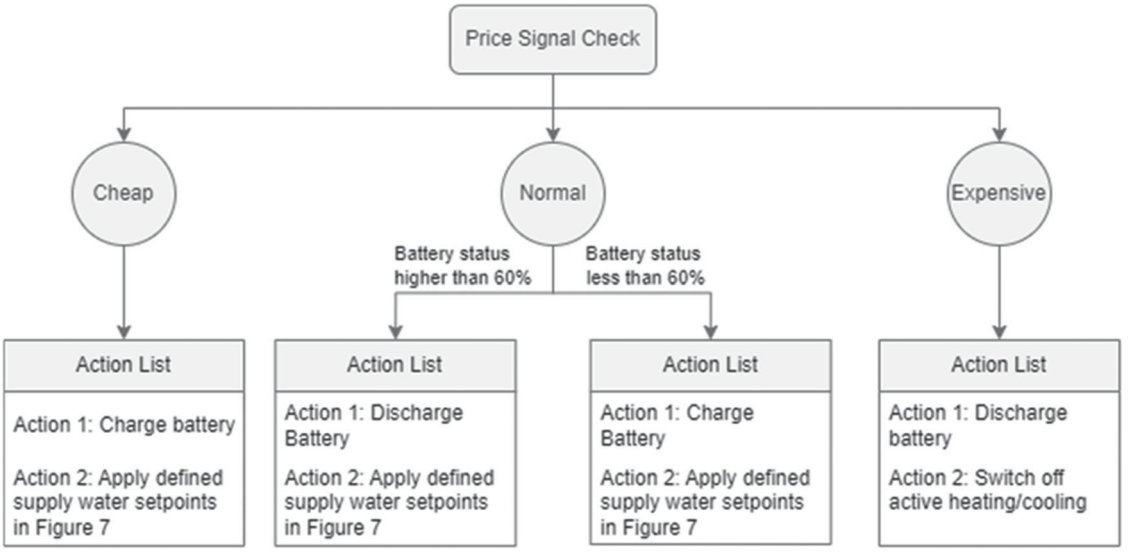

Figure 8. Building control application for flexible operation case.

expensive electricity periods, the building minimizes its demand to reduce costs. This likely translates to the lower temperature readings during peak price hours by switching off the active heating system. During these times, the building's electrical demand, excluding heating since the system is not running, is met by discharging the EES, provided sufficient charge is available.

In addition to controlling the supply water temperature setpoint, the EES charging/discharging cycle is simultaneously regulated, applying the same EES control strategy for both RBC and RBPC. During cheap price periods, the EES is charged until the State of Charge (SoC) reaches 100%, with no energy being discharged. Also, during normal price periods, the system monitors the SoC. If it falls below 60%, charging is initiated until the SoC reaches 60%. Conversely, if the SoC is higher, the system discharges the EES to meet the building's electrical demand. However, during expensive price periods, the EES can be discharged regardless of the SoC level, with no energy being charged.

The operational control strategies are presented in Figure 8. In addition to these control strategies, a feed-in approach is applied when there is excess energy; this is included in the shifted cost calculation by applying the same electricity unit tariff as shown in Figure 6.

Grid-oriented operation

For case(4), the primary objective is to reduce power demand by the exact amount requested by the aggregator. This process follows a sequential strategy: first, the EES is activated to discharge power, prioritizing demand reduction. The discharged power is intended to precisely match the grid request. However, if the discharged power is insufficient, supply water setpoints are adjusted to further lower demand. To find the most suitable setpoints ensures the closest power demand change close to the requested value, IDA-ICE simulates multiple setpoints. The effectiveness of demand adjustment in case(4) is evaluated using load matching grid index (LMGI).

$$\mathrm{LMGI} = \frac{P_{case(3)} - P_{case(4)}}{P_{request}} \times 100 \tag{1}$$

Traditionally, the LMGI has been used to assess the alignment between on-site generation and energy demand. We extend this concept by focusing on temporal alignment between building load and grid signals, particularly during grid-constrained periods. The LMGI used in our study evaluates how well the building adapts its load profile to match grid support needs. This adapted use of the matching index is conceptually consistent with the grid interaction indicators presented in the Salom et al. (2011), Voss et al. (2010), Sartori, Napolitano, and Voss (2012), and it allows for quantifying the effectiveness of building response during specific operational stress periods on the grid. Furthermore, while power-based indicators like demand response effectiveness offer fine-grained evaluation of instantaneous response, the LMGI provides a complementary system-level indicator that reflects both operational alignment and systemic impact during targeted grid events. This approach is aligned with expectations outlined in initiatives such as Enera (Projekt Enera 2025), GOPACS (GOPACS 2025), and NODES (NODESmarket 2025), where localized and time-coordinated demand shifts are rewarded as grid-supportive actions. Similarly, the U.S. Department of Energy's Grid-interactive Efficient Buildings performance

framework emphasizes the alignment with system signals (Schiller, Schwartz, and Murphy 2020).

As the LMGI approaches 100%, the system provides better support for ensuring grid stability. $P_{case(3)}$ and $P_{case(4)}$ represent the load demand from the power grid (in kW) in case(3) and case(4), respectively. $P_{request}$ denotes the power change requested by the aggregator. In both operation optimizations, the maximal power capacity of the heating system, as well as the surface temperatures are applied as constraints.

Substation Load

This study utilizes real monitored data from a local utility, capturing substation load fluctuations in a 100 kW neighbourhood grid. On average, demand exceeding 50 kW triggers a yellow status, indicating mild substation stress, while loads above 65 kW signal a critical condition, necessitating grid support. On December 5th, between 08:00–09:00, the substation load is projected to reach 60.55 kW, prompting the distribution system operator to request a 10.55 kW demand reduction via the aggregator. This research optimizes building operations to achieve the required reduction, ensuring grid stability through demand-side flexibility.

Rule-based predictive control

A primary challenge in implementing RBPC is reducing computational time, as running a white-box model can result in significantly long simulation times, e.g. lasting 25 hours as discussed in section Computational Benchmark. To address this challenge, two key simplifications are introduced as limiting the number of possible setpoints for scenario development and dividing the 24-hour prediction horizon into four control horizons to improve computational efficiency (Figure 9). Therefore, instead of solving an optimization problem at every control step, RBPC selects the best operational scenario from a predefined set, significantly reducing computational time. The best operational scenario means achieving the most cost-effective scenario during case(3) and highest LMGI for case(4).

The possible setpoints for the supply water temperature are determined based on the day-ahead price signal categorization, as detailed earlier. The approach follows these rules: during low-price periods, the supply temperature setpoint is increased by either 1°C, 2°C, or 3°C above case(1), whereas during normal-price periods, it is reduced by 1°C, 2°C, or 3°C below case(1). Users can customize setpoint options based on their specific case when applying RBPC. In RBPC, only scenarios that comply with predefined comfort limits are retained, and setpoints are adjusted based on historical performance to prevent inefficient operations.

By applying these values, a set of simulation scenarios is generated by combining all possible setpoints across a 24-hour prediction horizon. For example, if 01:00 falls within a cheap price period with three predefined setpoint options (A, B, or C), and 02:00 is a normal price period with another three predefined setpoint options (C, D, or E), then these values are combined to create nine possible scenarios as A–C, A–D, A–E, B–C, B–D, B–E, C–C, C–D, and C–E. Extending this method to a 24-hour window leads to a rapid increase in the number of possible scenario combinations, requiring computational efficiency improvements.

To reduce the computational burden while maintaining forecasting accuracy, the 24-hour prediction horizon is divided into four six-hour control horizons, as illustrated in Figure 9. Each control horizon follows a stepwise decision-making process. During the first control horizon (00:00–06:00), RBPC determines the most cost-effective demand profile for this period, and the selected setpoints are saved as inputs for the next control horizon. In the second control horizon (00:00–12:00), the previously determined setpoints from 00:00–06:00 remain fixed, while new setpoints for 06:00–12:00 are calculated using RBPC. Once finalized, the additional setpoints are stored for the following control horizon. This methodology is then applied to the next control periods as 12:00–18:00 and 18:00–00:00. In other words, subsequent control horizons follow the same iterative process until the full 24-hour prediction horizon is completed. After each control horizon, the power demand results from all simulated scenarios, computed by IDA-ICE, are stored in MATLAB. These values are then used for cost calculations, and the scenario yielding the lowest operating cost is selected as the final decision.

After each scenario, the load values from various building consumers as heat pump (P_t^{HP}), fans (P_t^{fans}) pump (P_t^{pumps}), lighting ($P_t^{lighting}$), plug-in loads ($P_t^{plug-inloads}$), PV generation (P_t^{PV}), and EES ($P_t^{EES\ charge}$, $P_t^{EES\ discharge}$) are stored in MATLAB to compute the cumulative power demand (P_h^{Total}) with hourly resolution.

$$P_h^{Total} = \sum_{t=1}^{T} (P_t^{HP} + P_t^{fans} + P_t^{pumps} + P_t^{lighting} + P_t^{plug-in\ loads} + P_t^{EES\ charge} - P_t^{EES\ discharge} - P_t^{PV}) \quad (2)$$

Subsequently, the cost for each scenario (C_h) is calculated using the day-ahead prices (λ_t), and the total cost is saved in the numerical tool.

$$C_h = \sum_{t=1}^{T} (P_t^{Total}\ \lambda_t - P_t^{feed-in}\ \lambda_t) \quad (3)$$

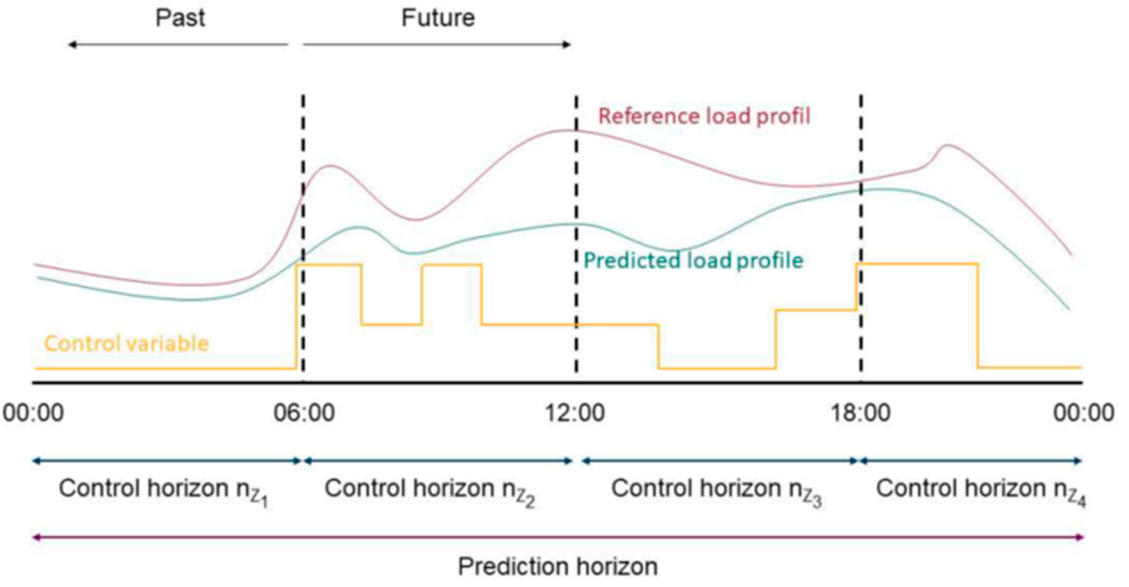

Figure 9. Control horizon of RBPC algorithm.

To determine the most cost-efficient scenario, the scenario with the minimum cost is selected for the respective control horizon. The setpoints of the selected scenario are then saved in MATLAB to serve as input for the subsequent control horizon, as described.

$$C_h^{Scenario} = \min(C_h^1, C_h^2, \ldots, C_h^n) \tag{4}$$

By this methodology, instead of computing optimal setpoints at each step, RBPC replaces iterative optimization with a predefined scenario selection approach, evaluating a limited set of pre-generated operational scenarios to determine the most suitable one based on predefined criteria. Unlike conventional RBC, which applies static control logic (fixed setpoint) without predictive capabilities, RBPC enables proactive decision-making by considering market prices in advance. While RBPC does not always guarantee a globally optimal solution, as MPC theoretically does, it strikes a balance between modelling feasibility and performance, making it a viable alternative.

In this study, the RBPC uses published day-ahead prices (at 12:00–13:00 for the next day's optimization), which are final and do not change once announced. Therefore, forecast errors are not present in this study. In scenarios where control decisions must be made before the official day-ahead prices are released, forecasting is required to estimate the expected price signals. In such cases, the forecasting error arises from uncertainty in market drivers and typically ranges between 10% and 15% under normal market conditions. The implemented quartile-based price categorization method in RBPC adds a degree of robustness to electricity price forecasting uncertainty, as the control logic depends on relative price levels (expensive, normal, cheap) rather than absolute values. Although the robustness of the RBPC under explicit price forecast errors was not directly tested in this study, we consider the approach to be moderately tolerant to typical day-ahead forecasting deviations, particularly because small variations are unlikely to shift a price value from one category to another.

In addition to price variability, other sources of uncertainty such as outdoor temperature fluctuations and variations in heat pump performance may affect the effectiveness of the proposed control strategy. In the current RBPC setup, temperature forecasts from the day before are used as inputs to generate control decisions. However, the model does not include a mechanism to update or recalibrate itself based on real-time deviations between forecasted and actual temperatures, which could reduce responsiveness in cases of abrupt weather changes. Similarly, the performance of the ground source heat pump can fluctuate due to changes in ground temperature or partial load operation, which may lead to deviations between expected and actual energy consumption. These performance shifts are not captured in the current framework.

One limitation of RBPC is that it follows a fixed-horizon approach, meaning that once a control horizon is completed, its setpoints remain unchanged. This could lead to suboptimal operation if new constraints emerge after a decision has been made. Unlike advanced control algorithms such as MPC, which continuously revises past decisions based on updated information, RBPC does not reconsider previous control horizons.

Another key consideration is the scalability of RBPC for finer time resolutions. Currently, RBPC operates on an

hourly resolution. However, if the system were to shift to a smaller time step, it would remain applicable, although the number of possible scenarios would increase significantly.

In grid-oriented operation, the optimization is applied to achieve the highest LMGI. First, the EES is activated to discharge power, aiming to meet the distribution system operator demand reduction request.

$$P_t^{case(4)} = P_t^{case(3)} - P_t^{EES\ discharge} \quad (5)$$

To verify whether the discharged amount is sufficient to meet the requested demand change, LMGI is calculated and compared to a 100% success benchmark.

$$LMGI_t = \min(LMGI_t, 100) \quad (6)$$

If the discharged power is insufficient to meet the requested demand reduction, the supply water temperature setpoints are adjusted to further lower demand. Initially, a 1°C lower setpoint is applied, and the total power demand P_h^{Total} is used to recalculate the $LMGI_t$. If the result does not meet the success benchmark, the setpoint is further reduced by 2°C and then 3°C, testing for the optimal adjustment. In other words, to determine the most suitable setpoints that achieve the closest match to the requested power demand change, IDA-ICE simulates multiple setpoints.

RBPC supports grid stability by reducing/increasing building load during congestion events, and it is not designed to provide direct frequency or voltage regulation. Frequency and voltage control require fast-reacting assets and grid-forming inverters, which are not within the operational scope of the HVAC systems.

Co-simulation environment

This research employs a co-simulation framework to perform two distinct calculations mentioned before, each requiring dedicated tools based on specific objectives as (a) BPS tool to calculate building energy system operation and assess thermal comfort, and (b) numerical computing tool to implement advanced control algorithm such as RBPC for optimizing load demand management based on aggregator request and cost-effective operation.

Since these calculations are interdependent, they must be executed concurrently within a dynamic simulation environment, where each time step's results serve as inputs for the next time step. To achieve this, a co-simulation framework was developed, integrating IDA-ICE (BPS tool) and MATLAB (numerical computing tool).

The initial connection between IDA-ICE and MATLAB was established using a standard MATLAB script provided by the IDA-ICE developers. This script was subsequently enhanced with RBPC functionalities, enabling data exchange and control implementation. The connection facilitates data transmission between IDA-ICE and MATLAB via functional mock-up interface, allowing MATLAB to send control setpoints and receive simulation results at each time step.

The co-simulation environment is primarily controlled by MATLAB, which automates the following processes: First, MATLAB establishes the channel connection with IDA-ICE. Then, it manages data storage and launches IDA-ICE, defining the simulation time window (e.g. specifying start and end times). Next, MATLAB transmits supply water setpoints and EES charging/discharging action to IDA-ICE and retrieves simulation results. At each time step, the simulation results are stored for post-processing. Finally, MATLAB ensures the proper termination of IDA-ICE upon simulation completion. This workflow is repeated for each RBPC scenario, ensuring that the co-simulation accurately captures both market-oriented and grid-oriented optimization cases.

To ensure data integrity and computational stability, the communication time step resolution is a highly sensitive parameter. While high-resolution time steps (e.g. 1 to 5 minutes) improve data accuracy, they impose a significant computational burden, leading to instability and premature termination of the simulation. To balance accuracy and stability, multiple tests were conducted, and a 15-minute time step was selected as the optimal resolution. The time step determination process considered key performance indicators, including simulation stability (ensuring uninterrupted execution), data transmission reliability (preventing missing values in data exchange), completeness of IDA-ICE simulation outputs (confirming all results are properly generated and stored). Scaling RBPC to finer time resolutions (e.g. 15-minute steps) requires further research, as increasing scenario complexity may challenge computational efficiency. It should be noted that the 15-minute interval refers to the communication time step in the co-simulation environment. The BPS still runs at a finer internal resolution (on the order of seconds). However, due to co-simulation limitations, only 15-minute averaged values are exchanged between simulation tools.

However, a data loss issue was identified when exporting results from IDA-ICE to MATLAB. Since these exported values serve as inputs for cost optimization calculations in MATLAB, any mismatch between actual simulation results and received values could introduce significant errors in RBPC, leading to discrepancies between simulated and real-world performance.

To resolve this issue, an alternative approach was implemented. IDA-ICE saves simulation results in '.prn' format in a local directory. A custom MATLAB script was developed to read and process the '.prn' files, ensuring

accurate input values for RBPC optimization. Data transmission through the export module was ignored, preventing reliance on potentially incomplete or incorrect exported values. Notably, this data loss problem was only observed in the IDA-ICE to MATLAB export process, whereas the import process (MATLAB sending data to IDA-ICE) remained stable and unaffected.

Results

This section presents a comprehensive evaluation of the building's operational performance under different control strategies. The analysis systematically investigates five distinct operational scenarios as Business-as-Usual [case(1)], market-oriented operation with RBC [case(2)], market-oriented operation with RBPC [case(3)], grid-oriented operation with RBPC [case(4)], and post-grid response market-oriented operation with RBPC [case(5)].

Case(1) and case(2) are analyzed over a week-long period from December 5th to December 11th, capturing long-term trends in baseline and RBC. In contrast, case(3), case(4), and case(5) are evaluated for a single representative day, December 5th, focusing on the impact of predictive control using RBPC. This distinction allows for a detailed comparison of daily response mechanisms under different control strategies.

Based on this operational analysis, the following section examines key performance indicators that characterize the impact of each case. The EES's charging and discharging cycles are investigated, emphasizing the effectiveness of short-term load shifting strategies. Patterns of energy consumption shifted from the grid are delineated, and the economic implications of these operational strategies are explored, underlining potential cost savings.

The operation of the heat pump, which corresponds with price signals, is evaluated. Variations in surface temperatures are examined to assess the impact of the control strategy employed. The simulation results of heat flux density offer insights into the thermal loading and unloading cycles of the building's thermal mass. Additionally, indoor temperature data demonstrates the effectiveness of our control approach.

EES charging /discharging cycle

Figure 10 depicts the EES charging and discharging patterns under case(1) and case(2). In case(1), EES usage is optimized for self-consumption, meaning that excess PV generated electricity is first used to meet the building's immediate electrical demands before charging the EES. Due to low PV generation in winter, minimal EES charging occurs from this source. Since no grid-charging strategy is in place, EES relies solely on PV generation.

In contrast, case(2) is characterized by an active EES cycle, with regular charging and discharging. Here, the system not only responds to PV generation but also actively manages the EES in anticipation of fluctuating electricity prices, irrespective of the lower winter PV output. Case(2) system's responsive charging strategy exploits periods of lower prices or excess PV generation, storing energy that can be used during peak price periods or when PV generation is insufficient.

Figure 11 illustrates that case(3) improves EES efficiency by applying predictive control, ensuring that charging and discharging are optimized for price fluctuations, thereby enhancing the overall cost saving strategy. In case(2), the EES charges and discharges a total of 24 kWh. In case(3), charging increases to 29 kWh, while discharging remains at 24 kWh.

As mentioned earlier, this research analyzes the optimization of a grid congestion event that occurs on December 5th between 08:00 and 09:00 at a substation, aiming to lower the power demand by 10.55 kW.

Case(4) prioritizes load curtailment during congestion events, requiring the EES to support demand reduction efforts as previously explained. During the congestion event between 08:00 and 09:00, the EES discharges up to −8 kW, with a higher discharge not being possible due to the current SoC. On the following hour, case(5) resumes market-oriented operation, applying new EES charging/discharging events. EES charging differs from case(3) after 09:00 as 8 kW was discharged before and SoC was 20%. On the following hour, EES is charged till the SoC reaches to 60% as it is normal price category.

Heat pump operation

Figure 12 illustrates the supplied water temperature by the heat pump. It compares case(1) and case(2), showing fluctuations in temperature across the monitored period. Case(1) operates within a narrower temperature range. Case(2) allows for more variability in temperature, which indicates adaptive strategies to optimize cost optimization based on price signals and demand response requirements.

The analysis reveals a distinct operational adjustment in case(2) during periods of low electricity prices. For instance, on December 6th at 00:00, the supply temperature in case(2) is approximately 10°C higher compared to case(1), suggesting thermal storage in anticipation of higher prices. Conversely, at around 23:00 on the same day, the temperature in case(2) decreases by an estimated 15°C below the case(1) level in response to a spike in electricity prices.

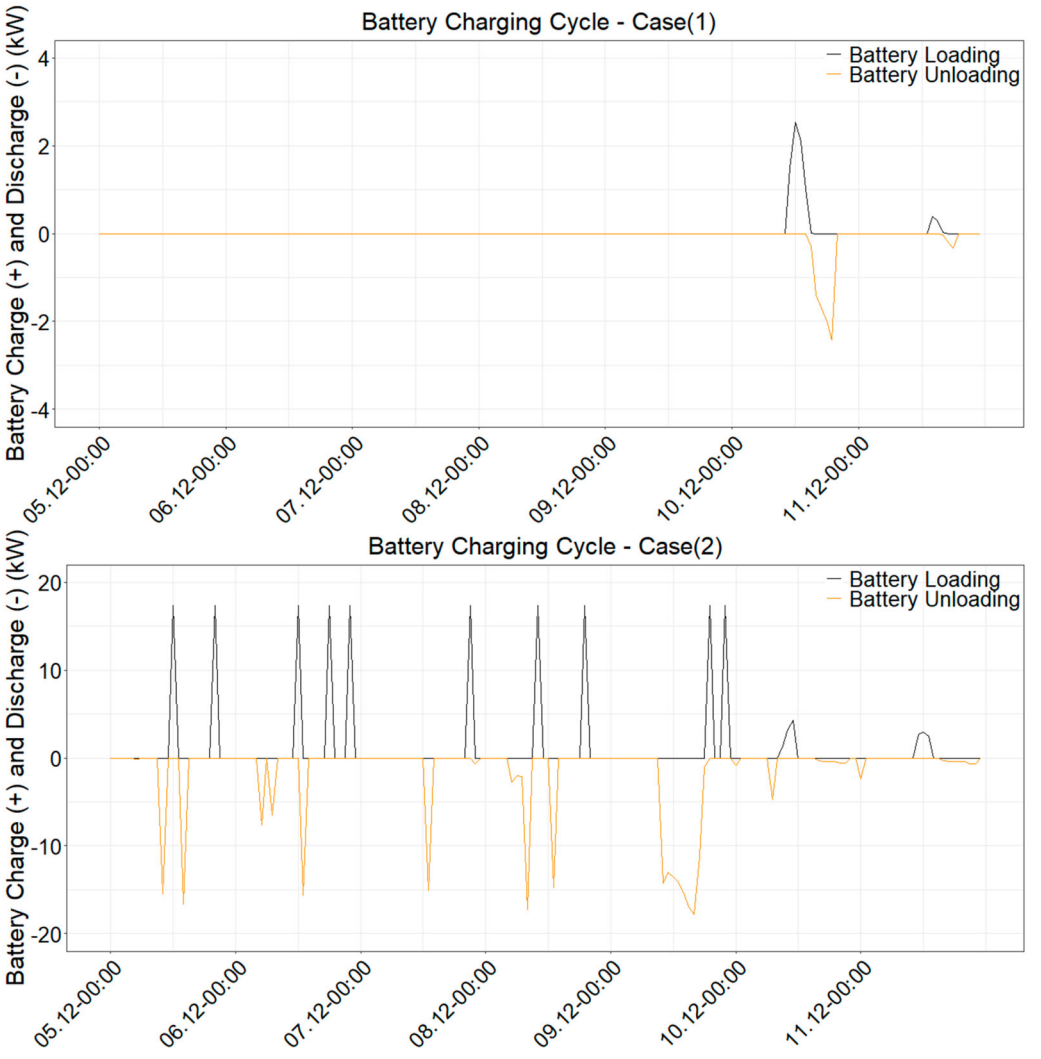

Figure 10. EES charging/discharging cycle for a representative week.

In the simulation, increasing the heat pump supply temperature to a higher level resulted in an immediate increase in compressor power demand within the same simulation timestep. The system responded to the assigned setpoint change in a few seconds and it reflected on the power grid demand in that certain. However, the thermal system response at the zone level was subject to hydronic inertia resulting in a delayed rise in delivered temperature over several minutes. Conversely, when the supply temperature was reduced, the compressor power decreased in a few seconds, however, the thermal system response takes longer.

The additional analysis in Figure 13 further explores the hourly variations in supply water temperature across all five cases on the representative day. Case(3) refines the flexibility approach of case(2) by incorporating predictive control strategies. Between 00:00 and 16:00, when the price is in the cheap or normal period, the supply temperature in case(3) fluctuates by approximately ± 1°C to ± 3°C compared to case (2).

The distribution system operator requested a power demand reduction of 10.55 kW compared to case(3) due to the congestion event, however, based on the EES capacity, only 8 kW could be discharged between 08:00 and 09:00 as presented in Figure 11. Since the LMGI falls below 100%, the heat pump operation is adjusted. In response to this, in case(4), the supply temperature is reduced by 1°C, 2°C, and 3°C, resulting in power reductions of 396 W, 840 W, and 1346 W, respectively. As the highest LMGI is achieved at the lowest supply temperature, a supply temperature of 34.8°C is applied in the operation as given in Figure 13. Once the congestion event passes, case(5) resumes market-oriented operation. As the EES is charged between 09:00 and 10:00 following its discharge in case(4), leading to increased demand from the grid, case(5) recalculates lower setpoints compared to

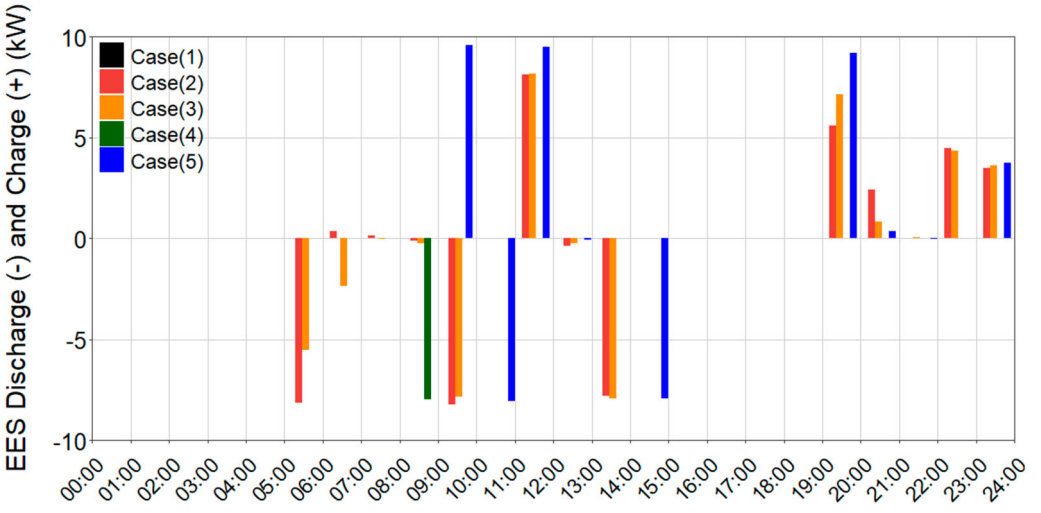

Figure 11. EES charging/discharging cycle across all operational cases for a representative day.

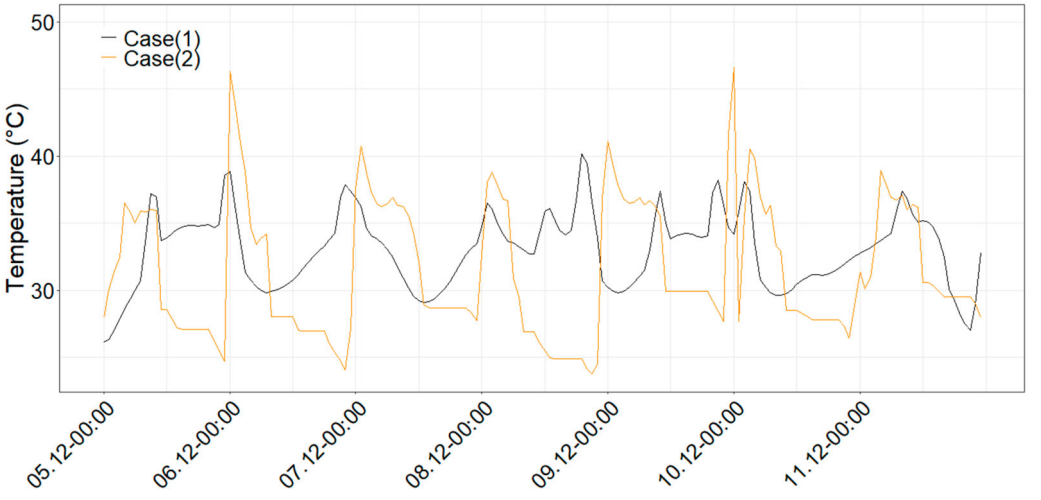

Figure 12. Heat pump supply water temperature for a representative week.

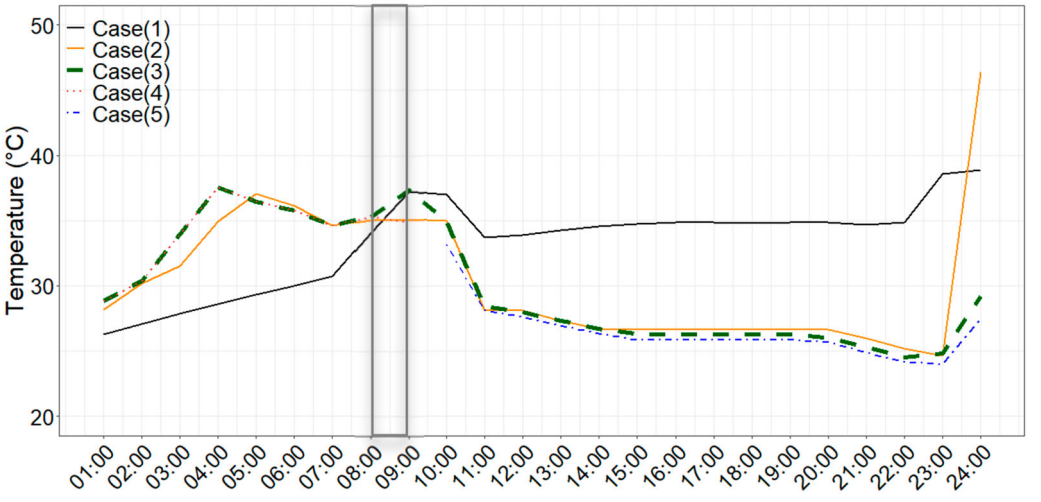

Figure 13. Heat pump supply water temperature across all operational cases for a representative day.

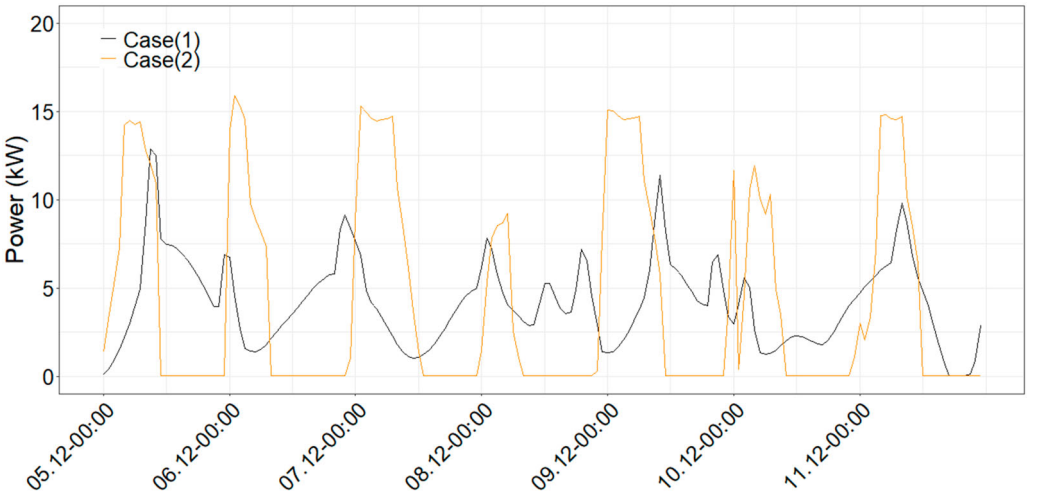

Figure 14. Heat pump power demand for a representative week.

case(3) to ensure cost-effective operation for the remainder of the day.

The electrical power demand of the heat pump is shown in Figure 14. Depending on the outdoor temperature and load variations, the COP of the heat pump was found to range between 3 and 5. The power demand in case(1) exhibits predictable peaks, likely corresponding to regular daily usage patterns and fixed setpoint temperatures.

Contrastingly, case(2) demonstrates periods where the power demand sharply decreases below case(1) levels, indicating adaptive energy use in response to variable pricing. These drops correspond to periods where the system load shifts and EES discharge to reduce power usage from grid when electricity prices are higher. Notably, on December 6th from 10:00 onwards, case(2) registers minimal to no power demand as a strategic response to the high prices. Conversely, at 00:00 on December 6th, there is a significant surge in the case(2) power demand, which is twice that of case(1), corresponding to the elevated supply temperature as given in Figure 12.

In Figure 15, the shifted peak demand in case(3) is observed, resulting from the increased supply water temperatures shown in Figure 13. During case(4), a demand reduction of 1346 W occurs during the congestion event. The total demand minimization period lasts for one hour, reducing stress on the local substation.

In case(5), power demand decreases between 10:00 and 11:00 compared to case(3) to compensate for the increased demand from EES charging, ensuring cost-effective operation. By the end of the 24-hour period, heat pump power demand is reduced by a total of 6% due to the adjustments made during case(4) and case(5).

Grid interaction

Figure 16 indicates that the building primarily demands power from the grid, rarely feeding power back due to the limited PV generation during the winter season. This unidirectional interaction suggests that the building under case(1) relies on the grid for its energy needs, without offering flexibility services to the grid. Case(2) shows a dynamic pattern of interaction with the grid, as EES is charged in addition to meeting the conventional building power demand, resulting in higher peak demands – reaching 40 kW in case(2) compared to 30 kW in case(1).

A daily representation of grid interaction for all cases is illustrated in Figure 17. In case(3), the building's load demand from the power grid is approximately 29.2 kW. By activating case(4), the EES discharges 8 kW, and heat pump power demand is reduced by 1.35 kW, resulting in a total demand reduction of 9.35 kW. Consequently, the power demand of case(4) from the power grid is reduced to 19.85 kW.

Short-term load shifting

Figure 18 shows the difference in total power demand of all consumers in the building except EES between case(1) and case (2) over time, with an hourly resolution. When the bars are above the zero line, this indicates that case(2) demands more power than case(1) during that hour. This occurs due to case(2) responding to lower price signals. Vice versa, when the bars are below the zero-line, case(2) demands less power than case(1).

The range of values spans from around −8 kW to 14 kW. This indicates that the maximum additional power demand in case(2) compared to case(1) is about 14 kW,

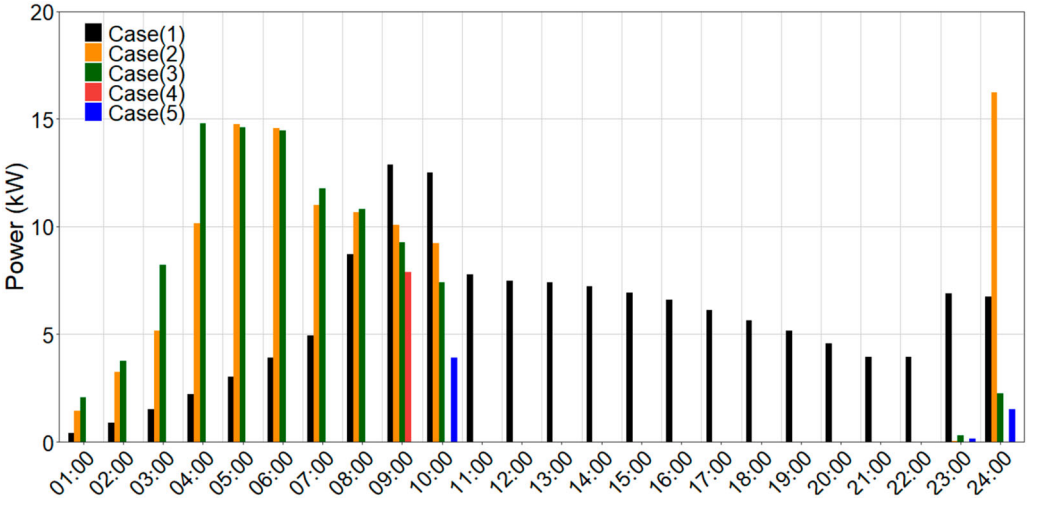

Figure 15. Heat pump power demand across all operational cases for a representative day.

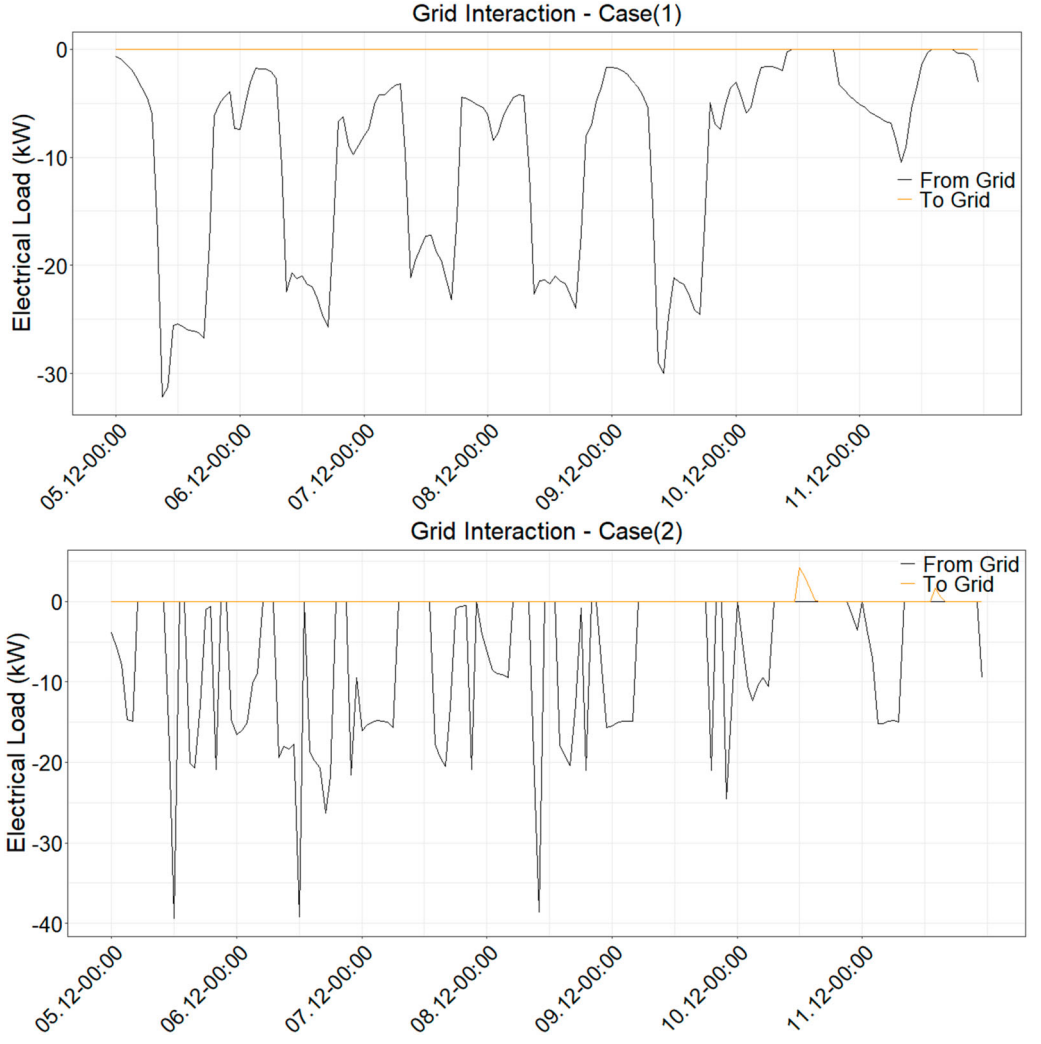

Figure 16. Building-grid interaction for a representative week.

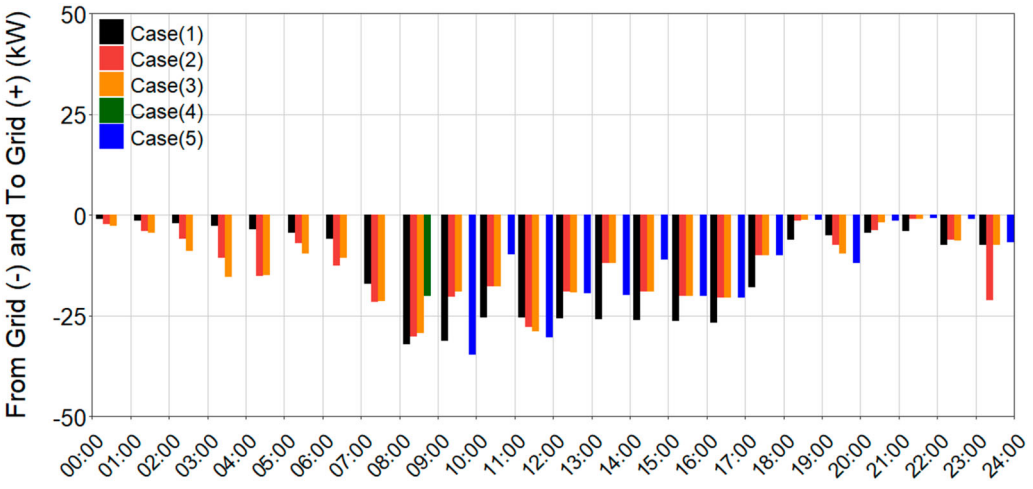

Figure 17. Building-grid interaction across all operational cases for a representative day.

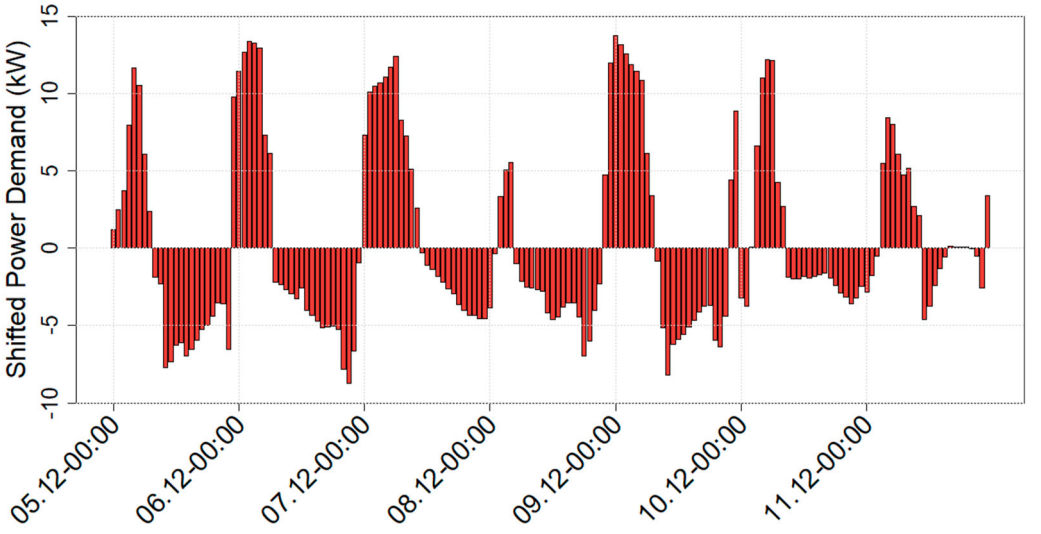

Figure 18. Shifted electrical power demand of all building actuators for a representative week.

and the maximum savings are about 8 kW. In case(2), a cumulative increase in demand of 450 kW has been observed for this representative week, which is consistent with the tendency for building-grid operations to amplify heating demand. This phenomenon often occurs as flexibility measures, such as load shifting, incentivizing the use of heating systems at times when electricity is less expensive.

Figure 19 presents the shifted load from all cases compared to case(1) for the representative day. During the early hours, the building takes advantage of cheap prices and the charging planned differently on case(2) and case(3) as case(3) also considers the cumulative favourable operation cost during the cheap and normal price period.

Figure 20 illustrates the difference in energy consumption from the power grid between case(1) and case(2), including the effect of the EES. The consumption difference ranges from approximately −15 kWh to +15 kWh. In case(2), weekly increase of 82 kWh in energy consumption from the power grid is observed.

Figure 21 illustrates the shifted demand across all building actors for the representative day by comparing all cases to case(1). In case(3), the maximum power demand shift exceeds that of case(2), with peaks reaching approximately 15 kW. The demand difference between case(3) and case(4) is 9.35 kW. Due to the limited discharge capacity of the EES, heat pump operation is adjusted by modifying temperature setpoints. Consequently, the LMGI is calculated at 88.6%.

The observed 88.6% LMGI indicates limitations in fully meeting the grid operator's demand reduction request, primarily due to the constrained capacity of the EES. While this study focused on heat pump and battery control, additional flexibility sources could be explored to enhance grid-oriented responsiveness. For instance,

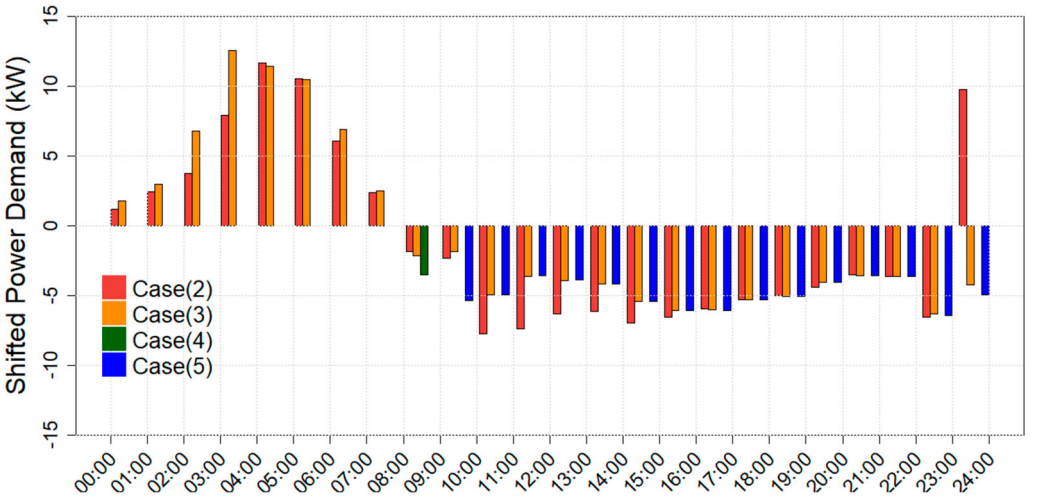

Figure 19. Shifted electrical power demand of all building actuators across all operational cases for a representative day.

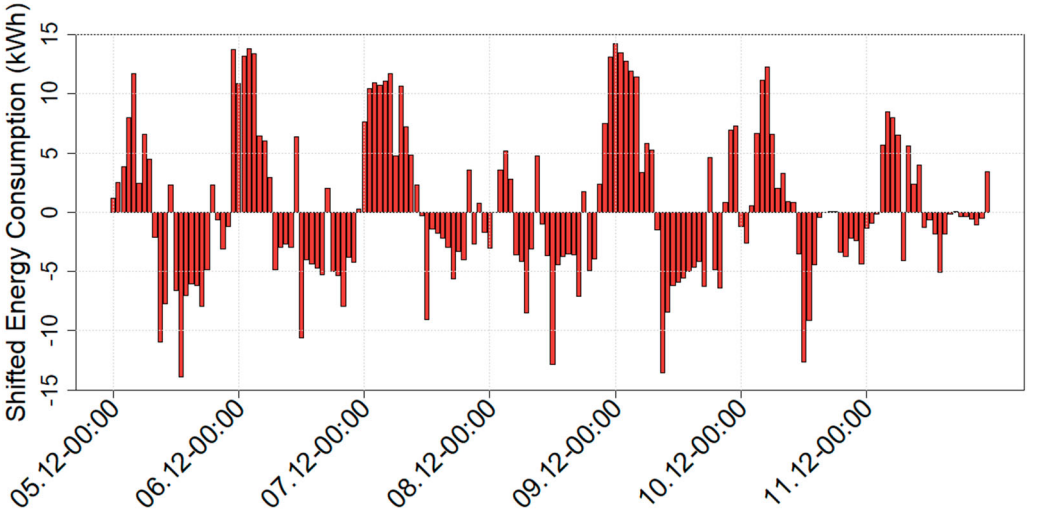

Figure 20. Shifted electrical energy consumption from power grid for a representative week.

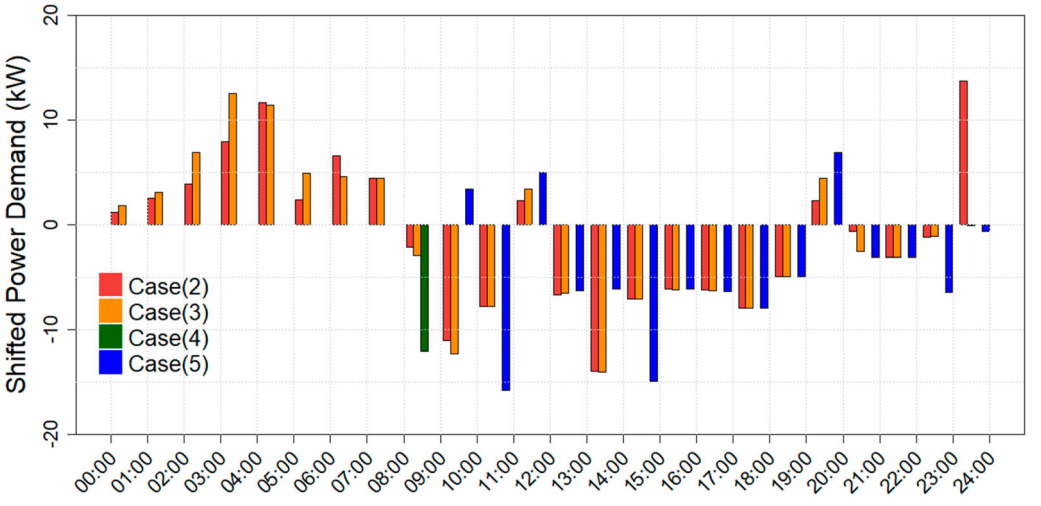

Figure 21. Shifted electrical energy consumption from power grid across all operational cases for a representative day.

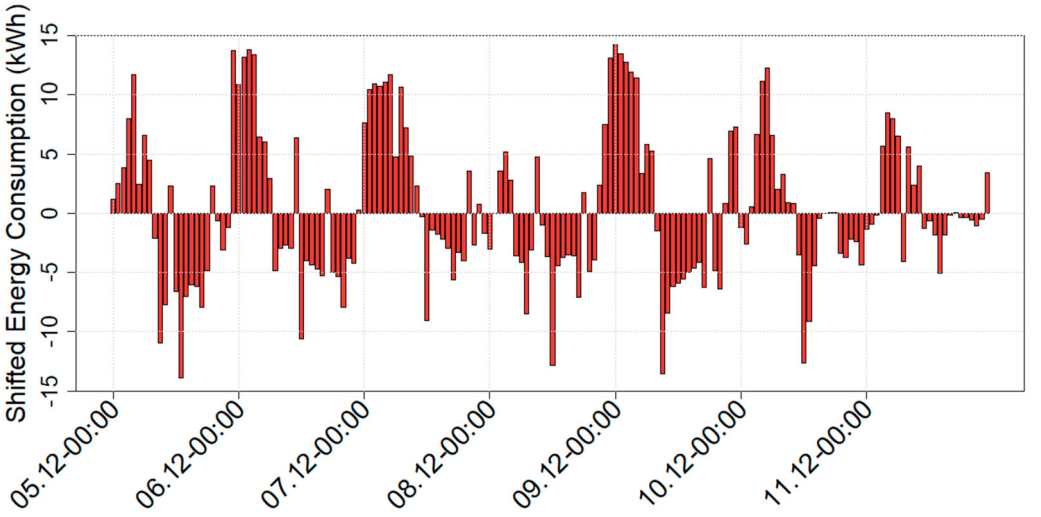

Figure 22. Shifted operational cost for a representative week.

temporary control of ventilation systems (e.g. switching off air handling units for short durations during non-critical hours) may contribute to power reduction without significantly compromising indoor air quality or occupant comfort, moreover, modulating lighting setpoints, dimming non-essential lighting. On the other hand, integrating occupant-driven flexibility, e.g. manual appliance shutdowns, offers limited potential in this context. Since demand must be reduced quickly following a grid signal, reliance on occupant intervention introduces uncertainty and delay. Moreover, the analyzed building is an office environment, where turning off computers or lighting could negatively affect productivity and user satisfaction.

Cost saving

Figure 22 illustrates the difference in cost between case(2) and case(1) over the representative week. The cost differences range from approximately −7 € to +5 €, with negative values indicating cost savings and positive values indicating additional costs compared to case (1). Similar to Figure 20, this cost graph also shows considerable volatility, which implies that the cost savings are not constant over time but fluctuate significantly. Although energy demand from the power grid increases by 82 kWh when building-grid interaction is activated in case(2), a 3.5% reduction of cost is achieved over the representative week, highlighting the economic benefits of this operational strategy. As a typical outcome of grid-interactive operation, increased consumption leads to lower costs by shifting demand to favourable periods.

To investigate further saving, RBPC is applied, and the cost results are compared to case(2) where RBC is implemented. Figure 23 illustrates the cost variations across all cases for the representative day. One of the key motivations for introducing RBPC was to achieve higher cost savings in case(3) compared to case(2). During this representative day, case(2) and case(3) resulted in cost reductions of 15 € and 20 €, respectively, with RBPC achieving a 2.5% greater reduction compared to RBC. When the congestion event occurs, costs decrease due to reduced heat pump demand and EES discharge in case(4). However, after transitioning to case(5), demand increases due to active EES charging. Despite this temporary rise, the cost optimization process in case(5) accounts for this increase and adjusts demand accordingly for the remainder of the day, resulting in cost savings of 18 €, which is 10% less than the initially planned reduction in case(3).

Surface temperature variations

The implications of the RBC strategy on the surface temperature profiles across the four different office orientations – Southeast (SE), Southwest(SW), Northeast (NE) and Northwest (NW) are observed. In all offices, there are noticeable differences between case(1) and case(2) temperature profiles, which suggest that case(2) operations affect the surface temperatures within the building (Figure 24).

In case(2), the curves exhibit greater fluctuations compared to case(1), indicating more dynamic control in response to price signals. The patterns appear relatively consistent across the four offices, which indicates a centralized control strategy for temperature management that affects all areas uniformly. In case(1), temperatures fluctuate between approximately 22.5°C and 24°C.

However, in case (2), the lower boundary has notably reduced to 21°C, and surface temperatures demonstrate a broader oscillation, spanning a 3°C range. At 18:00 on December 6th, the ceiling temperature in case(1) registers

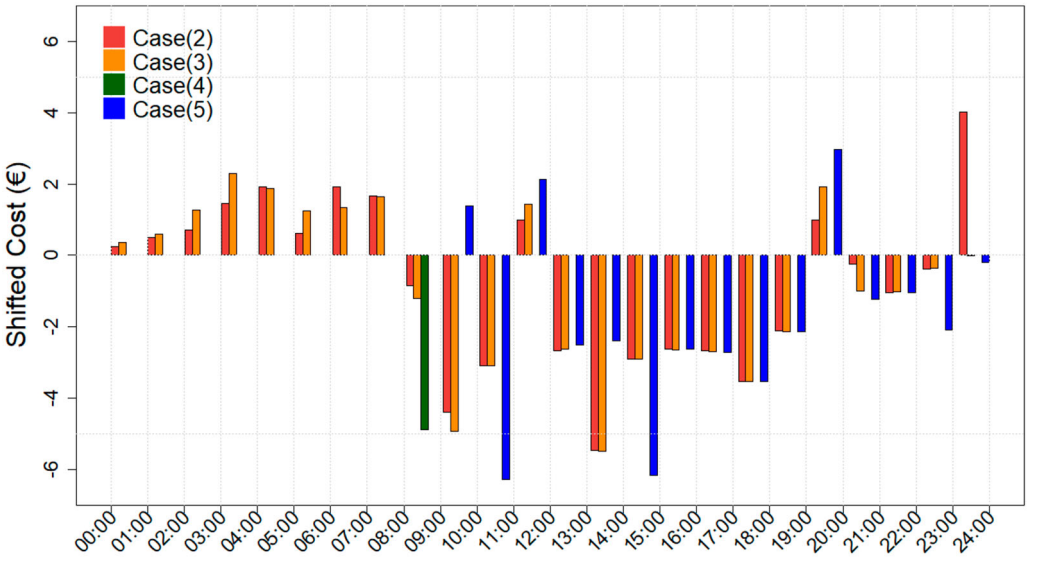

Figure 23. Shifted operational cost across all operational cases for a representative day.

at approximately 23.5°C, while in case(2), it measures around 22°C.

To analyze the effect of RBPC and congestion event control, Figure 25 presents a daily representation of surface temperature changes. Case(3) maintains temperatures within a range of 21.5°C to 22.75°C, similar to case(2), where slight variations occur at different times as RBPC shifts loads in alignment with the price signal. However, in case(4), due to the prioritization of grid stability, the heat pump supply temperature is reduced. The results, however, show that its impact on surface temperature is minimal, with no temporary surface temperature reductions observed.

Heat flux density

Figure 26 displays a cyclical pattern reflecting flux variations influenced by the building's operational schedules and the dynamic nature of internal heat gains and losses. Case(2) exhibits higher peaks and lower troughs in heat flux compared to case(1). This suggests that in case(2), the building's thermal mass is strategically utilized to absorb heat during times when energy prices are low, storing it for later use. Case(1), in contrast, shows a more uniform heat flux, indicating a consistent but no economically responsive energy use.

As observed in the surface temperature trend, the heat flux peak values are similar; however, they occur at different times to achieve higher cost savings when comparing case(2) and case(3), as shown in Figure 27. As the supply temperature decreases in case(4) during congestion events, there is no suppression of heat flux, with values remaining very close at $-0.5\,W/m^2$ in both case(3) and case(4). After the congestion event, the optimized operation in case(5) follows a similar pattern to case(3).

In the heating phase, TABS systems engage in thermal loading, capturing and storing heat within the building's mass. This stored energy is strategically released during thermal unloading to provide warmth, thus minimizing the need for active heating. The thermal energy storage behaviour under case(1) (Table 2) and case(2) strategies (Tables 3 and 4) for the 5th of December was observed for relevant office zones in the building, indicating distinct operational profiles.

The analysis pertains to the ceiling thermal loading and unloading cycles. Under case(1) condition, the SE zone underwent a thermal loading of 3.8 kWh, executed during the early morning hours (01:00–08:00), followed by an 8-hour unloading period (08:00–16:00). The case(2) strategy modified the loading to 3.4 kWh, distributed across three intervals (01:00–05:00, 11:00–12:00, 18:00–20:00), thereby demonstrating a segmented approach synchronized with periods of lower energy tariffs and thermal comfort optimization. Correspondingly, the thermal unloading was partitioned into three segments (05:00–11:00, 12:00–15:00, 20:00–21:00), indicative of a refined strategy to modulate indoor conditions.

The discernible pattern established for the SE zone provides a framework to interpret the thermal loading and unloading behaviours in the remaining zones. While the specific values and timings differ, the underlying principles observed in the SE analysis can be extrapolated.

The case(2) strategy's inclination toward segmented operations is evident, likely reflecting its price signal-driven approach, which governs the system's engagement with the energy market and thermal comfort requirements. The loading cycles of case(3), case(4), and case(5) are not presented, as they are relatively similar to case(2), with no significant variations to report.

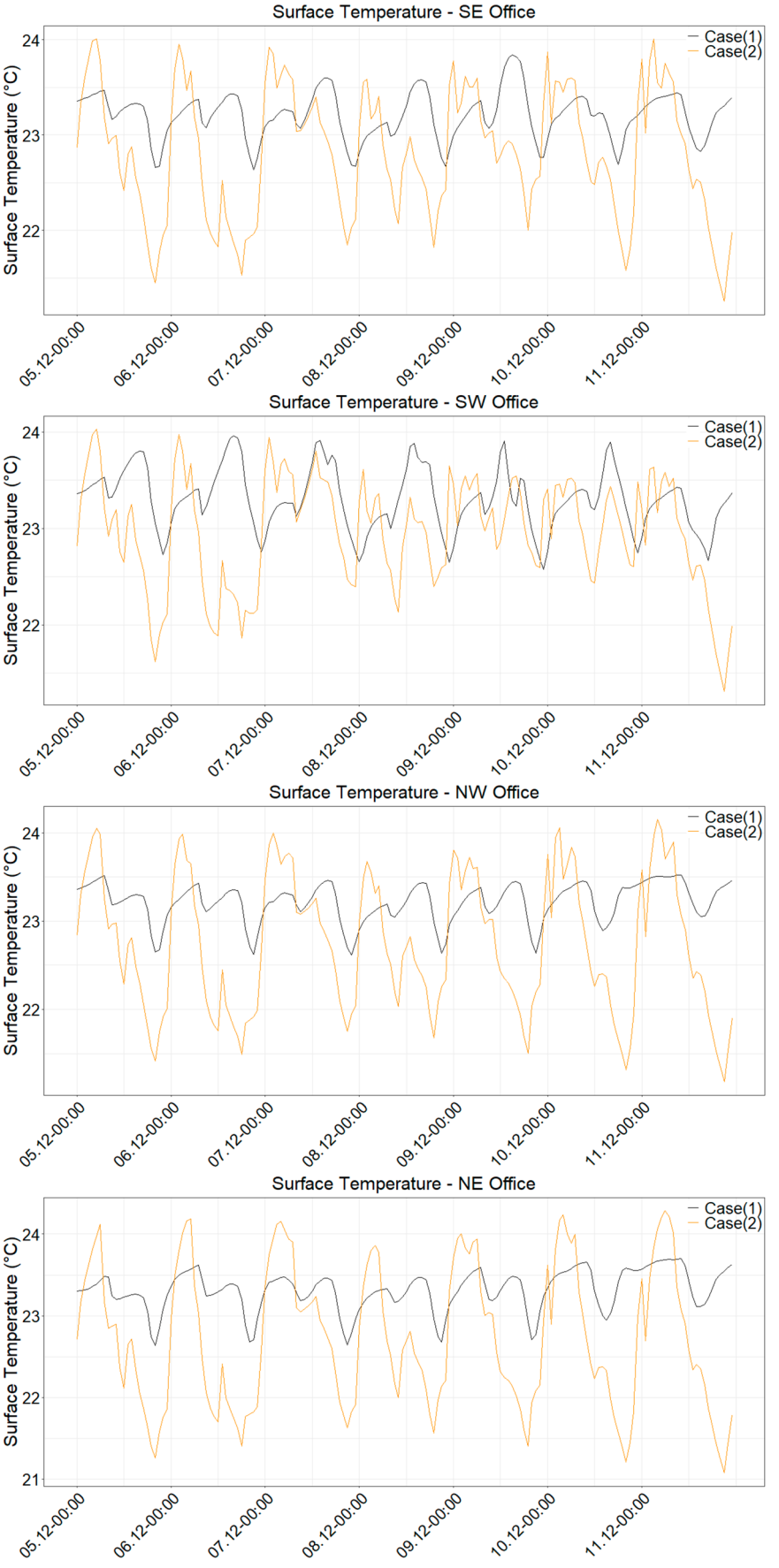

Figure 24. Surface temperature variations for a representative week.

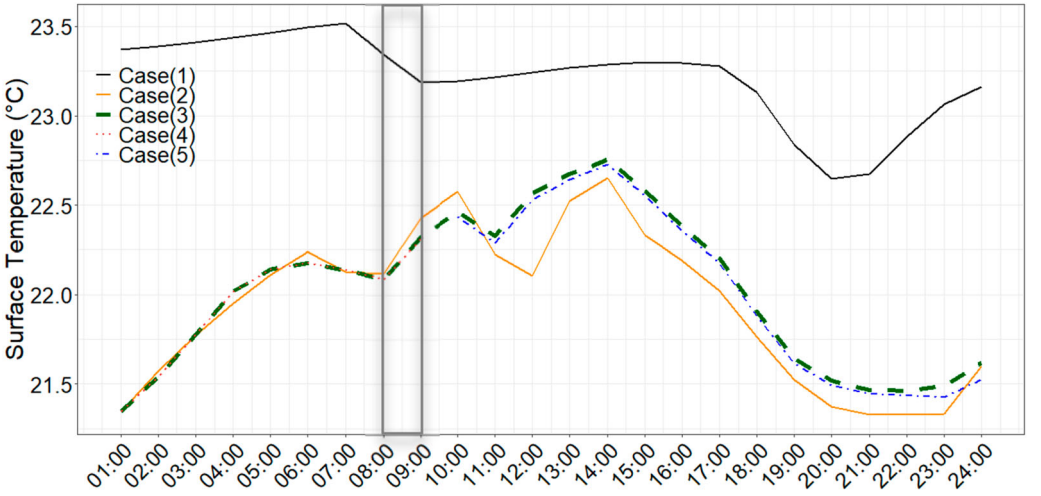

Figure 25. Surface temperature variations of NW office across all operational cases for a representative day.

Table 2. The loading cycle in SE, SW, NW and NE – case (1) scenario.

	SE		NW	
Loading (kWh)	3.8	0.6	3.4	0.4
Loading period (hour)	01:00–08:00	16:00–20:00	01:00–08:00	17:00–20:00
Unloading period (hour)	08:00–16:00	20:00–21:00	08:00–17:00	20:00–21:00
	SW		NE	
Loading (kWh)	2.7	0.9	4	1.5
Loading period (hour)	01:00–08:00	18:00–00:00	01:00–09:00	18:00–00:00
Unloading period (hour)	08:00–16:00	–	09:00–17:00	–

Table 3. The loading cycle in SE and SW – case(2) scenario.

	SE			
Loading (kWh)	3.4	0.5	0.3	0.5
Loading period (hour)	01:00–05:00	11:00–12:00	15:00–16:00	18:00–20:00
Unloading period (hour)	05:00–11:00	12:00–15:00	16:00–18:00	20:00–21:00
	SW			
Loading (kWh)	2.3	0.4	0.2	0.2
Loading period (hour)	01:00–05:00	11:00–12:00	15:00–16:00	17:00–19:00
Unloading period (hour)	05:00–11:00	12:00–15:00	16:00–17:00	19:00–21:00

Indoor temperature variations

In this section, the operative temperatures of four zones are compared between case(1) and case(2). Figure 28 represents the temperature variations, aligning with the response of the heat pump operation to the price signal.

In case(1), operative temperatures start rising around 08:00 and reach their peak in the afternoon. Notably, the temperature within the SE office peaks between 22°C and 24°C, an outcome attributable to increased solar gains given its orientation. In contrast, case(2) shows operative temperatures spanning from 20.5°C to 23°C, with the occurrence of multiple peaks throughout the day. These peaks correlate with the timing of thermal loading and unloading, as well as variations in surface temperatures. The extended duration of loading/unloading cycles under case(2) operations induces more pronounced temperature transitions; however, these transitions are gradual enough that occupants are unlikely to perceive them as discomfort.

Additionally, thermal comfort was assessed using the Predicted Percentage of Dissatisfied (PPD) calculated on an hourly basis in accordance with ISO 7730 (Ergonomics of the thermal environment 2005). A PPD value below 10% is considered indicative of acceptable thermal conditions. Across all analyzed zones, the maximum PPD remained below 10% during occupied hours, indicating satisfactory thermal comfort according to the standard, as presented in Table 5. Only the SE office exceeded 10% PPD, primarily due to the localized overheating from solar gains. No significant differences of PPD results between case(1), case(2) and case(3) are observed (Table 5).

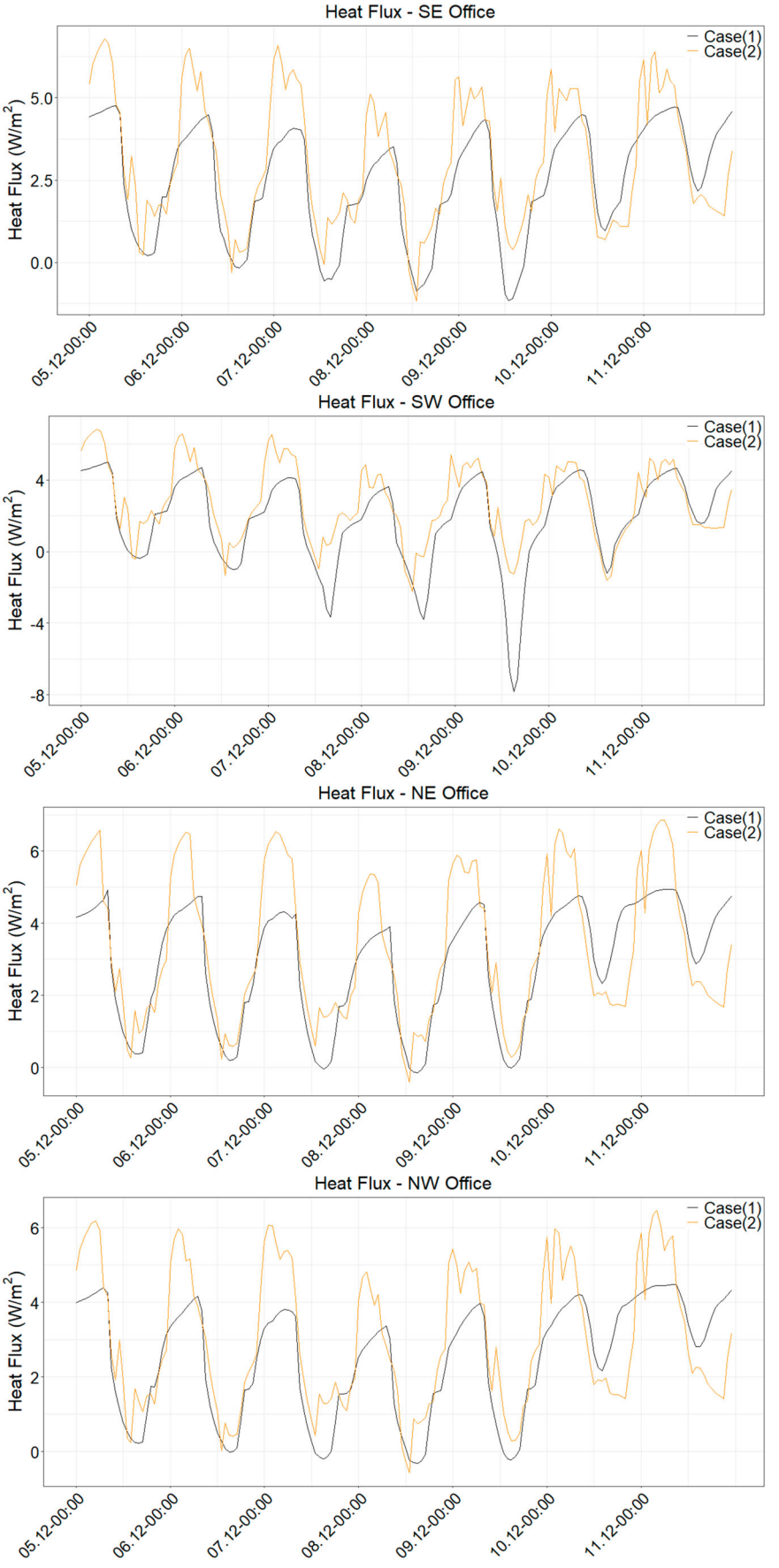

Figure 26. Heat flux variations for a representative week.

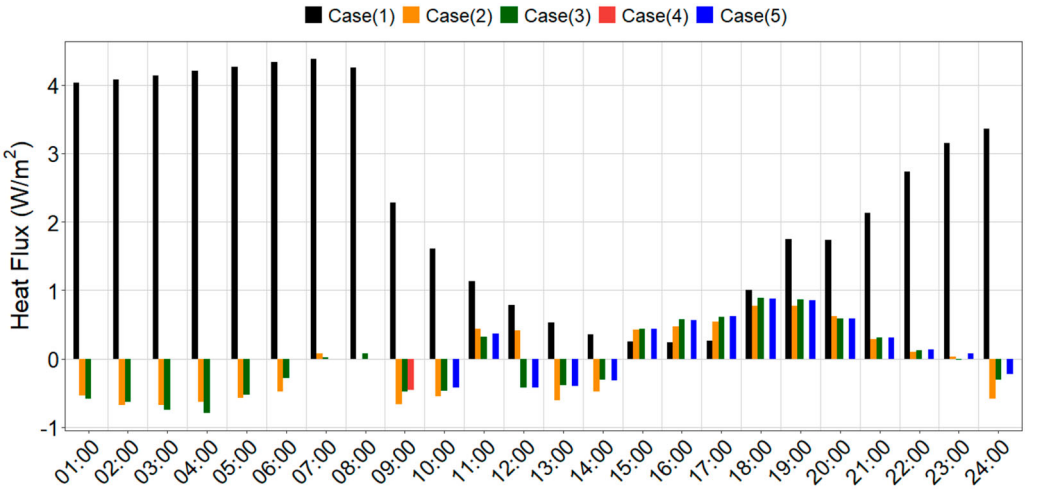

Figure 27. Heat flux variations of NW office across all operational cases for a representative day.

Table 4. The loading cycle in NW and NE – case (2) scenario.

		NW		
Loading (kWh)	3.4	0.5	0.3	0.5
Loading period (hour)	01:00–05:00	11:00–12:00	15:00–16:00	18:00–20:00
Unloading period (hour)	05:00–11:00	12:00–15:00	16:00–18:00	20:00–21:00
		NE		
Loading (kWh)	2.3	0.4	0.2	0.2
Loading period (hour)	01:00–05:00	11:00–12:00	15:00–16:00	17:00–19:00
Unloading period (hour)	05:00–11:00	12:00–15:00	16:00–17:00	19:00–21:00

Table 5. Zone-wise summary of PPD over the simulation period.

	case(1)	case(2)	case(3)
SE	8.6	8.7	8.5
SW	12.9	13.0	13.0
NE	8.3	8.4	8.5
NW	8.4	8.4	8.4

As given in Figure 29, which shows the indoor temperatures for all cases, case(3) presents moderate temperature fluctuations, keeping operative temperatures between 21.0°C and 23.0°C and ensuring smoother thermal transitions. No significant operative temperature decrement is observed in case(4). Case(5) resumes market-oriented operation, restoring indoor temperatures to slightly lower levels than those in case(3). This can be directly linked to the values given for case(5) in Figures 13 and 25 as follows: During the event, no significant temperature variation compared to case(3) is observed. However, to achieve cost-effective operation, case(5) reduces heat pump demand after the congestion event, resulting in a slightly lower operative temperature.

Computational benchmark

To clarify the computational advantages of the proposed RBPC, we compare it with the expected effort of standard MPC. A typical MPC setup with a 1-hour control interval and a 24-hour prediction horizon requires optimization over 24 control inputs. As discussed in Bamdad et al. (2023), even a shorter 3-hour horizon can require up to 120 solver iterations. Extrapolating to a full-day horizon for a multi-zone white-box model would increase this number to approximately 1000 iterations per control cycle. In our IDA-ICE co-simulation environment, a single 24-hour model evaluation, including software launching, data transfer, execution, and saving, takes approximately 1.5 minutes per given scenario. This results in a total computation time of around 25 hours per MPC optimization for a total of 1000 iterations, rendering real-time implementation infeasible in this setup. In contrast, the proposed RBPC approach evaluates a limited number of predefined control scenarios per hour. The complete daily simulation, including all scenario evaluations, is completed in approximately 8 hours, demonstrating a substantial reduction in computational demand compared to optimization-based control methods.

Conclusion

This study presents a comprehensive evaluation of a building's operational performance under different control strategies, focusing on energy consumption, cost

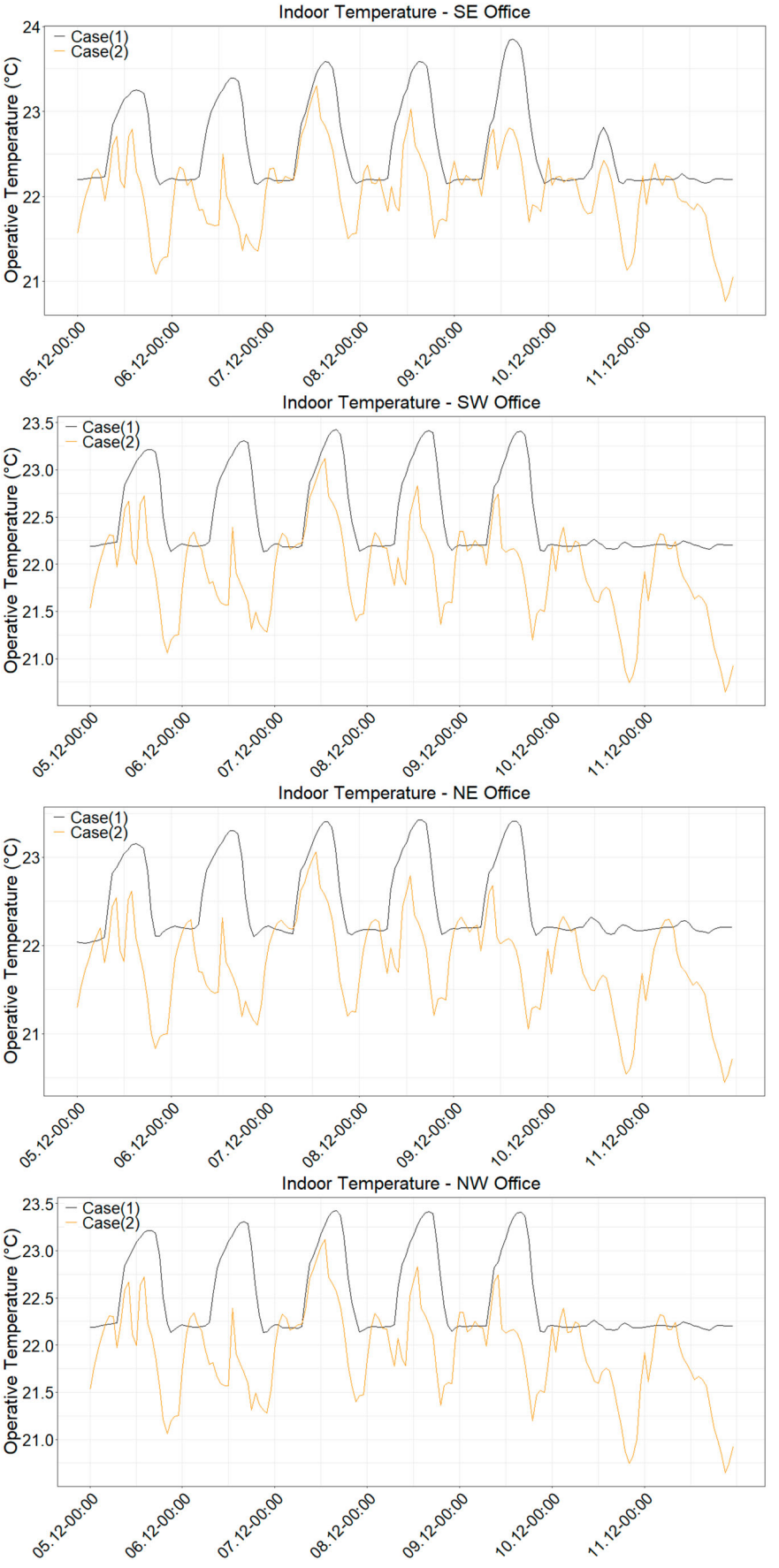

Figure 28. Operative temperature variations for a representative week.

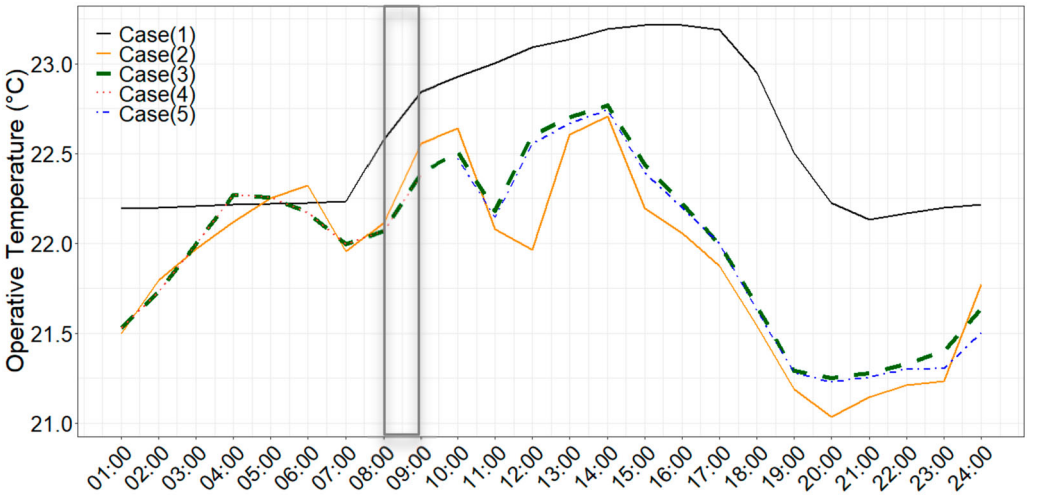

Figure 29. Indoor temperature variation of NW office across all operational cases for a representative day.

efficiency, and grid interaction. The comparative analysis of Business-as-Usual [case(1)], market-oriented RBC [case(2)], market-oriented RBPC [case(3)], grid-oriented RBPC [case(4)], and post-grid response RBPC [case(5)] provides valuable insights into the benefits of integrating predictive control strategies in TABS.

The results indicate that market-oriented operation with RBC [case(2)] enhances flexibility by shifting energy demand in response to price signals. Compared to case(1), case(2) achieves a 3.5% reduction in operational costs over a representative week, demonstrating the benefits of demand-side flexibility.

To address the limitations of RBC, RBPC is introduced in case(3) as a predictive control alternative. Unlike RBC, which adjusts setpoints reactively, RBPC proactively schedules heating operations based on anticipated price variations. RBPC achieves an additional 3.7% cost savings compared to RBC, showcasing its potential to enhance cost-efficiency while maintaining thermal comfort.

The TABS system serves as a valuable asset for enabling grid-interactive operation due to its sluggish thermal response. The slow responsiveness of the thermal building structure reduces fluctuations in surface and indoor temperatures, even as the heat pump supply temperature changes. During market-oriented events, variations in the supply temperature cause indoor temperatures to fluctuate by approximately 1.5°C over the course of the day. On the other hand, during grid-oriented events, no significant changes in surface or operative temperature are observed, indicating that the building envelope is not affected by short-term shifting.

Beyond market-driven optimization, RBPC is extended to grid-oriented operation in case(4). During a congestion event, the building successfully reduces power demand by 9.35 kW, demonstrating its capability to support grid stability. However, the energy systems capacities limit the full realization of grid flexibility, resulting in a LMGI of 88.6%. This highlights the need for additional flexibility measures, such as integrating ventilation control.

Following the congestion event, case(5) resumes market-oriented operation, optimizing setpoints based on previous grid-support actions. While post-event EES recharging slightly increases demand, RBPC still ensures overall higher cost savings of 2.2% compared to RBC, confirming its effectiveness in managing transitions between market and grid operations.

The findings clearly illustrate that RBPC outperforms RBC by integrating predictive capabilities, enabling buildings to participate in both market-driven optimization and grid support. While RBC provides basic load-shifting functions, it lacks adaptability to fluctuating electricity prices and grid constraints. In contrast, RBPC strategically adjusts setpoints ahead of time, avoiding unnecessary energy use while responding effectively to market and grid signals.

Compared to advanced control algorithms, which provide globally optimal solutions but have high modelling demands, RBPC offers a more efficient alternative. While RBPC does not continuously update its decisions in real time like MPC, it provides a structured rule-based predictive approach that balances cost-effectiveness for building-grid interaction applications.

In this paper, RBPC is applied on a single building. The scalability of RBPC in district-level applications is future work. When applied to multiple buildings, each building can independently evaluate a set of predefined scenarios, such as different temperature setpoints, preheating

periods. In cases where buildings share similar characteristics, such as system type or usage profile, a common set of control scenarios can be applied across the group, with each building selecting the most appropriate option based on its local conditions. For more heterogeneous districts, where building types, occupancy patterns, or HVAC systems differ, customized sets of predefined strategies may be developed per building category. While scenario evaluation remains local, some central coordination should be introduced if desired to align the overall operation with district-level objectives such as peak demand reduction or energy cost optimization. In particular, coordination becomes essential when flexibility actions, such as simultaneous charging or preheating, pose risks to the distribution network, especially transformer overloading. As shown in recent study (Kırant-Mitić et al. 2025), coordinated control signals may lead to accelerated transformer aging or overload, highlighting the need for transformer-aware coordination mechanisms.

Although this study focuses on a heating-dominated climate, the RBPC method is conceptually transferable to cooling-dominated regions. In such contexts, the majority of buildings rely on electricity-driven air conditioning systems to meet thermal comfort needs. Combined with the increasing penetration of rooftop PV, there is a similar opportunity to optimize control strategies based on day-ahead electricity prices. The RBPC framework, which relies on price categorization and predefined control scenarios, can be adapted by modifying the target variable, such as cooling buffer tank setpoint or precooling schedule, while preserving the underlying control logic.

In the case of district heating or cooling systems, the applicability of RBPC depends on the level of control available to individual buildings. If the energy supply is centrally controlled, building-level flexibility may be limited to thermal storage management or indoor temperature shifting within comfort constraints. In such cases, RBPC could still be applied at the building interface level but may require coordination with the district operator to ensure feasible and grid-supportive operation.

Future work could include a price sensitivity analysis using price forecasts to quantitatively assess the impact of forecast errors on cost and performance outcomes. This would explore the integration of adaptive control features or uncertainty-aware scenario selection to improve robustness under real-world variability in weather and system behaviour.

The findings of this study emphasize the critical role of predictive control strategies in enhancing energy flexibility, reducing operational costs, and supporting grid stability. By integrating sequential decision-making, predictive scheduling, and dynamic energy management, RBPC enables buildings to interact more effectively with electricity markets and power grids. The broader implications of this research contribute to the advancement of smart building controls, demand-side management, and sustainable energy systems, aligning with the objectives of future energy-efficient and resilient urban developments.

Declaration of generative AI and AI-assisted technologies in the writing process

During the preparation of this work the authors used OpenAI ChatGPT in order to improve the readability and language of the manuscript. After using this tool/service, the authors reviewed and edited the content as needed and take full responsibility for the content of the published article.

Acknowledgements

The authors would like to acknowledge IEA-EBC Annex 82 members for conducting scientific discussions and providing knowledge exchange.

Authors' contributions

Tuğçin Kırant-Mitić: Conceptualization, Software, Methodology, Investigation, Writing – Original Draft, ***Karsten Voss***: Conceptualization, Supervision, Writing – Review & Editing

Disclosure statement

No potential conflict of interest was reported by the author(s).

Data availability statement

The data underlying this study can be requested from the authors and will be made available upon justified interest.

ORCID

Tuğçin Kırant-Mitić http://orcid.org/0000-0002-1702-8822

References

Alahäivälä, A., J. Corbishley, J. Ekström, J. Jokisalo, and M. Lehtonen. 2017. "A Control Framework for the Utilization of Heating Load Flexibility in a day-Ahead Market." *Electric Power Systems Research* 145:44–54. https://doi.org/10.1016/j.epsr.2016.12.019.

Al Sayed, K., A. Boodi, R. Sadeghian Broujeny, and K. Beddiar. 2024. "Reinforcement Learning for HVAC Control in Intelligent Buildings: A Technical and Conceptual Review." *Journal of Building Engineering* 95:110085. https://doi.org/10.1016/j.jobe.2024.110085.

Arteconi, A., D. Costola, P. Hoes, and J. Hensen. 2014. "Analysis of Control Strategies for Thermally Activated Building Systems under Demand Side Management Mechanisms." *Energy and Buildings* 80:384–393. https://doi.org/10.1016/j.enbuild.2014.05.053.

Balaras, C. A. 1996. "The Role of Thermal Mass on the Cooling Load of Buildings. An Overview of Computational Methods." *Energy and Buildings* 24 (1): 1–10. https://doi.org/10.1016/0378-7788(95)00956-6.

Bamdad, K., N. Mohammadzadeh, M. Cholette, and S. Perera. 2023. "Model Predictive Control for Energy Optimization of HVAC Systems Using EnergyPlus and ACO Algorithm." *Buildings* 13 (12): 3084. https://doi.org/10.3390/buildings13123084.

Chen, Q., N. Li, and W. Feng. 2021. "Model Predictive Control Optimization for Rapid Response and Energy Efficiency Based on the State-Space Model of a Radiant Floor Heating System." *Energy and Buildings* 238:110832. https://doi.org/10.1016/j.enbuild.2021.110832.

Cho, S.-H., and M. Zaheer-uddin. 1999. "An Experimental Study of Multiple Parameter Switching Control for Radiant Floor Heating Systems." *Energy* 24 (5): 433–444. https://doi.org/10.1016/S0360-5442(98)00101-7.

Dey, S., T. Marzullo, X. Zhang, and G. Henze. 2023. "Reinforcement Learning Building Control Approach Harnessing Imitation Learning." *Energy and AI* 14:100255. https://doi.org/10.1016/j.egyai.2023.100255.

Drgoňa, J., et al. 2020. "All You Need to Know about Model Predictive Control for Buildings." *Annual Reviews in Control* 50:190–232. https://doi.org/10.1016/j.arcontrol.2020.09.001.

Du, P., X. Gong, W. Hu, and Y. Zhao. 2023. "A Multi-layer Scheduling Framework for Transmission Network Overload Alleviation considering Capabilities of Active Distribution Networks." *Sustainable Energy, Grids and Networks* 36:101188. https://doi.org/10.1016/j.segan.2023.101188.

ENTSO-E Transparency Platform. 2022. *Day-ahead Prices*. [Online]. Accessed December 2022. https://transparency.entsoe.eu/dashboard/show.

Ergonomics of the thermal environment. 2005. *Ergonomics of the Thermal Environment: Analytical Determination and Interpretation of Thermal Comfort Using Calculation of the PMV and PPD Indices and Local Thermal Comfort Criteria*, ISO 7730. https://www.iso.org/obp/ui/en/#iso:std:iso:7730:ed-3:v1:en.

Esmat, A., J. Usaola, and MÁ Moreno. 2018. "Distribution-Level Flexibility Market for Congestion Management." *Energies* 11 (5): 1056. https://doi.org/10.3390/en11051056.

Federal Ministry for Economic Affairs and Energy. 2015. "An Electricity Market for Germany's Energy Transition: White Paper by the Federal Ministry for Economic Affairs and Energy." Berlin. Accessed 15 February 2025. https://www.bmwk.de/Redaktion/EN/Publikationen/whitepaper-electricity-market.html.

GOPACS. 2025. *Congestion Management Makes More Possible*. Accessed 24 July 2025. https://www.gopacs.eu/.

Gwerder, M., B. Lehmann, J. Tödtli, V. Dorer, and F. Renggli. 2008. "Control of Thermally-Activated Building Systems (TABS)." *Applied Energy* 85 (7): 565–581. https://doi.org/10.1016/j.apenergy.2007.08.001.

Hanova, J., and H. Dowlatabadi. 2007. "Strategic GHG Reduction through the use of Ground Source Heat Pump Technology." *Environmental Research Letters* 2 (4): 44001. https://doi.org/10.1088/1748-9326/2/4/044001.

Haque, A., P. H. Nguyen, F. W. Bliek, and J. G. Slootweg. 2017. "Demand Response for Real-Time Congestion Management Incorporating Dynamic Thermal Overloading Cost." *Sustainable Energy, Grids and Networks* 10:65–74. https://doi.org/10.1016/j.segan.2017.03.002.

IDA-ICE. 2023. *Equa Simulation AB – IDA Indoor Climate and Energy 4.8 – Simulation Software | EQUA*. Accessed 15 August 2023. https://www.equa.se/en.

Jensen, SØ, et al. 2017. "IEA EBC Annex 67 Energy Flexible Buildings." *Energy and Buildings* 155:25–34. https://doi.org/10.1016/j.enbuild.2017.08.044.

Khatibi, M., S. Rahnama, P. Vogler-Finck, J. D. Bendtsen, and A. Afshari. 2022. "Investigating the Flexibility of a Novel Multi-zone air Heating and Ventilation System Using Model Predictive Control." *Journal of Building Engineering* 49:104100. https://doi.org/10.1016/j.jobe.2022.104100.

Killian, M., and M. Kozek. 2016. "Ten Questions concerning Model Predictive Control for Energy Efficient Buildings." *Building and Environment* 105:403–412. https://doi.org/10.1016/j.buildenv.2016.05.034.

Kırant-Mitić, T., M. Hall, G. Dawes, and R. A. Lopes. 2025. "Impact of Building-Grid Interaction Signals on Energy Flexibility at Cluster Level: Insights from two Case Studies." *Energy and Buildings* 346:116235. https://doi.org/10.1016/j.enbuild.2025.116235.

Le Dréau, J., et al. 2023. "Developing Energy Flexibility in Clusters of Buildings: A Critical Analysis of Barriers from Planning to Operation." *Energy and Buildings* 300:113608. https://doi.org/10.1016/j.enbuild.2023.113608.

Lee, C. K. 2011. "Effects of Multiple Ground Layers on Thermal Response Test Analysis and Ground-Source Heat Pump Simulation." *Applied Energy* 88 (12): 4405–4410. https://doi.org/10.1016/j.apenergy.2011.05.023.

Li, R., et al. 2022. "Ten Questions concerning Energy Flexibility in Buildings." *Building and Environment* 223:109461. https://doi.org/10.1016/j.buildenv.2022.109461.

Li, Y., J. Wang, Y. Han, Q. Zhao, X. Fang, and Z. Cao. 2020. "Robust and Opportunistic Scheduling of District Integrated Natural gas and Power System with High Wind Power Penetration considering Demand Flexibility and Compressed air Energy Storage." *Journal of Cleaner Production* 256:120456. https://doi.org/10.1016/j.jclepro.2020.120456.

Lichtmess, M. 2018. *Objektbericht Goblet Lavandier & Associés*.

Lim, J.-H., J.-H. Jo, Y.-Y. Kim, M.-S. Yeo, and K.-W. Kim. 2006. "Application of the Control Methods for Radiant Floor Cooling System in Residential Buildings." *Building and Environment* 41 (1): 60–73. https://doi.org/10.1016/j.buildenv.2005.01.019.

Liu, Z., Y. Chen, X. Yang, and J. Yan. 2023. "Power to Heat: Opportunity of Flexibility Services Provided by Building Energy Systems." *Advances in Applied Energy* 11:100149. https://doi.org/10.1016/j.adapen.2023.100149.

Lustenberger, M., F. Bellizio, H. Cai, P. Heer, and C. Ziras. 2024. "Introducing Price Feedback of Local Flexibility Markets into Distribution Network Planning." *Electric Power Systems Research* 236:110686. https://doi.org/10.1016/j.epsr.2024.110686.

NODESmarket. 2025. *Unlocking Flexibility, Driving Sustainability*. Accessed 24 July 2025. https://nodesmarket.com/.

Olesen, B. W. 2007. "Operation and Control of Activated Slab Heating and Cooling Systems."

Powell, J., A. McCafferty-Leroux, W. Hilal, and S. A. Gadsden. 2024. "Smart Grids: A Comprehensive Survey of Challenges, Industry Applications, and Future Trends." *Energy Reports* 11:5760–5785. https://doi.org/10.1016/j.egyr.2024.05.051.

Projekt Enera. 2025. *Der nächste Schritt der Energiewende*. Accessed 24 July 2025. https://projekt-enera.de/.

Reynders, G., T. Nuytten, and D. Saelens. 2013. "Potential of Structural Thermal Mass for Demand-Side Management in Dwellings." *Building and Environment* 64:187–199. https://doi.org/10.1016/j.buildenv.2013.03.010.

Rhee, K.-N., and K. W. Kim. 2015. "A 50 Year Review of Basic and Applied Research in Radiant Heating and Cooling Systems for the Built Environment." *Building and Environment* 91:166–190. https://doi.org/10.1016/j.buildenv.2015.03.040.

Rhee, K.-N., B. W. Olesen, and K. W. Kim. 2017. "Ten Questions about Radiant Heating and Cooling Systems." *Building and Environment* 112:367–381. https://doi.org/10.1016/j.buildenv.2016.11.030.

Salom, J., J. Widén, J. Candanedo, I. Sartori, K. Voss, and A. J. Marszal. 2011. *Understanding Net Zero Energy Buildings: Evaluation of Load Matching and Grid Interaction Indicators*.

Salt, H. 1985. "Preliminary Design Considerations for a Rockbed/Floor Space-Heating System." *Building and Environment* 20 (4): 221–231. https://doi.org/10.1016/0360-1323(85)90037-X.

Sartori, I., A. Napolitano, and K. Voss. 2012. "Net Zero Energy Buildings: A Consistent Definition Framework." *Energy and Buildings* 48:220–232. https://doi.org/10.1016/j.enbuild.2012.01.032.

Schiller, Steven R., Lisa Schwartz, and Sean Murphy. 2020. *Performance Assessments of Demand Flexibility from Grid-Interactive Efficient Buildings: Issues and Considerations*. Berkeley, CA: State and Local Energy Efficiency Action Network, Lawrence Berkeley National Laboratory.

Self, S. J., B. V. Reddy, and M. A. Rosen. 2013. "Geothermal Heat Pump Systems: Status Review and Comparison with Other Heating Options." *Applied Energy* 101:341–348. https://doi.org/10.1016/j.apenergy.2012.01.048.

Shin, M. S., K. N. Rhee, S. R. Ryu, M. S. Yeo, and K. W. Kim. 2015. "Design of Radiant Floor Heating Panel in View of Floor Surface Temperatures." *Building and Environment* 92:559–577. https://doi.org/10.1016/j.buildenv.2015.05.006.

Stackhouse, P. 2023. *NASA- Power – Data Access Viewer*. Accessed 10 November 2023. https://power.larc.nasa.gov/data-access-viewer/.

Staff, Andy. n.d. *Goblet Lavandier & Associés Ingénieurs-Conseils S.A. - Photo*

Sturzenegger, D., D. Gyalistras, M. Morari, and R. S. Smith. 2016. "Model Predictive Climate Control of a Swiss Office Building: Implementation, Results, and Cost–Benefit Analysis." *IEEE Trans. Contr. Syst. Technol* 24 (1): 1–12. https://doi.org/10.1109/TCST.2015.2415411.

Tian, Z., and J. A. Love. 2009. "Energy Performance Optimization of Radiant Slab Cooling Using Building Simulation and Field Measurements." *Energy and Buildings* 41 (3): 320–330. https://doi.org/10.1016/j.enbuild.2008.10.002.

Valkering, P., A. Moglianesi, L. Godon, J. Duerinck, D. Huber, and D. Costa. 2023. "Representing Decentralized Generation and Local Energy use Flexibility in an Energy System Optimization Model." *Applied Energy* 348:121508. https://doi.org/10.1016/j.apenergy.2023.121508.

Voss, K., J. A. Candanedo, S. Geier, H. Gonzalves, M. Hall, P. Heiselberg, B. Karlsson, et al. 2010. *Load Matching and Grid Interaction of Net Zero Energy Buildings*.

Wang, H., et al. 2023. "A Zoned Group Control of Indoor Temperature Based on MPC for a Space Heating Building." *Energy Conversion and Management* 290:117196. https://doi.org/10.1016/j.enconman.2023.117196.

Wei, Z., and J. K. Calautit. 2024. "Field Experiment Testing of a low-Cost Model Predictive Controller (MPC) for Building Heating Systems and Analysis of Phase Change Material (PCM) Integration." *Applied Energy* 360:122750. https://doi.org/10.1016/j.apenergy.2024.122750.

Yang, L., H. Li, D. Zheng, M. Cui, and X. Lv. 2024. "Flexible Market Trading Strategy for Business Integrated Energy Users considering Energy Cascade Utilization." *International Journal of Electrical Power & Energy Systems* 157:109755. https://doi.org/10.1016/j.ijepes.2023.109755.

Yang, X., et al. 2024. "Comparison of Different Control Methods on the Thermally Activated Building System (TABS) with Large Energy Flexibility." *Applied Thermal Engineering* 254:123863. https://doi.org/10.1016/j.applthermaleng.2024.123863.

5. PAPER 4

Impact of Building-Grid interaction signals on energy flexibility at cluster Level: Insights from two case studies

Energy & Buildings 346 (2025) 116235

Contents lists available at ScienceDirect

Energy & Buildings

journal homepage: www.elsevier.com/locate/enb

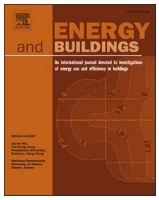

Impact of Building-Grid interaction signals on energy flexibility at cluster Level: Insights from two case studies

Tuğçin Kırant-Mitić [a,*], Monika Hall [b], George Dawes [c], Rui Amaral Lopes [d]

[a] Department of Building Physics and Technical Services, Faculty of Architecture and Civil Engineering, Wuppertal University, Wuppertal, Germany
[b] Institute of Sustainability and Energy in Construction, University of Applied Sciences and Arts Northwestern Switzerland, Muttenz, Switzerland
[c] Building Energy Research Group (BERG), Department of Architecture, Building and Civil Engineering, Loughborough University, Loughborough LE11 3UE, UK
[d] School of Science and Technology, UNINOVA-CTS and LASI, NOVA University Lisbon, Portugal

ARTICLE INFO

Keywords:
Building-Grid Interaction Signal
Transformer Aging
Building Energy Flexibility
Building Cluster

ABSTRACT

The increasing integration of renewable energy sources into power grids introduces operational challenges due to their time-varying electricity supply and limited predictability. Building-grid interaction (BGI) signals have emerged as a strategy to enhance energy flexibility, yet their impact on distribution transformer performance and aging remains underexplored. This study investigates the role of single vs. sequential BGI signals in two energy-efficient building clusters in Germany and Switzerland, using a co-simulation framework that integrates building performance simulation tools with numerical computing methods. Single BGI signals, such as electricity price and CO_2eq intensity, were compared to sequential BGI signals, which incorporate a transformer critical status signal to dynamically adjust flexibility responses. The results reveal distinct impacts on transformer aging and grid stress between the two clusters. In the German building cluster, sequential BGI signals effectively mitigated demand-driven transformer stress, reducing aging compared to single-signal cases, which impacted peak loads. Conversely, in the Swiss building cluster, photovoltaic feed-in was the dominant aging factor. Here, single BGI signals slightly lowered aging through improved self-consumption, while transformer critical status signals occasionally increased aging by reducing self-consumption during overload events. Across both clusters, energy and cost savings were analysed, with building-grid interaction signal integration successfully maintaining thermal comfort boundaries. These findings provide insights for energy flexibility aggregators on the potential trade-offs between grid stability, economic efficiency, and emission reductions in flexible building operations.

1. Introduction

In response to the global challenge of climate change, many nations have committed to achieving net-zero carbon emissions by 2050 [1]. A key strategy in this effort is the widespread deployment of renewable energy systems (RES) to decarbonise the power grid. However, as nations transition from traditional high inertia-based power generation to time-varying, low-inertia power generation from RES, they face significant operational challenges. Renewable energy sources, such as wind and photovoltaic (PV), are inherently variable, making it challenging to reliably predict power generation levels [2]. Such variability in energy supply can create stability issues for the power grid, particularly as RES penetration increases. To address these challenges, a whole-systems approach is required – one which incorporates the building sector as part of the solution. Building services, including heating, ventilation, and air conditioning (HVAC), thermal storage, energy generation, electrical storage systems and building automation systems, play a crucial role in this integration [3,4]. Building grid interaction (BGI) can be used to provide advanced services such as demand-side management (DSM). As the demand for electricity in buildings grows, driven by increased use of heat pumps and electric vehicles, the mismatch between renewable generation and consumption peaks becomes more pronounced.

The current power distribution networks were not designed to accommodate the energy transition [5], and their capacity may not be sufficient to meet the needs of widespread electrification as a major overload situation may occur for the distribution transformer [6]. For instance, full electrification of heating systems could increase peak electricity demand by 170 %, necessitating a 160 % expansion of grid capacity in the UK [7]. Besides, traditional power grids operate using a

* Corresponding author.
E-mail address: tugcin.kirant_mitic@uni-wuppertal.de (T. Kırant-Mitić).

https://doi.org/10.1016/j.enbuild.2025.116235
Received 4 May 2025; Received in revised form 7 July 2025; Accepted 30 July 2025
Available online 2 August 2025
0378-7788/© 2025 The Author(s). Published by Elsevier B.V. This is an open access article under the CC BY license (http://creativecommons.org/licenses/by/4.0/).

top-down approach, with one-way power flows from centralised generators to consumers [8]. However, the rise of decentralised energy sources, like rooftop PV, has introduced bidirectional flow [9], requiring a transition to smart grid systems for improved flexibility and resilience. Smart grids facilitate a high level of coordination between buildings and the power grid enabling more efficient energy management [10]. Utilising the information provided by smart grid systems through a control signal, the interaction between a building and the power grid can be exploited for operational optimisation [11]. BGI goals are linked to the optimisation or operational objectives of smart grid systems [12] such as frequency regulation [13] and voltage control to prevent fluctuations and maintain a reliable power supply [14]. Pricing also plays a crucial role, such as dynamic pricing schemes incentivise consumers to change their energy use during peak periods [15]. Furthermore, emissions-based signals encourage energy use when grid emissions are at their lowest, or when the supply of renewable energy is plentiful, thereby contributing to the decrease of greenhouse gas (GHG) emissions [16]. Load-based flexibility also features through programs for demand response and load-shifting, which serve to alleviate grid strain by modifying consumption during peak times, thereby enhancing stability.

On the other side, the effectiveness of these signals depends on their ability to transparently convey the value of flexibility to end-users. For instance, using a single control signal across a cluster of buildings can lead to unintended consequences. If all buildings respond to the same signal simultaneously, such as a favourable electricity price, this synchronised behaviour can overload the grid and cause congestion [17,18], bringing adverse peak-shifts and rebound peaks [19], which can destabilise the power grid. There is a positive motivation behind using a single signal, but it may lead to operational drawbacks, including distribution transformer overutilisation and accelerated aging, which can compromise the overall efficiency and reliability of power grid operation.

Existing BGI studies focus on single control signals such as price and CO_2 [19,20] but overlook their impact on transformer stress and aging. Research on optimized signals has improved joint influence of different single signals as price and CO_2, but lacks real-time power grid responsiveness [21]. [22] showed different agent functions such as price and grid stress signal from a peer-to-peer platform. By cooperating two different signals, the grid stability is always controlled while aiming cost effective operation. Similarly, [23] introduced a genetic algorithm-based flexibility optimization model, balancing grid stability and financial incentives. This approach optimizes electrical vehicle charging flexibility to reduce congestion costs. While they effectively reduce short-term costs and congestion, they do not incorporate transformer operational status. [24] developed a transformer model to assess aging impacts under varying load conditions, but their analysis was limited to signal-unaware demand scenarios. A more transformer-aware flexibility model was presented by [25], who developed a multi-stage optimization framework integrating home energy management systems and peer-to-peer trading. Their approach ensures grid-friendly flexibility activation by imposing transformer overload risk limits; however, their control approach does not include immediate operational changes to avoid transformer overload.

To this end, introducing additional signals is necessary to overcome operational challenges and ensure stable grid operation. Despite significant advancements in BGI research, several critical gaps remain:

- Priority between objectives: Current studies lack a systematic analysis for quantifying the relative impact of signals −such as cost and grid stability- within control strategies.
- Localized grid constraints: Grid-level impacts, such as distribution transformer operation status as overloading and fastened aging, are underexplored under dynamic signal scenarios.
- Sequential signal operation: Few studies have evaluated the effectiveness of sequential signals in mitigating transformer overload while maintaining BGI operation.
- Heterogeneity in building clusters: Most research focuses on one building cluster, failing to address the diverse properties and behaviours of different clusters.

Tackling these challenges, this study aims to examine the impacts of control signals on building clusters and power grid operation, by comparing the effects of single versus sequential penalty signals on distribution transformer performance and lifespan; a novel contribution to the field, as this is a previously underexplored aspect with significant implications to both the buildings, power grid networks and their interactions. However, the term “penalty signal” may carry negative connotations, making it less effective for engaging stakeholders, particularly in commercial contexts [26]. To address this, we propose the term “building-grid interaction signal” (BGI signal). A BGI signal is defined as “a dynamic signal that prompts adjustments in a building’s systems or services to align with operational goals and external factors such as grid service requirements”. Unlike penalty signals, BGI signals are not restricted to cost-specific factors and can encompass multiple control variables, offering a more inclusive and stakeholder-friendly approach to demand response initiatives. The literature outlines several types of BGI signals that can be applied to buildings:

1 Single BGI signal

A single signal is employed to achieve or optimise for a specific objective, such as minimising energy costs or reducing GHG emission [20,27]. This approach is straightforward, as it focuses on one parameter without accounting for trade-offs with other objectives.

2 Optimised or Compound BGI signal

Multiple parameters are simultaneously considered within a single signal, enabling a balance between objectives such as energy costs and GHG emission saving [28,29]. This requires pre-processing to generate a combined BGI signal at each time step. The process often involves a decision tree or weighted balancing method, where weights are assigned based on the importance of each parameter or the overall optimisation objective. This type of signal is particularly suited to scenarios where trade-offs between competing objectives must be resolved dynamically.

3 Sequential BGI signal

Multiple signals are applied concurrently, but only one signal is active at any given moment, based on a predefined priority hierarchy. For example, a baseline signal might optimise energy costs to minimise operational expenses. However, if a critical event occurs – such as power instability – a higher-priority signal is activated to address the urgent need for demand change. During this period, the priority signal temporarily overrides the baseline signal to tackle the greater issue. Once the issue is resolved, the system reverts to the baseline optimisation signal.

Sequential signals directly address the localized constraints by incorporating real-time feedback from grid infrastructure, such as transformer load and hot spot temperature (HST). However, the studies evaluating their impact on grid operations, particularly in the context of transformer aging, are limited. The integration of dynamic BGI signals into such models remains an open research question. This study focuses on these gaps by:

– Developing a co-simulation framework to evaluate the impacts of sequential BGI signals on building clusters and power grid operations.

Building performance simulations (BPS) are conducted in a co-simulation environment to analyse the use of *single signals* such as electricity unit price and power grid electricity carbon dioxide equivalent (CO_2eq) intensity in BGI operation, focusing on building clusters from Germany and Switzerland.

– Quantifying transformer aging and HST fluctuations under dynamic signal scenarios using sequential signals.

After performing the simulations using a *single signal*, further simulations were performed using a *sequential signal* arrangement; considering a single signal alongside a transformer critical status (TCS) signal, to evaluate the impacts that multiple signals (two signals are applied in the scope of this research) can have on flexibility objectives and grid

stability across building clusters. The distribution transformer model, which was used to create the TCS signal and calculate transformer aging, complies with the principles specified in the IEC 60076–7 standard [30]. Consequently, the distribution transformer load, energy costs, GHG emissions, distribution transformer aging and the indoor thermal comfort results are presented in this research.

The paper is structured as follows: Section 2 introduces the methodology, including the two investigated building clusters, a description of the signals used, and the numerical setup. In Section 3, the results of cluster and distribution transformer operation based on different signals are presented. Section 4 examines the context of different building cluster analysis, concluding with this study's key findings and outlining directions for future work.

2. Methodology

This research analyses two building clusters located in Germany and Switzerland as part of the IEA EBC Annex 82 – Energy Flexible Buildings Towards Resilient Low Carbon Energy Systems framework, which involves researchers from multiple institutions. The distinct characteristics of the case study areas, including country-specific standards, regulations, and operational practices, necessitated the application of different methodologies. Additionally, the institutions conducting the research employed varied BPS tools and numerical methods, reflecting their approaches. These differences, while inherent to international collaborations, contribute to a broader understanding of BGI by showcasing diverse strategies for building operations and control. The presented work represents a unified effort to address these variations and integrate insights from different contexts. This research does not aim to directly compare the clusters but rather to analyse them independently to understand how BGI signals function in distinct operational settings. The description of the clusters, BGI signal used, simulation cases, applied control strategies and numerical setup of co-simulation environments are described in the following section.

2.1. Cluster definition – Wuppertal, Germany

As part of the Solar Decathlon Europe 21/22 competition, which was organised in Wuppertal, Germany, 18 teams designed and built energy-efficient solar powered houses [31]. For further research activities to be conducted under the "Living Lab NRW" project, eight of these buildings remained in Wuppertal (Fig. 1). Wuppertal's climate is characterised by moderate winters and summers, with a long-term mean annual temperature of 10.5 °C and a total global solar radiation of 942 kWh/m^2 per year [32].

The buildings in the cluster were designed for residential use and exhibit considerable variation in size, with total net floor areas ranging from 67 m^2 to 155 m^2 and a combined living space of 850 m^2 (970 m^2 gross area), as well as differences in roof types. During the modelling phase of the buildings, limited monitored data was available. As a result, the building models may not fully represent actual performance. Nevertheless, the models were developed mainly based on data obtained during the project development phase. However, for the research purposes in this paper, the energy systems and their setpoints were modified and the obtained data from BPS were used for the paper analysis. Each building has unique thermal characteristics and HVAC system configurations tailor to their design purposes. In the existing arrangement, all buildings are equipped with heat pumps, some have specific designs to achieve passive heating and/or cooling. In this research, each building's HVAC was considered as a reversible air source heat pump with a thermal size of 10 kW and coefficient of performance (COP) of 4.4. The calculated space heating demand is 61 kWh/m^2 per year in the cluster. Additionally, the energy system of each building was modelled with two separate thermal storage tanks, each with a capacity of 500 L (for increased flexibility) —one designated for hot water, which is utilised for both space heating and domestic hot water, and one for cold water storage. The supply temperature for hot water utilised in space heating was modulated according to an ambient temperature-dependent heating curve (HC). Domestic hot water was charged for two hours during the day at a fixed 55°C temperature. The indoor temperature setpoints were established at 21 °C during the heating season and 25 °C during the cooling season. Certain houses were equipped with ceiling radiant heating systems, whereas others were fitted with floor radiant heating systems to serve as their primary heating and cooling room units. The indoor CO_2 level was maintained in the range of 400 ppm to 1000 ppm through mechanical ventilation in two buildings, while the remaining six buildings were ventilated naturally using automated window control. Each house also has its own PV panels with different orientations but a capacity of 2.5 kWp. No electrical energy storage systems were modelled in this research.

Each building had a distinct electrical load profile derived from lighting, equipment, and plug-in loads, in addition to the HVAC system demand. These profiles were correlated with a unique occupancy schedule. The cluster energy model was developed in a BPS tool where the actual recorded weather data for Wuppertal, Germany (by a local weather station) over an entire year is used. The energy model of the cluster, representing the baseline case (signal-unaware scenario), was developed with the actual thermal characteristics of each building defined. The calibrated model was obtained by the monitored data as described in [34]. However, the energy plants were modelled as non-electrical systems in the BPS tool to determine the transformer capacity before electrification

Fig. 1. The Wuppertal cluster buildings simulated in this work (Ref: © Sigurd Steinprinz, University Wuppertal).

2.2. Cluster definition – Basel, Switzerland

This building cluster comprises eight single-family terraced houses that were modelled on existing houses located in Basel, Switzerland (Fig. 2). The climate in Basel has moderate winters and summers, with an annual mean temperature of 11.2 °C and a total global solar radiation of 1273 kWh/m^2 per year. The data used was derived from the most recent 15 years (2007–2021) [35]. The total gross floor area is 137 m^2 (net floor area 114 m^2) for each building, which are of solid-wall construction (brick wall, concrete floors/ceilings), without basement and oriented south/north. The top level of the pitched roof is unheated. The building models retain only the geometric form of existing buildings, reflecting their actual physical shape. However, all other modelling parameters were based on assumptions in accordance with the SIA 380/1 standard. Based on the modelling assumption, each house has a heating demand of 38.6 kWh/m^2 (gross floor area per year) according to [36].

For the modelling purposes, a brine-to-water heat pump with a thermal capacity of 15 kW and a COP of 3.5 was used for each building to meet their heating and domestic hot water demands. Each heat pump fed a 300-liter buffer tank and a 200-liter domestic hot water tank (HWT). The heat was emitted via radiators that draw their heat from the buffer tank. The domestic hot water was produced for two hours in the early morning during the whole year. During summer, between the 1st of May and the 15th of September, the heat pump heating function was switched off and, no mechanical cooling was implemented in the cluster. All buildings have roof mounted south-facing PV systems at 40° inclination. Two buildings have a PV-system with a capacity of 1.5 kWp and the other six buildings 3.0 kWp.

Eight unique household electricity load profiles based on 10-minute increments were used [37] and varied between 7.6–23.5 kWh/m^2 per year. The daily occupancy profiles were based on Swiss standard [38] and were customised for each building, alongside daily hot water usage – both apply to all days of the year.

Ventilation was modelled based on a fixed daily window-opening behaviour, with windows opened four times a day for 10 min each as given in the reference [39]. The four ventilation times vary for each building, and they were independent of the ambient temperature. The range of the ventilation times for all buildings was in the morning between 6:50 – 8:20, after lunch between 13:10–14:50 (except of one building: 17:30–17:40), in the early evening between 18:40–20:20 and late in the evening between 21:50–23:20 as given in the supplementary document – Fig. 1. The radiators were switched off during ventilation times; however, the heat pumps continued to charge the buffer tanks if the monitored temperature fell below the setpoint. In midsummer, between the 15th of June and the 15th of August, additional nighttime natural ventilation was provided in the upper rooms between the evening and morning ventilation time in each building. The external blind was activated when the solar radiation on the outer façade exceeds 120 W/m^2 for two buildings and 150 W/m^2 for the other buildings. The building energy models were created using DesignBuilder [40] and simulated using EnergyPlus [41] at 10-minute simulation steps. In Table 1, the key parameters of both clusters are given.

2.3. Building-Grid interaction signals

Sequential BGI signals differ from single or optimized signals by their dynamic prioritization mechanism, as described in Section 1, which activates specific signals based on predefined grid conditions, such as transformer overload, cost or GHG emission. Unlike single-signal approaches, sequential signals aim to balance competing objectives by integrating real-time feedback from the grid into control strategies. This study incorporates a novel sequential signal framework that evaluates the impacts of combining price- or CO_2-driven signals with TCS signals, thus addressing previously unquantified trade-offs between energy flexibility and grid stability.

2.3.1. Price-driven and emissions-driven Building-Grid interaction signal

Day-ahead prices (DAH) (before tax and surcharge) were utilised as the electricity unit price, with data accessible on the ENTSO-E Transparency Platform [42]. Similarly, CO_2eq intensity data was obtained

Table 1
The key parameters of the clusters.

	German building cluster	Swiss building cluster
Area	Ranging from 67 m^2 to 155 m^2 (net) – in total 850 m^2 (net)	137 m^2 (gross) for each building – in total 1080 m^2 (gross)
Heating system	8 reversible heat pumps – each with a thermal capacity of 10 kW and 4.5 COP	8 heat pumps – each with a thermal capacity of 15 kW and 3.5 COP
Cooling system	8 reversible heat pumps and 8 tanks – each with a volume of 500 L	No mechanical cooling
HWT	8 combi tanks – each with a volume of 500 L	8 tanks – each with a volume of 200 L
Buffer tank	No	8 tanks – each with a volume of 300 L
DHW	From HWT	From HWT
PV	2.5 kWp	1.5/3.0 kWp
Space heating demand (Thermal)	61 kWh/m^2	38.6 kWh/m^2
Space cooling demand (Thermal)	26 kWh/m^2	No mechanical cooling
Cluster total peak demand (Electrical)	11.5 kW	13.6 kW

Fig. 2. The Swiss building cluster simulated in this work (Ref: © Monika Hall).

from the Electricity Maps – Data Portal [43]. Both datasets are from 2023 – they are freely accessible and provided in hourly resolution. DAH are announced every day around 12:00 pm and present the dynamic electricity unit prices for the next entire day. For the purposes of this research, it was assumed that the bidding process in the DAH market was successful throughout the year. This assumes that the building is part of an aggregator's portfolio, enabling participation in the DAH market. Utilising this information, the building energy systems were optimised to use economic operation (i.e., objectively minimise operational costs) by controlling building energy systems within specific indoor thermal comfort setpoints. Accessing average emission data before energy price data is not easy. However, there are some studies that conduct forecasts using artificial intelligence technology, allowing such a signal to be used for environmentally friendly operation of the energy system. In this research, the German and Swiss datasets for price and emissions were exploited under the assumption that the datasets are known 24-hours in advance.

2.3.2. Transformer Building-Grid interaction signal

To generate a TCS BGI signal, a transformer model developed using IEC 60076–7 standard [30] was used in this study. The transformer's rated power was obtained by considering the peak cluster load observed over a year, before the use of available energy flexibility to modify the buildings' load according to the considered BGI signals. In practical applications, transformer design typically includes a security factor above the peak expected load to ensure operational safety. However, in this study, the transformer capacity was intentionally set equal to the peak load of the building cluster, without an additional safety margin. By not incorporating a built-in safety margin, the model exposes the transformer to its full load potential, thereby enabling a more sensitive evaluation of how BGI signals influence transformer heating, aging, and overloading. Since all control strategies and simulations were benchmarked using the same transformer capacity across cases in the specific cluster, the relative differences in aging and critical status are internally consistent and valid for comparison. Although absolute aging values might vary with a different transformer sizing strategy, the observed trends and relative performance of BGI signals remain robust.

The broader district typically consists of a large number of buildings (e.g. more than 50) that are connected to a shared transformer. However, for the purpose of this research, we focused on a smaller representative cluster of eight buildings in to balance computational complexity with a realistic level of detail. While in practice, a transformer would not be dedicated solely to this limited number of buildings; we scaled the transformer size in our models to match the aggregated peak demand of the simulated cluster under baseline conditions. This approach allowed us to isolate the impact of BGI signals on transformer performance under computationally manageable conditions. This resulting transformer capacity is therefore hypothetical, yet aligned with the actual load profile of the selected buildings.

The yearly power demand of the cluster is output at one minute resolution by the BPS tool. The highest demand value was found to be 11.5 kW and 13.6 for the German and Swiss building cluster, respectively which was used as the transformer capacity for the simulation scenarios executed in this research. It is important to note that a distribution transformer in real operation would have higher rated power values, for that reason, the model used based on IEC 60076–7 standard considers the load factor, i.e., absolute load normalised to the rated power, and not the absolute load.

This sizing approach allows future increases in peak load (e.g., resulting from increasing electrification and integration of PV systems) as the transformer does not operate above nominal power during the baseline scenario. At a constant transformer HST of 110 °C, the lifetime of a transformer is specified as 180,000 h, which corresponds to approximately 20.5 years. Since the transformer HST varies depending on the transformer utilisation and the ambient temperature, this must be calculated for each time step. If the transformer HST in the time step is lower than 110 °C, the lifetime is extended; if it is higher, it is shortened. This results in equivalent aging days. A higher number of equivalent aging days corresponds to a faster transformer aging.

The method from IEC 60076–7 was used to calculate the transformer HST and transformer aging. In [24], the standardised method according to IEC 60076–7, for calculating the transformer HST and equivalent aging based on one minute time steps was presented as a difference equation.

In this research, when the transformer HST exceeded 110 °C, TCS BGI signal was switched from zero to one (inactive to active). When this BGI signal became active, it suspended the price or CO_2eq intensity driven operation. More information about the utilisation of these signals is provided in Section 2.4.

2.4. Simulation scenarios

Two single BGI signals, specifically, DAH (€/kWh) and CO_2eq intensity (gCO_2eq/kWh) were used in the building simulations, as described in Section 2.3.1. To conduct the sequential signal analysis, each of these two signals were paired separately with a TCS signal (given in Section 2.3.2) in order to consider the transformer HST. This way it is possible to also evaluate the impact of these signals on building and power grid operation. In total, five different operation simulation scenarios were developed for each of the building clusters as presented in Fig. 3.

The baseline case of a cluster – the REF case was simulated as a reference scenario (no BGI load management is applied) to compare to BGI cases. In the single BGI signal cases, DAH (the DAH case) and CO_2eq intensity signals (the CO_2 case) were used to perform economic and environmental operation, respectively. Their impact on the power grid operation was analysed separately by incorporating TCS BGI signal in the DAH_TR case "DAH and transformer critical status" and "electricity CO_2eq intensity and transformer critical status" in the CO_2_TR case. More information about the utilisation of DAH, electricity CO_2eq intensity and TCS signals as drivers of the cluster control strategies are given in Section 2.5.

2.5. Building cluster control strategies

The basic assumption for the BGI is that a building operates in an economical or environmental-friendly manner. In this way, power demand is used to a greater extent when DAH or GHG emissions are low, or 'favourable'; conversely, higher or 'unfavourable' BGI signal values would trigger reduced demand. To define the 'favourable' and 'unfavourable' hours, an interquartile analysis was applied to categorise the signals for each day. This resulted in, six hours of low (favourable), six hours of high (unfavourable) and 12 h of medium (nominal) signal

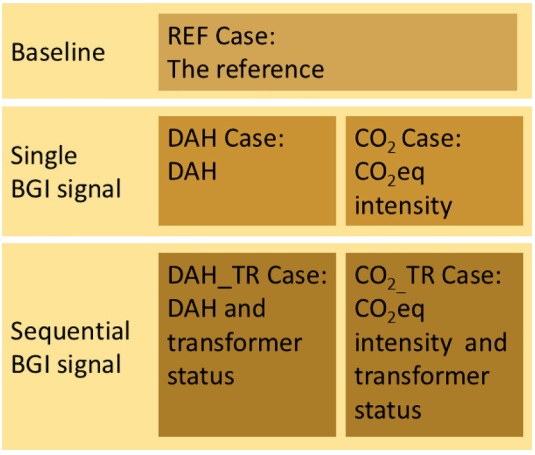

Fig. 3. The simulation cases performed in this research.

categories being established. This process was repeated for each simulation day based on the new daily BGI signal values. During low signal periods (≤ 25 % daily quartile), DAH and CO_2eq intensity are more favourable, allowing the building to operate at a lower cost or in a more environmentally friendly manner compared to the nominal operation. Conversely, during high signal periods (≥ 75 % daily quartile), prices and emissions are at their peak, leading to more expensive or less environmentally friendly building operation. Similar methodology was applied in the previous researches [16,44,45]. The illustration of price categorization using quartile analysis for an example date is included in the supplementary document – Fig. 2. Within the examined cases, ensuring thermal comfort remains a primary constraint at the building level.

In this framework, the control strategies were established based on the defined signal categories and rule-based control was implemented. In the German building cluster, the temperature of the hot and cold water storage tanks were controlled, whilst in the Swiss building cluster the temperatures of the indoor air, buffer and domestic hot water tanks were directly controlled. This approach indirectly manipulated the operation of the heat pump in both cases. It was assumed that all houses in the clusters receive the same signal simultaneously and reacted homogenously. During low (favourable) operating periods, the buildings were thermally charged by increasing the setpoints during the heating period. When the BGI signal entered the high (unfavourable) category, the setpoints were adjusted to slightly lower temperatures to reduce costs/emissions. During medium (nominal) operating periods, the setpoints remained at the same level as in the REF case. It should be noted that in the German building cluster, the heat pumps operated during the cooling season with setpoints adjusted using a similar methodology. However, in the Swiss building cluster, no active BGI signal was applied during the cooling season as there is no mechanical cooling operation.

Table 2 shows the heating season setpoints for the indoor air temperature and the HWT for both clusters respectively. Only the space heating buffer tanks and domestic hot water tank in the Swiss building cluster had direct setpoint temperature control. In the German building cluster, a HC (responding to the ambient temperature) determined the HWT setpoint temperature. Depending on the BGI signal, the temperatures were set to different levels, whereby the medium (nominal) setpoint temperatures were the standard HC values of the REF case operation. In low and high BGI signal periods, the setpoint was increased or reduced, respectively, by 5 °C than the HC value applied in the REF case. In cooling season, the cold-water tank was charged by 5 °C lower and 5 °C higher compared to the REF case cooling curve temperatures, when the BGI signal was at low and high level, respectively. Domestic hot water was charged for two hours during the day at a fixed 55°C temperature, and BGI strategies were not applied to its operation. Prior BPS studies for the German building cluster showed that the indoor temperature was maintained between 21 °C and 25 °C within this HWT temperature ranges. Therefore, there was no additional control strategy applied to retain indoor temperatures. In the Swiss building cluster, the indoor air temperatures were directly controlled based on the BGI signal, e.g. 23 °C and 18 °C were assigned during low and high BGI signal periods, respectively. When the BGI signal was at medium (nominal) levels, 21 °C was applied as in the REF case. If a setpoint of 23 °C was required, more heat from the buffer tank was used to supply the radiators and the buffer tank temperature increased from 50 °C to 55 °C. If the setpoint was at 18 °C, then, the buffer tank set point was set to 40 °C. Additionally, in the Swiss case, domestic hot water was supplied from the HWT. If the charging time coincided with a high BGI signal period, the setpoint was set to 45 °C; otherwise, it remained at 55 °C.

During price- and emission-driven BGI operation, rebound effects may increase stress on the transformer. For example, transformer HST can reach 110 °C when the applied setpoint temperature leads to higher peak loads from the power grid. It Is crucial for the control strategies to be adjusted to resolve the critical status on the transformer as presented in Fig. 4.

In this event, price- and emission-driven BGI operation was overridden, and transformer management took priority. To allow the transformer to cool down after the maximum temperature of 110 °C had been exceeded, the HWT temperature in the German building cluster was set to 10 °C lower than the HC temperature. In the Swiss building cluster, the heat pumps were switched off until the transformer temperature cooled down to a certain temperature. As there is no definition of a lower boundary for the transformer HST, 90 °C was assumed as the lower limit in this research. Occupant comfort was considered a priority, and so the "off" status remained until this hard limit was reached. Therefore, a minimum room temperature of 19 °C and 18 °C must be maintained for the German and Swiss building clusters, respectively.

It should be noted that, in the Swiss building cluster model, the transformer manager had no access to room or tank temperature data, nor to BGI signals. It sent a request to switch off the heat pumps when the transformer temperature was too high. The individual houses complied by adjusting their heating setpoint temperatures to the TCS levels, and the heat pumps were turned off individually if this revised thermal comfort requirement was met.

2.6. Co-simulation environment

In this research, two distinct simulation approaches were performed, each utilising specialised tools designed to meet specific requirements. The simulation approaches both comprise two main steps: (1) the computation of the transformer HST in order to generate a TCS BGI signal and (2) the determination of building performance metrics, such as HVAC operation values and thermal comfort levels. Step (1) was implemented by numerical computing tool and for step (2), BPS tool was utilized. These signals are crucial for implementing control algorithms aimed at demand optimization and for calculating yearly transformer aging. To ensure accuracy, these calculations must be performed concurrently, as each time step's results depend on the preceding step within this dynamic computational framework. To address this challenge, a co-simulation framework was established as per Fig. 5, enabling an in-depth analysis of different BGI signals.

Since this study was conducted through collaboration between two

Table 2
The applied setpoint control strategies for both clusters during heating and cooling seasons. GER: Germany, CH: Switzerland, HS: Heating Season, CS: Cooling Season, HC: Heating Curve, HWT: Hot Water Tank, TCS: Transformer Critical Status.

BGI signal	Cluster GER		Cluster CH		Buffer Tank Cluster GER	Cluster CH	HWT Cluster GER	Cluster CH
	HS	CS	HS	CS				
Baseline	21 °C	25 °C	21 °C	–	–	50 °C	HC	55 °C
Low level DAH/CO_2eq	21 °C	25 °C	23 °C	–	–	55 °C	HC + 5°C	55 °C
Medium level DAH/CO_2eq	21 °C	25 °C	21 °C	–	–	50 °C	HC	55 °C
High level DAH/CO_2eq	21 °C	25 °C	18 °C	–	–	40 °C	HC − 5 °C	45 °C
TCS	If TCS = 1, 19 °C		If TCS = 1, 18 °C		–	If TCS = 1, 40 °C	If TCS = 1, HC − 10 °C	If TCS = 1, 45 °C

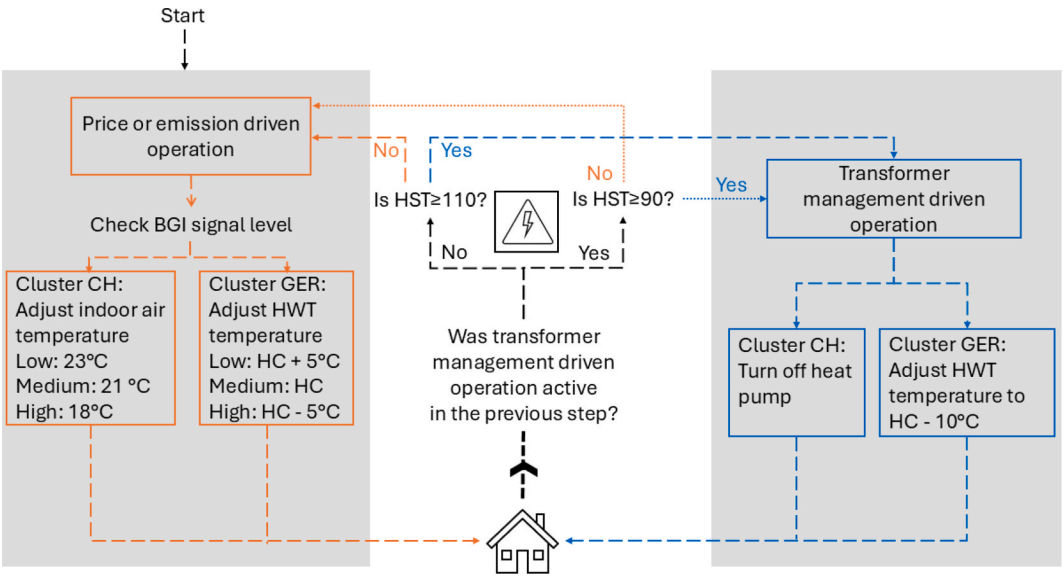

Fig. 4. The operational changes based on the sequential BGI signals in a building cluster. The orange line presents the operation flow described for the DAH case and the CO_2 case. The dynamic interaction with the transformer status is integrated with blue line in the DAH_TR case and the CO_2_TR case. HC: Heating Curve, HST: Hot Spot Temperature, HWT: Hot Water Tank.

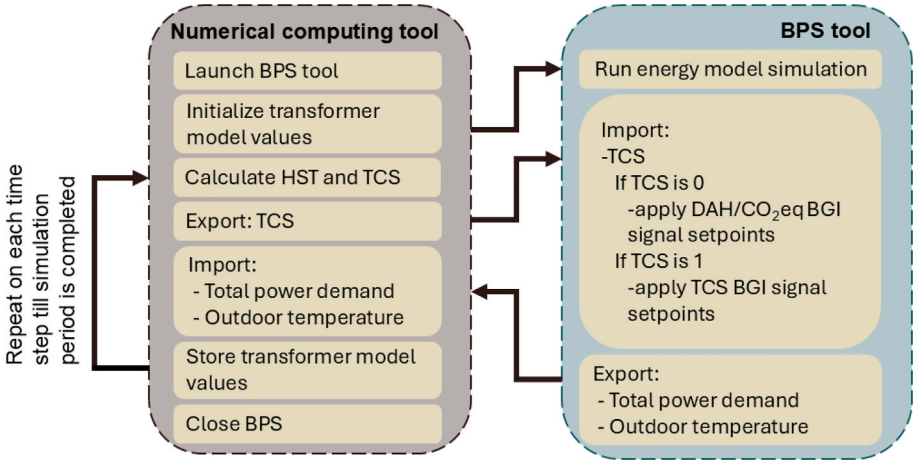

Fig. 5. The workflow between numerical computing tool and BPS tool in co-simulation environment.

institutions, one based in Germany and the other in Switzerland, each team employed the BPS tool standard to their institutional practices. Specifically, this study used a co-simulation environment that integrates BPS tools IDA-ICE [33] and EnergyPlus with numerical computing tools, Matlab [46] and Python [47] in the German and Swiss building cluster, respectively. In German building cluster, the co-simulation environment was established using communication channel as the data exchange pathway in Functional Mock-up Interface, and the Mosaik platform [48] was used in the Swiss building cluster. The time step for the transformer model described in Section 2.3.2 was set to one minute for calculation, as standard practices from IEC 60076–7 suggest this high resolution to accurately mode the thermal phenomena in the internal components of the transformer (e.g., windings temperature variation). In the German building cluster, the co-simulation environment was set up with a 1-minute time step to align with the given standard.

On the other side, this high-resolution calculation resulted in long simulation times and increased computational burden. As a solution to decrease the simulation time, the Swiss institution applied a modified method for calculating the transformer HST, accordingly. The differential equations were reformulated as integrals to enable a more flexible calculation across varying time steps and the simulation time step in the Swiss building cluster was set to 10 min. For verification purposes, the results were compared, showing a close agreement. The deviation of the predicted value of the modified method compared with the standardised method is approximately + 0.2 % for the maximum transformer temperature and approximately + 2 % for aging between the standard method at a 1 min time step, and the modified approach at a 10 min time step [49]. In the supplementary document, Fig. 3 presents the numerical difference between the standard method and modified method. In

Table 3
The used tools and parameters in this research.

	BPS Tool	Numerical Tool	Co-simulation environment	Co-simulation time step
German building cluster	IDA-ICE	Matlab	Channel connection	1 min
Swiss building cluster	EnergyPlus	Python	Mosaik	10 min

Table 3, the tools and parameters to set the co-simulation environment for the clusters are shown.

The objective of using a 1 min or adapted 10 min resolution in the co-simulation is to align with the transformer HST calculation time step. If the time steps of the two tools – namely, the numerical computing tool and the BPS tool – do not align, communication issues may arise, potentially resulting in failure of the co-simulation environment. Moreover, using larger time steps in the BPS tool, such as 30 min or one hour, can lead to missed peak loads, as the tool would compute results based on averaged data over the larger interval, also resulting in limitations for the transformer thermal model due to larger than expected time constants. This, in turn, could result in incorrect estimation of transformer stress.

3. Results

This section presents the simulation results for the two building clusters, evaluating how the same BGI signals influence building and grid operations under distinct operational conditions. Rather than conducting a direct comparison between clusters, this study aims to demonstrate how BGI signals interact with different building characteristics and control strategies. The findings provide insights into the adaptability of sequential BGI signals across varying grid and building contexts.

3.1. Daily load profile under different simulation cases

This section analyses representative daily load profiles from both clusters to illustrate demand variations across different simulation cases. Fig. 6 illustrates the operational demand and transformer state for the German building cluster on the 22nd of January at one minute resolution where the TCS BGI signal for the heating season was observed for the first time. The figure displays the REF case, economic optimisation the DAH case, and economic optimisation with TCS DAH_TR case in subplots A, B, and C, respectively. Since the analysis results exhibit a similar overall profile, the remaining cases – CO_2 and CO_2_TR – are not included in the figure. However, their impacts on transformer operation and other cluster metrics are presented in the next sections. In these three subplots, the cluster power demand, heat pump power demand and PV generation in kW are given on the left axis. The cluster power demand includes all the loads from building cluster, namely the heat pump power demand and baseloads as lighting, equipment, and plug-in loads. In the right axis, transformer HST (°C) and transformer utilisation (%) are illustrated by the dotted lines. In Fig. 6-D, the price BGI signal is

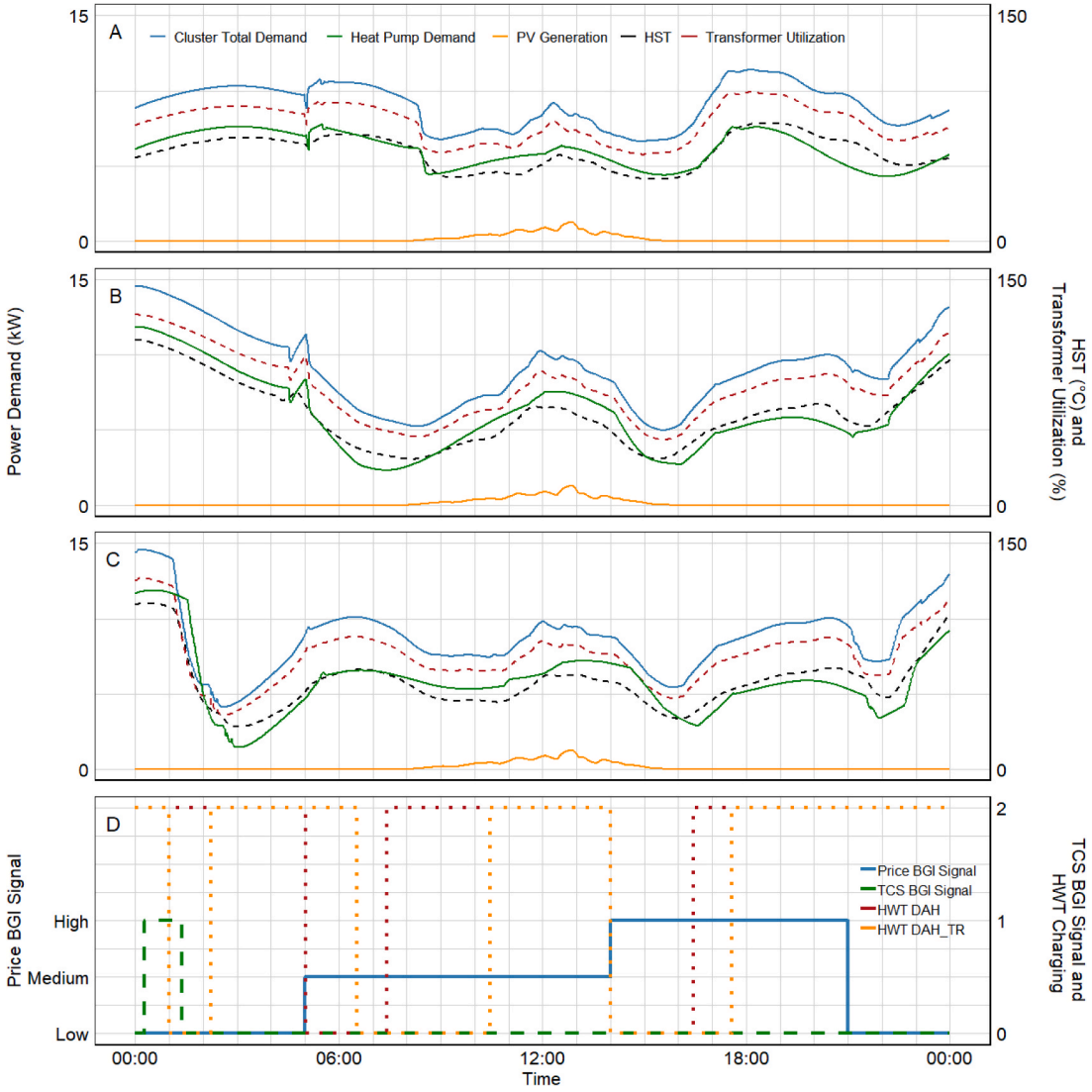

Fig. 6. The daily load profile presentation of the German building cluster for a day in January. Subplots A, B and C present the results from the REF case, the DAH case and the DAH_TR case, respectively. HST: Hot Spot Temperature, HWT: Hot Water Tank, TCS: Transformer Critical Status.

given on the left axis in high, medium and low levels where TCS and HWT charging signals are presented on the right axis. TCS status is defined as 0 (not active) and 1 (active), while HWT charging signal is 0 (no charge) and 2 (charge) on the right axis. The same price signal is exploited in both the DAH case and the DAH_TR case, however, the HWT charging signal varies for these cases since the operation control is in response to the HWT temperature value in addition to the price signal, thus it is presented as HWT DAH case and HWT DAH_TR case. TCS is only introduced for the DAH_TR case as described in Section 2.4. In the REF case, the operation of the heat pumps in the cluster was controlled relative to the ambient temperature HC as baseline operation scenario and the heat pump power demand was the main actor of the total cluster consumption. The highest heat pump and cluster total demand for this representative day were 8.0 kW and 11.5 kW, respectively. The transformer utilisation remained under 100 %, with the transformer HST reaching a safe level of up to 80 °C. Between 08:00 and 14:00, there was a slightly higher PV generation, but as there was no additional control strategy for PV generation in this research, the generation profile was same for all given cases. In Fig. 6-B, the DAH case results showed that, with the price driven strategy, the cumulative demand of eight heat pumps increased to 12 kW when the price was at low level at 00:00 and correspondingly the cluster total demand reached 15 kW. The transformer capacity in the German building cluster was limited to 11.5 kW and during thermal charging of the HWTs, the transformer HST increased to 115 °C, corresponding to a transformer utilisation of 125 %, exceeding its rated capacity. However, since the TCS BGI signal was not implemented in the DAH case, no additional control strategies were available to address the transformer overload when transformer HST reached 110 °C. As the HWT temperature reached the charging setpoint value, the heat pump power demand decreased and, based on the dynamic setpoint varying with the ambient temperature together with price level, the thermal charging was activated during the day at different times as 07:00 and 16:30. If the HWT temperature value was below the setpoint, even though it was a high price event period, e.g. 16:30–21:00, the heat pumps operation continued to ensure thermal comfort.

For the DAH_TR case, to keep the transformer HST below the desired maximum value of 110 °C, the TCS BGI signal was introduced in addition to the price BGI signal in the cluster control strategy. The first low price period started at 00:00 and the power demand of all heat pumps rapidly reached to 11 kW inducing the transformer HST increase (Fig. 6-C). However, when transformer HST raised to 110 °C, the TCS switched from 0 to 1 between 00:15 and 01:20 as given in Fig. 6-D. This event immediately supressed the thermal charging of HWT, and heat pumps' power demand decreased till the transformer HST drops to 90 °C. After ensuring the transformer HST was at 90 °C, the heat pumps again

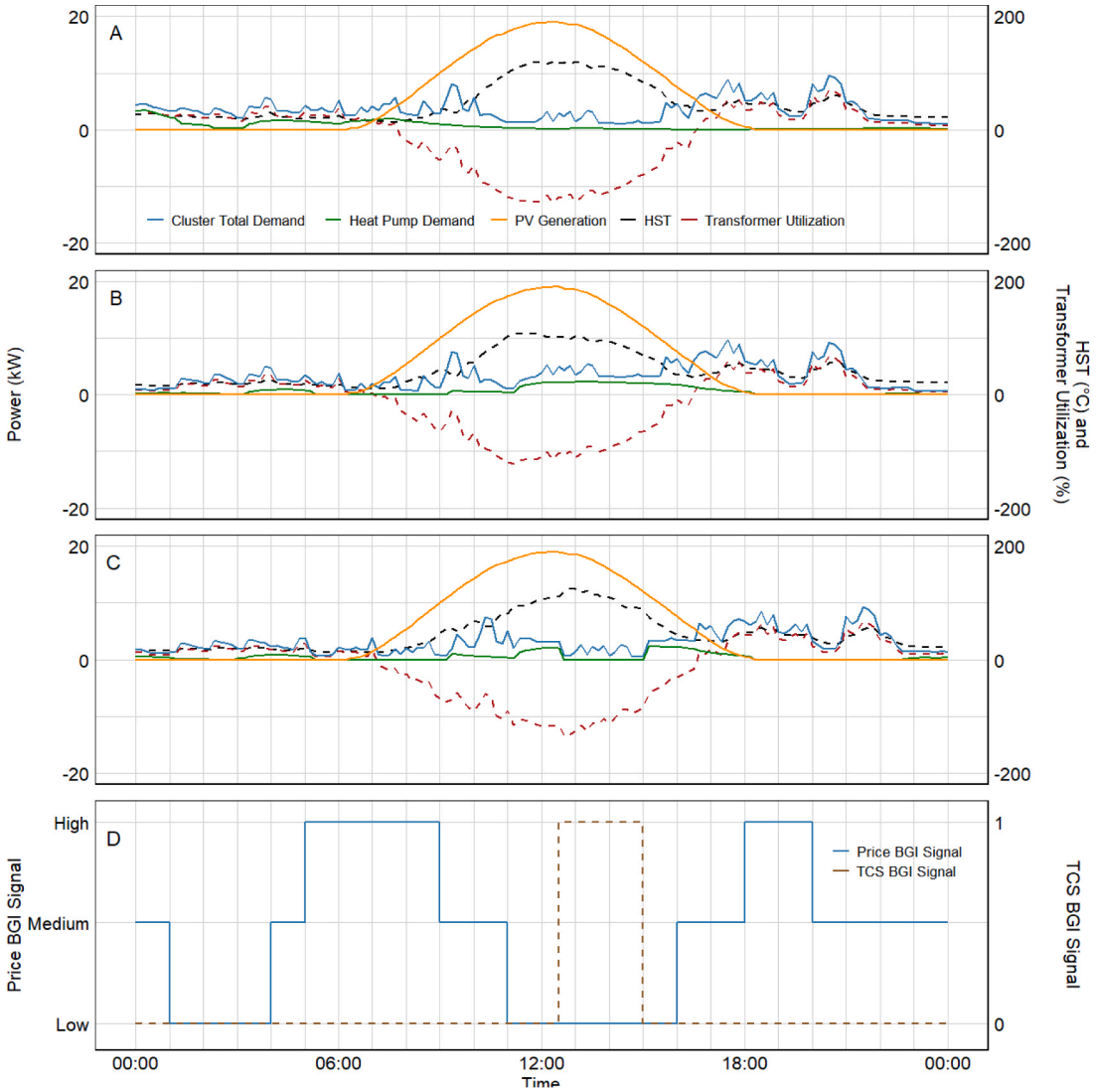

Fig. 7. The daily load profile presentation of the Swiss building cluster for a day in April. Subplots A, B and C present the results from the REF case, the DAH case and the DAH_TR case, respectively. HST: Hot Spot Temperature, TCS: Transformer Critical Status.

charged the HWTs based on the dynamic setpoint value at that certain moment. By falling 20 °C less than the critical transformer HST value, a secured time was ensured to avoid a repetitive TCS event since the following heat pump operation occurred in a short time if the HWT temperature was lower than the charging setpoint. The delayed activation of the HWT charging, kept the transformer HST at a normal range, thus, avoids the rapid transformer aging. This analysis is discussed in Section 3.2.

The operational analysis of the Swiss building cluster under different load management scenarios – REF, DAH, and DAH_TR cases – are presented in Fig. 7 (A), (B), and (C), respectively, using the 7th of April as a representative day.

This date was selected as it marks the first occurrence of the TCS BGI signal during the year. In contrast, in the German building cluster, the first occurrence of the TCS BGI signal (22nd of January) took place on a different day due to differences in climatic conditions, building thermal properties, and control strategies. Since the objective of this study is not to compare the clusters directly but to demonstrate how the operational scenarios apply under different conditions, each cluster was analysed based on the first occurrence of the TCS BGI signal within its respective operational context. This approach ensures that the analysis remains consistent with the goal of evaluating BGI signal utilization across diverse building configurations rather than drawing direct comparisons between clusters.

The Swiss building cluster total demand represents all loads from the entire cluster, including heat pumps as well as baseloads such as lighting, equipment, and plug-in loads. In Fig. 7-D, the price BGI signal and TCS BGI signal are presented. Unlike in the German building cluster, heat pump operation in this case was controlled by the manipulated indoor and buffer tank temperature. Consequently, no HWT thermal charging signal is designated in Fig. 7-D. In Fig. 7-A, which presents the operational analysis for the REF case, the power demand for heat pumps remained low, indicating that most of the cluster total demand was attributed to household loads. The peak heat pump demand and cluster total demand were approximately 3 kW and 10 kW, respectively. Given that PV generation significantly exceeds the total power demand, transformer utilisation was surpassed due to feed-in to the power grid, for instance, exceeding −120 % at 12:00. Consequently, the transformer HST surpassed 100 °C.

The results of the DAH case are presented in Fig. 7-B. As the price fell into the low category around 11:00 (as shown in Fig. 7-D), the indoor and the buffer tank setpoint temperatures raised, leading to an increased power demand from the heat pumps. The cluster total demand, including the additional heat pump demand, was covered by PV generation and the residual load was reduced, which resulted in a slight reduction in transformer utilisation, i.e. −110 %, and transformer HST.

The results of the DAH_TR case are presented in Fig. 7-C. As the transformer HST exceeded 110 °C after 12:00, the TCS switched to 1 (Fig. 7-D), and consequently, electricity consumption by the heat pumps dropped to 0 as they were switched off. However, PV generation remained high, and due to the reduced self-consumption after the heat pumps were deactivated, grid feed-in increased. This, in turn, raised transformer utilisation and further increased the transformer HST. To reduce the transformer HST, the heat pumps need to be activated at midday when there is a high PV surplus in order to increase self-consumption. As the transformer HST must first go down to 90 °C before the heat pumps are allowed to start again, an event extends over a longer period, e.g. two hours. This results in a counterproductive outcome, where the control strategy in the DAH_TR case inadvertently exacerbates transformer loading. This issue is further discussed in Section 4. Fig. 7-B shows that during low prices at midday, the heat pumps are activated with higher indoor setpoint temperatures. In the REF case, only medium target temperatures were set, resulting in a lower electricity demand for space heating than the DAH case.

3.2. Transformer hot spot temperature and aging

The fluctuations in transformer HST across different representative weeks are illustrated in Fig. 8, highlighting the transformer HST peaks. Representative weeks from January (when first TCS BGI signal occurs) and July are given for the German building cluster, whereas weeks from April (when first TCS BGI signal occurs) and July are shown for the Swiss building cluster.

In the heating season, the control of HWT setpoint temperatures in response to the single BGI signals in the German building cluster resulted in a broader range of transformer HST values in January compared to the REF case. For example, the transformer HST varied between 20 °C and 110 °C, whereas in the REF case, it reached up to 80 °C. The broadened setpoint temperatures altered heat pump operation, leading to changes in power demand from the grid. During the cooling season in July, some transformer HST peaks were higher in the REF case since PV generation partially covered the power demand of the building, and the rest was fed into the power grid. In the DAH case and the DAH_TR case, the setpoint of the cold-water storage tank was lower during the favourable BGI signal periods, thereby increasing demand and reducing the surplus electricity feed-in by covering the increased heat pump demand. This leaded to a decreased transformer HST since the transformer stress was mitigated. In some events, transformer HST was higher than the desired maximum value of 110 °C such as 125 °C which occurred a few times due to the feed-in from surplus PV generation. One such event spans the period during which the transformer HST rises above 110 °C and subsequently returns to 90 °C, with the duration of these events varying. Except the feed-in event times, the transformer stress was less in the German building cluster during cooling season because the feed-in was decreased with BGI control strategies exploited by increased active cooling.

As presented in Section 3.1, the transformer was stressed due to PV feed-in event in the Swiss building cluster. In the Swiss building cluster during April, higher transformer HST occurred during midday when feed-in was at its peak. On the 7th of April, the transformer HST value reached 110 °C in the REF case, and when TCS was introduced in the DAH_TR case, the heat pump operation was suspended which lowered the self-consumption and caused higher transformer HST. In the cooling season, there was no mechanical cooling as described in Section 2.2, thus, the transformer HST values remained the same for the cooling season in all cases. Feed-in from the PV generation was the main driver that the transformer HST reached to 130 °C in July.

The transformer aging results, relative to the reference scenario, are presented in Fig. 9. To provide a standardized reference for comparison of transformer aging the overall annual value of the REF case transformer aging was normalized to 100 % as can be seen for the German building cluster in Fig. 9-A and Swiss building cluster in Fig. 9-B. The normalization allows us to compare the transformer aging of the different cases easier.

In the REF case of the German building cluster, where no BGI signal was applied, transformer aging was the lowest at 1.9 days. In this baseline case, the cluster power demand did not have sharp peaks that the transformer capacity was approached frequently. However, when a single BGI signal was used, such as in the DAH case and CO_2 case, the applied control strategy caused significant peaks resulting in reaching to the transformer capacity, where faster transformer aging ensued.

The most rapid aging occurred in the DAH case and then following in the CO_2 case with slightly less difference as 262 % and 253 %, respectively. When the TCS signal was included in the DAH_TR case and the CO_2_TR case, the building energy systems operation could align with the transformer needs, e.g., the cluster's power demand was reduced, alleviating transformer stress. As seen, by the introduction of this signal, the relative aging was found lower as 250 % and 230 % in the DAH_TR case and CO2_TR case compared to the CO_2 and DAH cases, respectively. The rapid aging during heating season addresses the impact of demand peak developments from BGI control strategies, e.g., applying higher

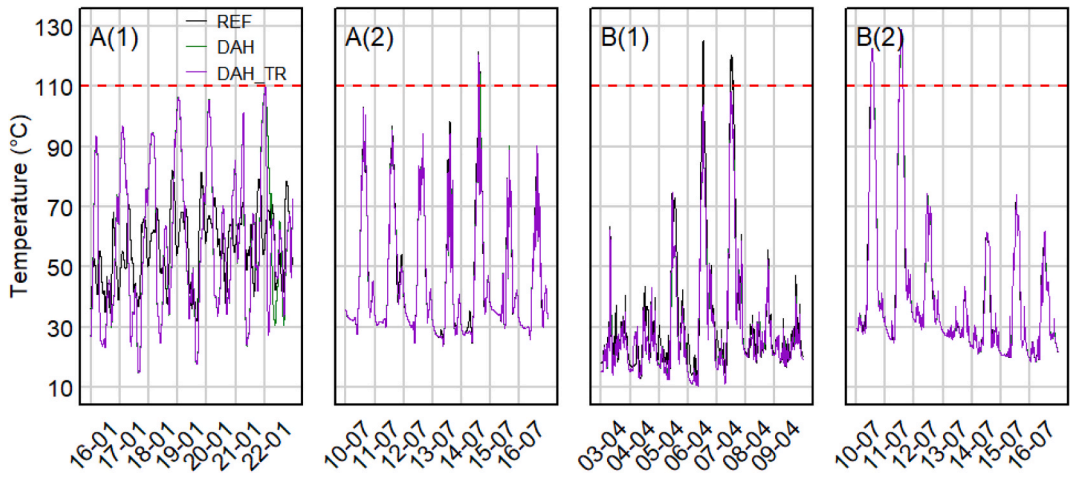

Fig. 8. The transformer HST change for the selected cases for representative weeks, where the red line represents the HST limit which triggers a TCS BGI signal. A(1) and A(2) present the results from the German building cluster, whereas B(1) and B(2) show the results for the Swiss building cluster.

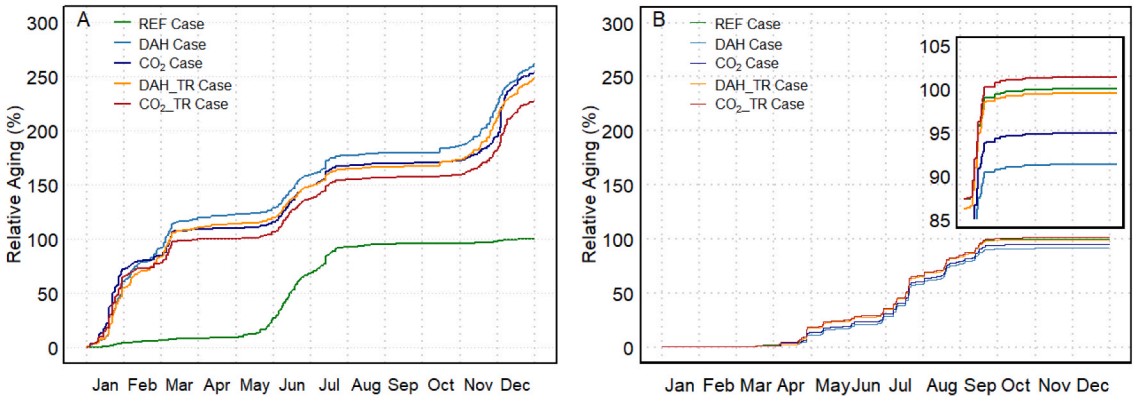

Fig. 9. The transformer relative aging for both clusters over a year. A – German building cluster, B-Swiss building cluster. The Swiss building cluster relative aging between September and December is illustrated in a zoom view.

setpoints compared to the REF case. In the cooling season, PV generation was at the highest level where it covered mainly the cooling demand. Besides, when there was relatively less demand and surplus generation, it was fed into the power grid. As seen during June and July, the aging accelerated where the feed-in caused higher transformer HST in all cases. During the transition season, i.e., May and September, the building heating and cooling demands were lower, hereby, BGI control could not take place often as applied during the rest of the year.

In the Swiss building cluster, the equivalent aging days in the REF case is 16.7 due to PV feed-in. The PV feed-in in the German building cluster is relatively lower compared to the Swiss building cluster. Therefore, there is a significant difference in transformer aging between the two clusters. In general, the single BGI signal operations in the DAH case and CO_2 case showed the lowest relative aging as 91 % and 95 %, respectively (Fig. 9-B). In those cases, the heat pumps often ran around midday during the heating season, when PV yield was also available. This increased the self-sufficiency and reduced the grid feed-in, which had a positive influence on aging. In the DAH_TR case and the CO_2_TR case, since the TCS BGI signal was rarely activated, they showed almost the same aging curve as 99 % and 101 %, respectively. As the main aging took place in summer due to the high grid feed-in the aging of all Swiss building cluster cases were close. The impact of PV feed-in is evaluated more in the Discussion section.

3.3. Transformer load, cost, greenhouse gas emissions and thermal comfort change

The cases DAH, CO_2, DAH_TR and CO_2_TR, where BGI signal were exploited in the cluster operation, were compared to the baseline operation – the REF case. The analysis under different operation scenarios revealed distinct results between the two building clusters located in Germany and Switzerland. In Fig. 10, the transformer load observed at the power grid meter connected to the transformer is shown, reflecting values after accounting for self-consumption.

In the German building cluster, transformer load increased in the range of 6.0 % to 7.1 % when BGI control strategies were applied. In the single BGI signal operation, the transformer load was slightly lower than sequential BGI signal cases. In the Swiss building cluster, the transformer load increased in the DAH case and the DAH_TR case in the range of 2.6 % to 2.8 % where price BGI signal was used in the cluster operation. However, in the CO_2 case and the CO_2_TR case –where CO_2eq intensity BGI signal was utilised- transformer load decreased 0.9 % because CO_2eq intensities changed very often and rarely longer periods with high or low setpoints occur. Since TCS BGI for CO_2eq. was more rarely activated than the DAH cases, no change was observed between the CO_2 case and the CO_2_TR case in the Swiss building cluster.

The cost saving was higher in the DAH case and the DAH_TR case around 4.0 % and 8.0 % for the German and Swiss building clusters respectively, as presented in Fig. 11. Fewer savings in the CO_2 case and CO_2_TR were calculated since the DAH and CO_2eq intensity are not

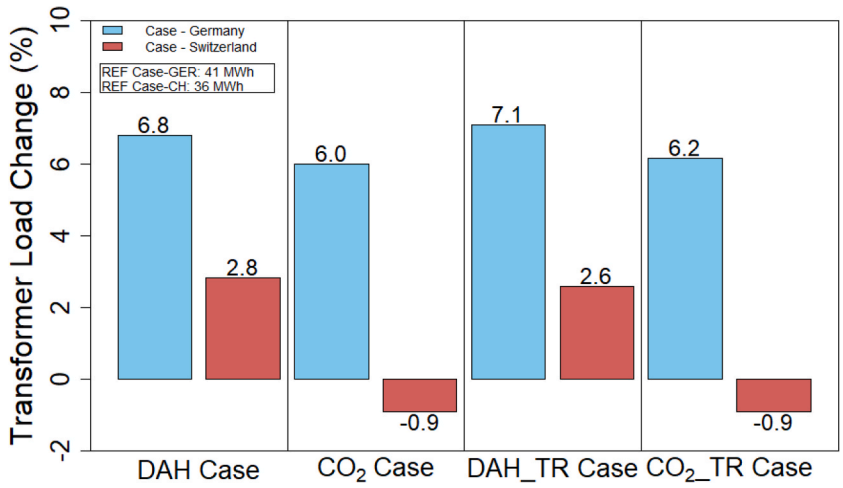

Fig. 10. Yearly transformer load change relative to the REF case for both clusters.

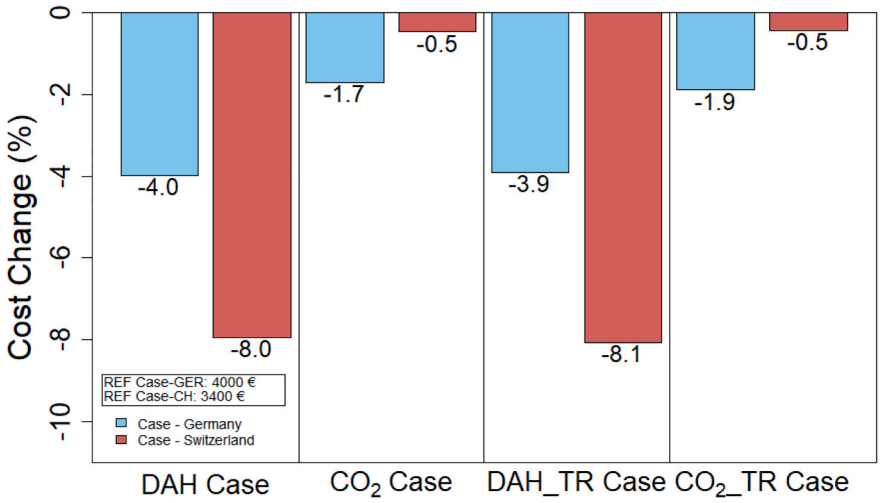

Fig. 11. Yearly energy cost change relative to the REF case for both clusters.

correlated positively among year all the time. When a cluster is operated using a BGI signal with a certain objective, e.g. a price signal to achieve economical saving, this may reflect oppositely on the operational savings of cases where different objective is aimed such as reducing GHG. The results of DAH and DAH_TR case were close to each other on both clusters since the TCS occurred a few times during the year which did not change the operational savings significantly. The same behaviour also was seen for the CO_2 case and the CO_2_TR case. As mentioned above

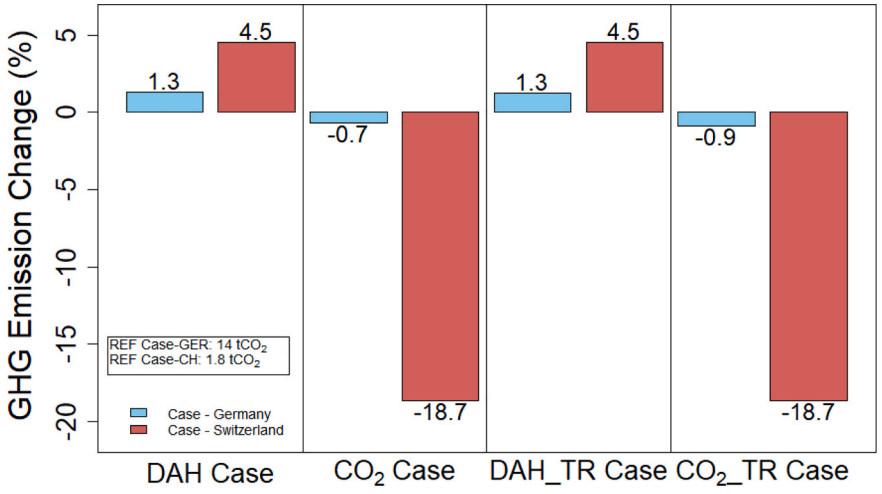

Fig. 12. Yearly GHG emission change relative to the REF case for both clusters.

TCS BGI for CO2eq. was more rarely activated than the DAH cases, no change was observed between the CO_2 case and the CO2_TR case in the Swiss building cluster.

As given in the cost change analysis, the uncorrelated trend of DAH and CO_2eq intensity BGI signal affected GHG emission saving differently on the DAH case and the CO_2 case. In Fig. 12, the GHG emission was 0.7 % less in the CO_2 case compared to the REF case and it was found 0.9 % less in the CO_2_TR case for the German building cluster. In the Swiss building cluster, the GHG emission had a reduction of 18.7 % under the CO_2eq intensity signal operation in the CO_2 case and (5). As described before, TCS occurs rarely, therefore the results were the same or did not differentiate significantly. Conversely, the GHG emissions increased by 1.3 % and 4.5 % in the DAH case and the DAH_TR case for the German and Swiss building cluster, respectively.

The BGI operational control strategies must be implemented without compromising thermal comfort as discussed in Section 2.5. To assess this, the operative temperature of one selected building from the German building cluster (Fig. 13-A) and the Swiss building cluster (Fig. 13-B) under the DAH_TR case operation is presented for the entire year. In German building cluster, active heating and cooling were utilised to maintain indoor temperatures between 21 °C and 25 °C, in alignment with the ISO 7730 standard [50]. In contrast, the Switzerland case lacked mechanical cooling, adhering instead to the comfort range defined by the SIA 180 standard [51]. This standard considers the moving average of the ambient temperature over 48 h as a benchmark for acceptable comfort levels. In both clusters, there were instances where temperatures exceeded or fell short of the prescribed limits: 21 °C in the German building cluster and the SIA 180 limits in the Swiss building cluster. In the German and Swiss building cluster, the lowest indoor temperature for the representative buildings was 20.3 °C and 18.0 °C, respectively. These deviations arose because ventilation, achieved through manual window operation, was controlled either by indoor CO_2 levels or a fixed window opening schedules. In the Swiss building cluster, where the BGI control strategy was limited to heat pump operation during the heating period, deviations below the lower temperature limit for heating were highlighted in the grey area. Nonetheless, temperatures below the lower limit occurred only within a narrow range in both clusters.

Temperatures below the lower limit and above the higher limit occurred during the non-heating season (white area). The shortfalls occurred due to the fix nighttime ventilation between the 15th of June and the 15th of August. The excesses are based on the window opening times during daytime. As mentioned, the ventilation time is based on a fix time schedule and independent of the ambient temperature. Crucially, for both occupant comfort and the effective implementation of this control strategy, thermal conditions were maintained in both clusters. However, slightly lower indoor temperatures were observed due to natural ventilation.

4. Discussion

This research analysed the operation of the building clusters and their transformers over an entire year. Single day building operation results showed distinct differences between the examined building clusters. In the German building cluster, the TCS was triggered due to the increased heat pump demand in the cluster. However, in the Swiss building cluster, the heat pump demand was comparatively less than the overall cluster demand. Especially because of the high amount of PV generation, where the excess power was fed into the grid resulting in transformer overload triggering the TCS. When the transformer is overloaded, in principle, the demand should be reduced. In the Swiss building cluster, reducing demand led to a decrease in PV energy consumption during heating season, which reduced self-sufficiency. Consequently, the amount of power fed into the grid increased. To avoid this situation, we want to highlight the importance of integrating advanced control strategies specific to each building within the cluster. If transformer HST is high due to feed-in, large consumers should adjust their setpoint temperatures to peak values within the acceptable range of thermal comfort levels or switch on their HVAC systems. If no grid feed-in occurs during times with high transformer HST, the building/s with high demand should minimise their demand or switch off their HVAC systems. In this research, all buildings in the same cluster were controlled with the same control strategy and no individual control was applied for each building. Our future work involves developing customized control strategies for each building, aligned to its demand profile.

While the clusters are not meant to be compared in a normative sense (e.g., which performs better), their differences allow us to observe how system behaviour and control outcomes vary due to system-specific properties. For example, in the German building cluster, where the cluster peak heating demand is higher than the Swiss building cluster, the load shifting could be applied on a larger scale. Higher setpoints lead to greater demand on the heat pump and the thermal storage, enabling effective peak shaving during periods of low BGI categories. However, the increased peaks resulted in faster aging during heating season. In contrast, the peak heating demand is lower because of buildings thermal properties in the Swiss building cluster, and the higher setpoints setting did not accelerate the transformer aging on the heating system since the increased heating demand was partially covered by PV generation. Therefore, the aging resulted in a lower value compared to REF case. During the cooling season, the rapid transformer aging was slowed down in the German building cluster as PV generation partially covered the

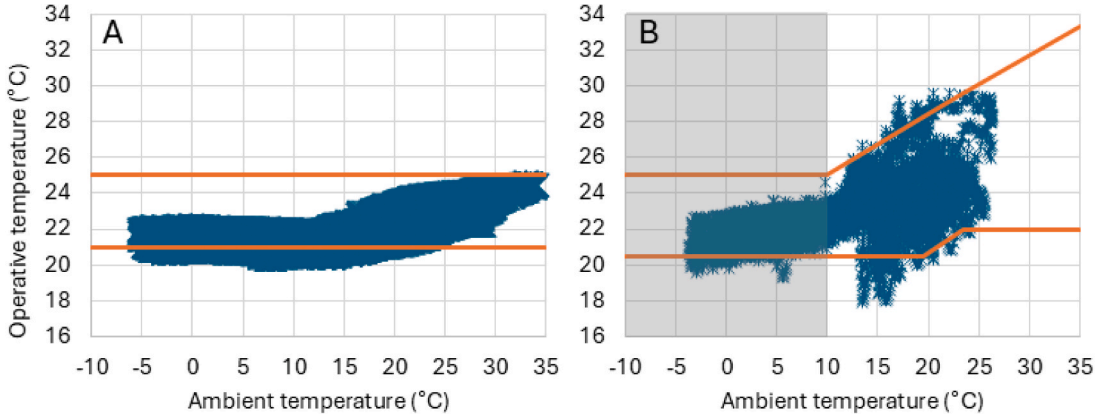

Fig. 13. The indoor operative temperature of representative buildings from the cluster Germany (A) and Switzerland (B). In (A), ISO 7730 standard with fixed temperature boundaries is applied. In (B), the moving average of the ambient temperature over 48 h according to SIA 180 is applied and presented on the x-axis. Grey area in (B) presents the heating season.

cooling demand and there were less feed-in events compared to the REF case. Conversely, the Swiss building cluster's lack of mechanical cooling system limits its summer flexibility, leading to TCS events and fewer opportunities for dynamic control, which results in rapid transformer aging during the cooling season, i.e., the transformer aging was less than REF case in DAH and CO_2 cases. This leads to observable differences in transformer HST profiles and aging rates under the same BGI control structure between clusters. It is important to note that the transformer HST is affected not only by the cumulative cluster power demand, but also by the ambient temperature as previously mentioned. If this research were conducted in a region with vastly different climate characteristics, the TCS could activate more frequently, potentially accelerating the transformer aging and maintenance cost.

When evaluating yearly metrics such as transformer load, cost, and GHG emission savings, no significant differences were observed between DAH and the DAH_TR cases and also between CO_2 and the CO_2_TR cases. However, the timing of peak events during the day differed. This discrepancy arises because the CO_2eq intensity value is not always positively correlated with the price value [29]. In future, when the electricity market dynamic aligns closer with the RES supply and demand imbalances, an integrated strategy can be applied for both cost and GHG emission saving. Although electric vehicles are not examined in this study, their increasing share is expected to influence transformer load. Incorporating charging strategies have to be included in the BGI signal controls.

On the other side, both clusters include highly insulated, energy-efficient buildings. This raises questions about the future viability of building–grid interaction as the stock of energy-efficient buildings grows. When most buildings have minimal heating and cooling demands, their ability to relieve congestion events will be limited, and the resulting cost savings may not be sufficient to motivate end users to participate. Consequently, more innovative business models and incentive structures will be needed to sustain engagement in building-grid interaction schemes.

These variations underscore a key finding: BGI signals perform very differently depending on each cluster's system setup, seasonal operating patterns and flexibility reserves. Rather than aiming for uniform results, our study stresses the importance of fitting control strategies to each scenario and shows how signals can produce varied effects, even when driven by the same protocols, because of each cluster's distinct composition. A key insight from this study is the importance of distinguishing between load-driven and generation-driven transformer stress when designing flexibility control strategies. In load-driven scenarios, such as peak heating or cooling demand, reducing or shifting consumption is a viable means to relieve transformer stress. In contrast, generation-driven stress, e.g., caused by high PV feed-in, requires alternative strategies, such as coordinated load activation or storage integration, to absorb excess generation and avoid back feeding-related transformer overload. Therefore, applying identical control signals across clusters without accounting for the dominant source of transformer stress may lead to suboptimal outcomes. Including two clusters helps to highlight that flexibility solutions are not one-size-fits-all. This is particularly relevant for stakeholders developing scalable demand side management strategies or integrating flexibility into building stock.

Additionally, authors consider three operational control strategies that could be applied as future work: curtailment of PV generation, implementation of an electrical energy storage system and scheduling the preheating of domestic hot water system during high PV generation. The first option provides a complete solution by curtailing generation in proportion to the extent of transformer overloading. In some countries like Germany, this approach is applied. However, this also would mean a reduction in renewable energy usage, which does not align with the transition efforts from fossil-based systems to RES. Charging electrical energy storage systems, electrical vehicles and preheating the domestic hot water storage could assist the power grid operation during feed-in times. This also would increase the self-sufficiency of the system. Additionally, in the case of applying these advanced control strategies, we suggest considering energy sharing solutions within a building cluster where the energy is shared within the local grid. Various business models can be applied that the power is sold to the grid/local network or traded between the neighbours.

5. Conclusion

In this research, we address the growing demand for Building-Grid Interaction (BGI) applications at cluster level which plays a significant role for electrification and full integration of renewable energy systems (RES) into power grid. In this study, single and sequential BGI signals were exploited to unlock energy flexibility and present their impact on the power grid. The single BGI signals used were day-ahead prices and electricity CO_2eq intensity to enable economical and grid-friendly operation in different simulation cases, respectively. To reflect the status of power grids, especially when there is peak shift event occurring during favourable BGI signal times, a transformer model that complies with the IEC 60076–7 standard was integrated into the Building Performance Simulation (BPS) environment and the research was conducted under a co-simulation framework. Two energy-efficient building clusters from Germany and Switzerland, were used as case studies. Since the power grid robustness has priority over the price or the CO_2eq intensity BGI signal operation, a hierarchical approach was applied where TCS BGI signal overrides the in-use BGI signal and changes the operational control strategies in order to support the reliable power grid operation.

The results reveal that while single BGI signal implementation optimise demand side management, their simultaneous application within a cluster can trigger grid instabilities, highlighting the need for additional BGI signal such as TCS. The sequential integration of TCS with other BGI signal effectively prevents transformer overloads. However, the control strategy should be building customized focusing on the transformer stress ground as load-driven or generation-driven transformer. The findings suggest future research on integrating advanced controls and advanced control technologies such as electrical energy storage utilisation and energy-sharing models within a cluster to enhance energy system resilience and flexibility. These outcomes offer strategies for integrating buildings into the power grid and supporting the shift to a low-carbon future.

Another important point the authors want to highlight is the challenges to conduct a BGI analysis in a co-simulation environment. In the market, there are various BPS tools that can be purchased or freely used. During the transition of energy supply systems, the users require a platform where the cluster of buildings and energy grid analysis can be performed together without requiring heavy additional effort. In this research, to carry out the BGI analysis, different tools were coupled, and considerable time was spent to obtain stable communication between the tools and print high resolution data. Moreover, this output data was stored in those tools individually and required additional time for post-processing. With the growing electrification and BGI applications, the demand for user-friendly, fast and stable tools will be increasing.

Declaration of Generative AI and AI-assisted technologies in the writing process

During the preparation of this work the authors used OpenAI ChatGPT in order to improve the readability and language of the manuscript. After using this tool/service, the authors reviewed and edited the content as needed and take full responsibility for the content of the published article.

CRediT authorship contribution statement

Tuğçin Kırant-Mitić: Writing – review & editing, Writing – original draft, Visualization, Validation, Methodology, Formal analysis, Data

curation, Conceptualization. **Monika Hall:** Writing – review & editing, Validation, Methodology, Formal analysis, Data curation, Conceptualization. **George Dawes:** Writing – review & editing, Methodology, Conceptualization. **Rui Amaral Lopes:** Writing – review & editing, Software, Resources, Methodology, Conceptualization.

Declaration of competing interest

The authors declare that they have no known competing financial interests or personal relationships that could have appeared to influence the work reported in this paper.

Acknowledgements

The authors would like to gratefully acknowledge the IEA EBC Annex 82 for providing the framework in which this work was completed. The analysis of the German building cluster in this research was carried out in the framework of the project "Living Lab NRW" supported by the Ministry of Economic Affairs, Industry, Climate Action and Energy of North Rhein-Westphalia under the contract number EFO 0027. The Swiss work described in this paper was funded by the Swiss Federal Office of Energy SFOE under contract number BFE SI/502154. The UK contribution to this work was made possible by support from the EPSRC & SFI Centre for Doctoral Training in Energy Resilience and the Built Environment (ERBE CDT) (grant EP/E21671/1). The Portuguese contributions were supported by the Portuguese "Fundação para a Ciência e a Tecnologia" (FCT) in the context of the Center of Technology and Systems CTS/UNINOVA/FCT/NOVA, reference UIDB/00066/2020.

Appendix A. Supplementary data

Supplementary data to this article can be found online at https://doi.org/10.1016/j.enbuild.2025.116235.

Data availability

Data will be made available on request.

References

[1] United Nations, *The Paris Agreement | United Nations.* [Online]. Available: https://www.un.org/en/climatechange/paris-agreement (accessed: Jul. 21 2024).
[2] C. Peng, J. Zou, L. Lian, Dispatching strategies of electric vehicles participating in frequency regulation on power grid: a review, Renew. Sustain. Energy Rev. 68 (2017) 147–152, https://doi.org/10.1016/j.rser.2016.09.133.
[3] Y. Chen, et al., Experimental investigation of demand response potential of buildings: combined passive thermal mass and active storage, Appl. Energy 280 (2020) 115956, https://doi.org/10.1016/j.apenergy.2020.115956.
[4] W. Liao, F. Xiao, Y. Li, H. Zhang, J. Peng, A comparative study of demand-side energy management strategies for building integrated photovoltaics-battery and electric vehicles (EVs) in diversified building communities, Appl. Energy 361 (2024) 122881, https://doi.org/10.1016/j.apenergy.2024.122881.
[5] D. J. S. Coumans, M. O. W. Grond, and E. J. Coster, "Impacts of future residential electricity demand and storage systems on 'classic' LV-network design," in *2015 IEEE Eindhoven PowerTech*, Eindhoven, Netherlands, 2015, pp. 1–6.
[6] S. Shao, M. Pipattanasomporn, S. Rahman, Demand Response as a load Shaping Tool in an Intelligent Grid with Electric Vehicles, IEEE Trans. Smart Grid 2 (4) (2011) 624–631, https://doi.org/10.1109/TSG.2011.2164583.
[7] P. Hoseinpoori, A.V. Olympios, C.N. Markides, J. Woods, N. Shah, A whole-system approach for quantifying the value of smart electrification for decarbonising heating in buildings, Energ. Conver. Manage. 268 (2022) 115952, https://doi.org/10.1016/j.enconman.2022.115952.
[8] J. Kossahl, J. Kranz, N. Opitz, and L. Kolbe, Eds., *A Perception-based Model for Smart Grid Adoption of Distribution System Operators - An Empirical Analysis*, 2012.
[9] A. Usman, S.H. Shami, Evolution of Communication Technologies for Smart Grid applications, Renew. Sustain. Energy Rev. 19 (2013) 191–199, https://doi.org/10.1016/j.rser.2012.11.002.
[10] F.R. Albogamy, et al., Real-Time Energy Management and load Scheduling with Renewable Energy Integration in Smart Grid, Sustainability 14 (3) (2022) 1792, https://doi.org/10.3390/su14031792.
[11] M.J. Kalani, M. Kalani, Controlling the energy supply and demand of grid-connected building integrated photovoltaics considering real-time electricity prices to develop more sustainable and smarter cities, Optik 300 (2024) 171629, https://doi.org/10.1016/j.ijleo.2024.171629.
[12] European Union Directorate-General, *European Energy Performance of Buildings Directive: Smart readiness indicator.* [Online]. Available: https://energy.ec.europa.eu/topics/energy-efficiency/energy-efficient-buildings/smart-readiness-indicator_en (accessed: 12-Dec-24).
[13] Y.-J. Kim, G. Del-Rosario-Calaf, L.K. Norford, Analysis and Experimental Implementation of Grid Frequency Regulation using Behind-the-Meter Batteries Compensating for Fast load demand Variations, IEEE Trans. Power Syst. 32 (1) (2017) 484–498, https://doi.org/10.1109/TPWRS.2016.2561258.
[14] Y. Ding *et al.*, "Development of a DSO-market on flexibility services," 2013. Accessed: Aug. 2 2024.
[15] Z. Afroz, H. Wu, S. Sethuvenkatraman, G. Henze, R. Grønborg Junker, M. Shepit, A study on price responsive energy flexibility of an office building under cooling dominated climatic conditions, Energ. Buildings 316 (2024) 114359, https://doi.org/10.1016/j.enbuild.2024.114359.
[16] J. Clauß, S. Stinner, C. Solli, K.B. Lindberg, H. Madsen, L. Georges, Evaluation Method for the Hourly Average CO2eq. Intensity of the Electricity Mix and its Application to the demand Response of Residential heating, Energies 12 (7) (2019) 1345, https://doi.org/10.3390/en12071345.
[17] M. You, Q. Wang, H. Sun, I. Castro, J. Jiang, Digital twins based day-ahead integrated energy system scheduling under load and renewable energy uncertainties, Appl. Energy 305 (2022) 117899, https://doi.org/10.1016/j.apenergy.2021.117899.
[18] L. Zheng, B. Zhou, Y. Cao, S. Wing Or, Y. Li, K. Wing Chan, Hierarchical distributed multi-energy demand response for coordinated operation of building clusters, Appl. Energy 308 (2022) 118362, https://doi.org/10.1016/j.apenergy.2021.118362.
[19] N.G. Paterakis, O. Erdinc, I.N. Pappi, A.G. Bakirtzis, J.P.S. Catalao, Coordinated operation of a Neighborhood of Smart Households Comprising Electric Vehicles, Energy Storage and distributed Generation, IEEE Trans. Smart Grid 7 (6) (2016) 2736–2747, https://doi.org/10.1109/TSG.2015.2512501.
[20] R.G. Junker, et al., Characterizing the energy flexibility of buildings and districts, Appl. Energy 225 (2018) 175–182, https://doi.org/10.1016/j.apenergy.2018.05.037.
[21] M. Song, K. Alvehag, J. Widén, A. Parisio, Estimating the impacts of demand response by simulating household behaviours under price and CO2 signals, Electr. Pow. Syst. Res. 111 (2014) 103–114, https://doi.org/10.1016/j.epsr.2014.02.016.
[22] M. Kilthau, et al., Integrating Peer-to-Peer Energy Trading and Flexibility Market with Self-Sovereign Identity for Decentralized Energy Dispatch and Congestion Management, IEEE Access 11 (2023) 145395–145420, https://doi.org/10.1109/ACCESS.2023.3344855.
[23] D. Cano-Tirado, M. Forchheim, M. Asman, M. Zdrallek, and S. Palmer, Eds., *Potential Grid-Oriented and Market-Oriented Optimisation of a Local Charging Infrastructure Through a Genetic Algorithm*. Austria, 2024.
[24] R.A. Lopes, P. Magalhães, J.P. Gouveia, D. Aelenei, C. Lima, J. Martins, A case study on the impact of nearly Zero-Energy buildings on distribution transformer aging, Energy 157 (2018) 669–678, https://doi.org/10.1016/j.energy.2018.05.148.
[25] S. Hussain, M.I. Azim, C. Lai, U. Eicker, New coordination framework for smart home peer-to-peer trading to reduce impact on distribution transformer, Energy 284 (2023) 129297, https://doi.org/10.1016/j.energy.2023.129297.
[26] J. Langevin, et al., Customer enrollment and participation in building demand management programs: a review of key factors, Energ. Buildings 320 (2024) 114618, https://doi.org/10.1016/J.ENBUILD.2024.114618.
[27] A. Nilsson, P. Stoll, N. Brandt, Assessing the impact of real-time price visualization on residential electricity consumption, costs, and carbon emissions, Resour. Conserv. Recycl. 124 (2017) 152–161, https://doi.org/10.1016/j.resconrec.2015.10.007.
[28] Z. Pooranian, J. Abawajy, V. P, and M. Conti, "Scheduling Distributed Energy Resource Operation and Daily Power Consumption for a Smart Building to Optimize Economic and Environmental Parameters," *Energies*, vol. 11, no. 6, p. 1348, 2018, doi: 10.3390/en11061348.
[29] T. Kirant Mitić, K. Voss, Development of a Joint Penalty Signal for Building Energy Flexibility in operation with Power Grids: Analysis and Case Study, Buildings 13 (5) (2023) 1338, https://doi.org/10.3390/buildings13051338.
[30] IEC 60076-7:2005, *Power transformers - Part 7: Loading guide for oil-immersed power transformers*: International Electrotechnical Commission, vol. 29.180. Accessed: 2024. [Online]. Available: https://webstore.iec.ch/en/publication/605.
[31] Solar Decathlon Europe 21/22, *SDE.* [Online]. Available: https://sdeurope.uni-wuppertal.de/de/ (accessed: 15-Aug-23).
[32] K. Voss, I. Kalpkirmaz Rizaoglu, A. Balcerzak, H. Hansen, Solar energy engineering and solar system integration – the solar Decathlon Europe 21/22 student competition experiences, Energ. Buildings 285 (2023) 112891, https://doi.org/10.1016/j.enbuild.2023.112891.
[33] IDA-ICE, *Equa Simulation AB - IDA indoor climate and energy 4.8 - Simulation Software | EQUA.* [Online]. Available: https://www.equa.se/en (accessed: 15-Aug-23).
[34] T. Kırant-Mitić and K. Voss, "Enhancing Grid Stability and Economic Operation through Heuristic Control: A Simulation Case Study," in *Proceedings of BauSim 2024: 10th Conference of IBPSA-Germany and Austria*, 2024.
[35] Lawrie, Linda K, Drury B. Crawley, *Development of Global Typical Meteorological Years (TMYx).* [Online]. Available: https://climate.onebuilding.org/ (accessed: 09-Dec-24).
[36] SIA 380/1, *Heizwärmebedar*. Zürich, Schweiz: Schweizerischer Ingenieur- und Architektenverein. Accessed: 2024. [Online]. Available: https://shop.sia.ch/normenwerk/architekt/380-1_2016_d/D/Product.

[37] N. Pflugradt, *LoadProfileGenerator*. [Online]. Available: https://www.loadprofilegenerator.de/references/ (accessed: 09-Dec-24).
[38] SIA 2024:2021, *Raumnutzungsdaten für die Energie- und Gebäudetechnik*. Zürich, Schweiz: Schweizerischer Ingenieur- und Architektenverein.
[39] EnergieSchweiz, *Suche*. [Online]. Available: https://www.energieschweiz.ch/search/?searchInput=Besser+Wohnen (accessed: 25-Jun-25).
[40] DesignBuilder Software Ltd, *DesignBuilder*, 2002. Accessed: 09-Dec-24. [Online]. Available: https://designbuilder.co.uk/.
[41] National Renewable Energy Laboratory, *EnergyPlus*: The U.S. Department of Energy's Building Technologies Office, 1996. Accessed: 2024. [Online]. Available: https://energyplus.net/.
[42] ENTSO-E Transparency Platform, *Day-ahead Prices*. [Online]. Available: https://transparency.entsoe.eu/dashboard/show (accessed: Dec-2022).
[43] Electricity Maps, *CO_2 emissions of electricity consumption*. [Online]. Available: https://app.electricitymaps.com/map (accessed: 09-Dec-24).
[44] M. Hall, A. Geissler, Comparison of Flexibility Factors and Introduction of a Flexibility Classification using Advanced Heat Pump Control, Energies 14 (24) (2021) 8391, https://doi.org/10.3390/en14248391.
[45] J. Le Dréau, P. Heiselberg, Energy flexibility of residential buildings using short term heat storage in the thermal mass, Energy 111 (2016) 991–1002, https://doi.org/10.1016/j.energy.2016.05.076.
[46] MATLAB, *(R2015b)*. Natick, Massachusetts: The MathWorks Inc, 2015.
[47] Python Software Foundation, *Python*, 2001. Accessed: 2024. [Online]. Available: https://www.python.org/.
[48] C. Steinbrink, et al., CPES Testing with mosaik: Co-simulation Planning, Execution and Analysis, Appl. Sci. 9 (5) (2019) 923, https://doi.org/10.3390/app9050923.
[49] Hall, M., Geissler, A., *FlexiCluster - Energy flexibility of building clusters*. [Online]. Available: https://www.aramis.admin.ch/Grunddaten/?ProjectID=47510.
[50] ISO, *ISO 7730: Ergonomics of the thermal environment: Analytical determination and interpretation of thermal comfort using calculation of the PMV and PPD indices and local thermal comfort criteria*. Geneva.
[51] SIA 180, *Wärmeschutz, Feuchteschutz und Raumklima in Gebäuden*: Schweizerischer Ingenieur- und Architektenverein. [Online]. Available: https://shop.sia.ch/normenwerk/architekt/sia%20180/d/2014/D/Product.

6. DISCUSSION

This dissertation set out to understand how buildings can be operated as flexible prosumers in a way that is technically, economically and environmentally meaningful and feasible at the distribution level. The four papers approach this question from complementary angles:

- signal analysis (how to combine price and CO_2eq. intensity information into one controllable objective),
- a residential reference case (what control can and cannot deliver in a highly efficient dwelling),
- control algorithm design at the single-building scale (how to plan and apply actions under comfort and equipment limits), and
- cluster operation across two countries (how transformer stress shape the value of demand-side flexibility).

Read together, the studies show that signal choice, control architecture, and system scale are interdependent: none can be treated in isolation if flexibility is to be applicable, verifiable, and aligned with local network constraints. Below, the answers to the research questions with paper-specific discussion are given.

RQ1 - Composite objective vs single-signal control.

Paper 1 demonstrates that a joint penalty signal can deliver balanced gains across cost and emissions relative to single-signal control. Over the heating season, the combined case reduced CO_2 emission by 21-24% and cost by 24-34%, tracking the best single-signal outcome on each metric while avoiding one-sided optimizations. The study also shows that aggregation choice matters: biweekly thresholds smoothed activation even though annual averages converge. Since day-ahead price and average CO_2eq. intensity are not reliably aligned, the paper concludes that composite signaling is valuable, but it must be embedded in a controller with priorities or adaptive weights and always remain bounded by DSO feasibility. It further documents that cross-border exchanges influence national CO_2 intensity, complicating price/carbon alignment.

RQ2 - Controller architecture for flexibility under price and congestion signals.

Paper 2 provides a calibrated reference in a very efficient dwelling: a predictive heuristic reduces the daily bill from 5.64 € to 5.45 € underprice response, with 5.50 € after the post-congestion event; indoor temperatures remain essentially stable by design (fluctuation around by 1 °C). The residential case indicates a limit set by efficiency itself: with well-insulated envelopes, high coefficient of performance equipment, and narrow comfort bands, the available flexibility margin is relatively limited. Most demand is essential and closely connected to maintaining comfort, leaving little scope for preheating/precooling or prolonged shifting to later periods without violating temperature or equipment constraints. Accordingly, both bill savings and congestion load reductions are limited and are delivered primarily via minor scheduling adjustments rather than large energy shifts. This should be understood as an inherent characteristic of efficient buildings, not a weakness of the control approach, and it underscores the need for portfolio aggregation and realistic program targets.

RQ3 - Co-optimizing grid and market-oriented operation at the single-building level.

Paper 3 shows that an RBPC control architecture can plan preheating/precooling and use the slab's thermal storage to follow price signals while enforcing slab/zone temperature limits and respecting DSO constraints. In market operation, RBPC achieved additional cost savings by 2.2% over RBC; during a congestion event it delivered a 9.35 kW power reduction with LMGI 88.6%, then resumed market-oriented operation with overall cost still lower. Comfort was maintained, i.e., market-oriented actions produced only modest operative temperature fluctuations over a representative week. Together with Paper 2, the studies show that RBC provides as a simple reference, whereas RBPC introduces predictive control and resolves objective conflicts with lower computational cost under DSO constraints compared to other complex control architecture models. White-box MPC in the loop remains a theoretical benchmark but is generally too computationally intensive for short decision intervals in co-simulation. For current practice, RBPC offers a practical balance of capability, computational feasibility, and transparency/verifiability.

RQ4 - Multi-building clusters: signaling strategies that balance cost, CO_2, and grid reliability.

Paper 4 shows that local network context determines which actions create real value. In the German cluster, a sequential strategy, i.e., price/CO_2 signals by default, overridden by a transformer critical status signal and mitigated demand-driven aging relative to single-signal cases. In the Swiss cluster, price/CO_2 signals could slightly lower aging via self-consumption, whereas overriding with transformer-critical status at inopportune times could increase aging by curtailing useful on-site PV utilization. Comfort bounds are preserved in both clusters. Accordingly, transformer-aware control must be root cause oriented and context specific. Before acting, the controller should determine whether the local stress stems from high imports or from surplus generation and then choose measures that address that cause. For example, reducing evening imports via preheating versus increasing midday consumption through storage charging or modest setpoint increases.

Taken together, these findings establish an integrated picture of grid-interactive buildings: signals, controllers, and local network context must be treated as a coupled design problem. Joint price/CO_2 signaling helps, but only when embedded in priority-aware control that treats DSO limits as hard constraints; RBPC provides a practical arrangement layer for this task. At the same time, the available flexibility in highly efficient dwellings is modest, so programs should privilege verifiable adherence and reliability over headline-grabbing shift quantities, and aggregate portfolios to achieve system impact. At the multi-building scale, transformer-aware, context-specific actions, i.e., reducing imports versus increasing on-site utilization, are essential to avoid re-creating peaks or curtailing useful self-consumption. Methodologically, the calibrated co-simulation and key performance indicators framing offer a reproducible way to test such strategies end-to-end.

7. CONCLUSION

This dissertation examined how building-side demand flexibility can be signaled, controlled, and verified so that buildings deliver bidirectional value, specifically lower cost and emissions for end users and dependable, verifiable support for the distribution grid, without compromising comfort. Transmission-level signals were treated as boundary conditions; the focus was distribution-feasible operation. The contributions cover signal analysis (Paper 1), a high-efficiency residential dwelling (Paper 2) and single-building control in a non-residential TABS building (Paper 3), and transformer-aware cluster operation in Germany and Switzerland (Paper 4).

Beyond the paper-level findings, the thesis contributes a coherent framework for grid-interactive buildings: (I) a joint penalty signal that synthesizes economic and environmental drivers with tested thresholding schemes; (ii) a rule-based predictive controller that ensures priority-aware and enforces comfort/equipment limits while planning thermal actions; (iii) a co-simulation pattern (calibrated white-box plant + numerical controller) with a transparent key performance indicator set and (iv) transformer-aware cluster scheduling that makes the load vs generation-driven distinction operational.

7.1 Summary

Finding 1: Signal design is decisive but not sufficient. The joint penalty signal developed in Paper 1 demonstrates that a composite objective that is both economical and lower carbon can be achieved. This directly addresses a gap in much of the literature, where buildings are asked to follow a single signal and then evaluated unfavorably when that signal is misaligned with other objectives. The study also makes clear that price and CO_2eq. intensity do not always move together. When they diverge, composite control alone cannot resolve the conflict: it must be embedded in a controller that ensures explicit priorities. The implication is that signal design should be evaluated as a critical design variable.

Finding 2: Requirement for an applicable controller. Paper 2 complements the picture from the residential side. In a very efficient dwelling, a controller reduces cost and shape demand without comfort penalties when sequential grid and market-oriented optimization are applied. Together with paper 3, they show that an RBPC architecture can schedule preheating/precooling and charge thermal storage in the building mass while applying slab and zone temperature limits and respecting DSO constraints. These two papers justify RBPC as a middle ground: capable and reliable than static rules (as in RBC), yet far lighter than white-box-in-the-loop MPC for short decision periods.

Finding 3: Scale and locality shape outcomes. Paper 4 moves from single buildings to clusters and shows why the main cause of the transformer stress must be central. In one cluster, transformer stress is primarily load-driven; in the other, it is generation-driven. A sequential strategy that defaults to price/CO_2eq. intensity control and is overridden by local limits. This argues against one-size-fits-all approach.

Finding 4: Methods and transferability. Methodologically, the dissertation contributes to a reproducible co-simulation workflow that couples a calibrated white-box building energy performance model with a numerical controller, harmonizes signals and decision periods, and evaluates outcomes with a transparent key performance indicator set. Further research can be supported by covering both residential and non-residential buildings and by testing clusters in different locations such as broader climates, tariffs, and feeder topologies will further strengthen research.

7.2 Limitations and outlook

Modeling workflow and toolchain. Conducting BGI studies at research quality is still slow. High-resolution inputs (weather, prices, CO_2eq. intensity, occupancy, congestion windows), device-level actuation, closed-loop co-simulation, and calibration all raise the bar. Today there is no helpful tool that makes modeling, control, and evaluation seamless. A practical next step is to package the workflow demonstrated here into a modular toolbox: a hub for co-simulation, importers for price/CO_2/DSO signals, ready-to-use control architectures as RBPC templates, and a key performance indicator/validation suite with automatic reports. To reduce study time, surrogate models (reduced-order or grey-box) can stand in for parts of the white-box plant once

calibrated; scenario pruning and parallelization can cut compute without losing decision quality.

Data needs and standards. The quality of any flexibility assessment is capped by the quality of the data. Many sites lack reliable, high-frequency dataset for the assets that matter (heat pumps, DHW, TABS sensors, EES and more). A sensible outlook is to define a minimal, standard data layer for BGI studies such as timestamps, basic device setpoints and feedback. Where measured data are incomplete, digital-twin techniques, combining short calibration runs with synthetic time series, can fill gaps while keeping uncertainty explicit.

Control evolution under uncertainty. RBPC demonstrates that much of the value of predictive control can be achieved at manageable computational cost. The next step is to make the controller uncertainty aware such as represent forecast bands for prices, CO_2, and weather.

From single sites to portfolios. Because highly efficient dwellings have limited shiftable energy, impact comes from aggregation. As the stock of efficient buildings grows, there is simply less energy to move without touching comfort. Value will concentrate on products that pay for being available at the right place and at the time.

The methodological gap (tools and data), the physical reality (limited shiftability in efficient homes), and the market gap (products that pay for time- and location-specific availability) are the three levers that will determine whether building flexibility scales. The work in this dissertation provides patterns as signal analysis, controller design, and evaluation practice to act on all three.

7.3 Implications for pilot markets and building typologies

The findings of this dissertation indicate that not all building types contribute equally to system-relevant flexibility. While highly efficient dwellings demonstrate technical feasibility and provide an ideal testbed for verifying control approaches under strict comfort and equipment constraints, their absolute flexibility potential remains modest. The combination of low heating and cooling demand, narrow comfort ranges, and high-efficiency systems limits the available energy that can be temporally shifted without compromising comfort. Consequently, the system-level impact of individual residential buildings is small, and aggregation is required to achieve measurable

network effects. However, this aggregation requires high coordination effort, substantial data exchange, and increased uncertainty due to occupant diversity, which collectively reduce cost-effectiveness in early-stage flexibility programs.

From an impact–effort perspective, other building typologies such as particularly non-residential and mixed-use buildings, come forward as promising pilot candidates. Commercial and public buildings, such as offices, schools, and retail facilities, typically feature larger conditioned floor areas, centralized HVAC systems, and occupancy-driven schedules that provide distinct flexibility windows outside working hours. Their thermal inertia, combined with reduced comfort constraints during unoccupied periods, enables meaningful load shifting with moderate control complexity. Similarly, small industrial sites or community-scale energy systems, where several loads are already monitored and centrally managed, offer high controllable capacity per site and more straightforward data acquisition.

Therefore, early market pilots should focus on clusters that combine diverse load types under a common transformer, for instance mixed-use neighborhoods or business parks, where both the coordination effort and verification requirements remain manageable while the overall system impact is enhanced by diversity.

The CV has been removed for data protection reasons.